Cardiac oxidative stress and antioxidant status in response to radiation and monocrotaline induced cardiac dysfunction

A Thesis Presented to the Faculty of Graduate Studies of Lakehead University

by Stephanie Puukila

Submitted in partial fulfillment of requirements for the degree of Doctor of Philosophy in Biotechnology

December 1, 2015

PERMISION TO USE STATEMENT

In presenting this thesis in partial fulfillment of the requirements for the Doctor of Philosophy degree at Lakehead University, I agree that the Library shall make it available to use under rules of the Library. Permission for extensive quotation from or reproduction of this thesis may be granted by my major professor, or in their absence, by the Head of Biotechnology department when in the opinion of either, the proposed use of the material is for scholarly purposes. Any copying or use of the material in this thesis for financial gain shall not be allowed without my written permission.

Requests for permission to copy or make other use of material in this thesis in whole or in part should be addressed to:

Head of the Biotechnology Program,

Lakehead University

955 Oliver Road

Thunder Bay, Ontario, Canada

P7B 5E1

Abstract

Cardiovascular disease is the leading cause of death and disability worldwide. Oxidative stress has been implicated in many types of cardiovascular disease. Chronic cardiac stress conditions have been shown to be associated with an increase in myocardial oxidative stress following myocardial infarction, which in turn may lead to depressed contractile function, myocardial remodeling and heart failure. Antioxidants play a protective role against oxidative stress damage through the removal of free radical intermediates and inhibition of oxidation reactions. An imbalance of free radicals and antioxidants results in cellular and sub-cellular damage. Therefore, treatment with non-enzymatic antioxidants may provide protection against high levels of free radicals. We investigated, in three different studies, if treatment with antioxidants can protect the heart under conditions of oxidative stress. In the first study, a complex dietary supplement composed of numerous antioxidants and anti-inflammatory components was given to C57BL/6 mice that received a whole body radiation dose of 5 Gy to investigate potential cardioprotective effects by measuring cardiac antioxidant status and apoptosis. In the second study, the same complex dietary supplement was given to Thy1-GFP mice that received a radiation dose of 10 Gy to the head to investigate the abscopal effect on the heart by measuring cardiac inflammation and fibrosis. In the final study, the potential cardioprotective effects of secoisolariciresinol diglucoside, a compound found in flaxseed, was investigated in a Wistar rat model of pulmonary arterial hypertension by correlating cardiac functions with oxidative stress. We have shown that treatment with antioxidants may offer some protection to the heart in these models of oxidative stress though it is important to consider the extent of oxidative stress and when developing a antioxidant treatment protocol.

Acknowledgements

I can't stress enough how grateful I am to the many people who have worked with me for the past three years; from NOSM, Lakehead, McMaster and especially Brazil. First, I need to thank my supervisor Dr Neelam Khaper, who I've worked with for about 7 years now. I am grateful for her guidance, mentorship and support. It is because of her that I've had the opportunity to find my passion and work in molecular research.

I want to give special thanks to my co-supervisor Dr Doug Boreham for getting me started in the fascinating field of radiation research by giving me a PhD position after a quick visit to NOSM. Also, for his guidance and support these past three years.

I would like to thank my committee members Dr Marina Ulanova and Dr Guangdong Yang for providing feedback as well as offering/providing help when needed.

I was fortunate enough to spend 3 months in Porto Alegre, Brazil to work on a research project. I'd like to acknowledge everyone else in Dr Belló-Klein's lab group at UFRGS: Jéssica Poletto Bonetto for organizing the work and tissue collection, Bruna Gazzi de Lima for i.p. injection training and performing the hemodynamic data collection, Rayane Teixeira for performing the hemodynamic data collection, blood collection and aiding with the rats, Denise Lacerda for gavage training and administering anesthesia, Vanessa Ortiz and Gaina Corssac for aiding with the rats, Dalvana Broilo Muller for aiding with tissue collection, Tania Gattelli for chemiluminescence training and Patrick Turck and Christina Campos Carraro for aiding with the rats, tissue homogenization, protein measurement and ROS, chemiluminescence, and antioxidant enzymatic activity analysis. I want to acknowledge Ana Lucia Hoefel for aiding in ALT and AST analysis. I'd also like to acknowledge Dr Alex Sander Da Rosa Araujo for aiding in analysis of data and suggestions of further study.

I want to thank Dr Pawan Singal and those at DFATD for the opportunity to go to Brazil. I want to give a very big thank you to Dr Adriane Belló-Klein and her staff and students at UFRGS for making my stay a fantastic experience. I need to give a special mention to Rafael Fernandes for organizing EVERYTHING, from the project to where I was staying. It would not have been possible without his help.

Finally, I want to thank everyone at NOSM, especially those in 'Khaper lab' (especially Yue Sun and Ashley NemecBakk) for their help with running experiments when I was overrun with work. I'd also like to thanks Jessica Sarvas, Sarah Niccoli and Shuangshuang Li for their help with the western blot protocol. I of cousre need to thank those at McMaster, Jen Lemon and Mary Ellen Cybulski, for collecting/shipping the hearts, teaching me their protocols and giving feedback on my work.

I gratefully acknowledge Lakehead University Faculty of Graduate Studies and Department of Biology and the Ontario Graduate Scholarship program for the financial support.

I also want to give a special thank you to Roger Page for the Michael John Page NOSM Summer Research Award.

Table of Contents

List of Tables

List of Figures

Chapter 2

Chapter 3

Chapter 4

Abbreviations

8-oxodG - 8-hydroxyguanine

ACE - Angiotensin-converting enzyme

ALT - Alanine aminotransferase

Apaf - Apoptotic protease activating factor

ATG - Autophagy-related proteins

AST - Aspartate aminotransferase

Bcl - B-cell lymphoma

Bax - B-cell lymphoma-associated X protein

β2M - Beta-2 microglobulin

CVD - Cardiovascular disease

CAD - Coronary artery disease

DCF-DA - 2′, 7′ - dichlorofluorescein diacetate

DNA - Deoxyribonucleic acid

ECM - Extracellular matrix

GPx - Glutathione peroxidase

GSSG - Glutathione (oxidized)

GSH - Glutathione (reduced)

GSR - Glutathione reductase

Gy - Gray

H & E - Hematoxylin and eosin

H_2O_2 - Hydrogen peroxide

$^{\bullet}OH$- Hydroxyl radical

ICAM - Intercellular adhesion molecule

IL - Interleukin

IR - Ionizing radiation

LET - Linear energy transfer

LC3 - Light chain 3

MMP - Matrix metalloproteinases

mTOR - Mammalian target of rapamycin

Mn-SOD - Manganese superoxide dismutase

MCT - Monocrotaline

PAF - platelet-activating factor

PVC - Polyvinyl chloride

PAH - Pulmonary arterial hypertension

ROS - Reactive oxygen species

SDG - Secoisolariciresinol diglucoside

SV - Sievert

TGF - Transforming growth factor

TNF-α - Tumor necrosis factor-alpha

$O_2^{\bullet-}$ - Superoxide anion

ULK1 - Unc-51-like kinase

UFRGS - Universidade Federal do Rio Grande do Sul

WBD - Whole body dose

Chapter 1 - Introduction

Cardiac Remodeling and Failure

The heart pumps blood that carries oxygen and nutrients to all parts of the body. The heart muscle receives its own blood supply from a system of coronary arteries. Adequate blood supply is crucial for normal function of the heart [1]. The left and right side of the heart are anatomically and electrically connected resulting in identical contraction rates between the chambers. In the case of an abnormality of one pump it is essential to take into account the effects of the other pump [2]. Impaired blood flow can occur because of cardiovascular disease (CVD). CVD is responsible for over 17.3 million deaths per year, and is the leading cause of death and disability worldwide [1; 3]. Types of CVDs include those due to atherosclerosis, such as: ischemic heart disease, stroke, and diseases of the aorta and arteries; or those due to other causes such as cardiomyopathy [1].

Atherosclerosis is the major source of morbidity and mortality in the developed world and claims more lives than all types of cancer combined [4]. It is characterized as a thickening of the arterial wall caused by the accumulation of cholesterol deposits in macrophages. This thickening forms an atherosclerotic plaque, which narrows the lumen of the artery, reducing blood flow. Progressive narrowing and reduced blood flow to the point that metabolic needs of the heart are no longer met will cause ischemia [5]. Atherosclerotic plaques can abruptly rupture, causing a blood clot, compromising oxygen supply to target organs even further [4; 5]. Blockage in the coronary artery leads to ischemic death of cardiomyocytes and eventually myocardial infarction. Restoring blood flow is crucial, but reperfusion can lead to further damage to endothelial cells and cardiomyocytes [6]. After ischemic insult to the myocardium the

inflammatory repair response is activated. Stressed myocardial cells release cytokines which leads to microembolism, platelet activation, neutrophil plugging, and endothelial cell dysfunction further reducing blood flow and increasing myocyte damage and death [6; 7]. To compensate with the loss of myocytes, hypertrophy is activated in the remaining viable cells. There are two different hypertrophic phenotypes depending on how the shape of the myocyte is changed. Concentric hypertrophy, due to pressure overload, is characterized by parallel addition of sarcomeres and increase in diameter of cardiomyocytes, resulting in wall thickening. Eccentric hypertrophy, due to volume overload or prior infarction, is characterized by addition of sarcomeres in series and lengthening of cardiomyocytes. This results in thinning of the wall and ventricular dilation [8-10]. Atherosclerosis is not the only cause of hypertrophy in CVD. Hypertrophic cardiomyopathy, specifically hypertrophy of the myocardium, is the most common form of monogenically inherited heart disease [11]. Prolonged hypertrophy can lead to myocardial scarring, where fibrotic tissue replaces normal tissue lost by damage [10]. Cardiac fibroblasts account for up to two-thirds of all heart cells and are regulators of extracellular matrix (ECM) remodeling [12; 13]. In myocardial infarction the infarct area is infiltrated by modified fibroblasts called myofibroblasts. Myofibroblasts form granulation tissue used to clear dead cells, breakdown ECM and stimulate angiogenesis to re-vascularize the ischemic tissue. Prolonged myocardial infarction causes myofibroblasts to increase synthesis of structural ECM proteins which leads to scar formation. This scar formation is essential to repair where cardiomyocytes were lost due to damage in order to prevent rupture of the myocardial wall, but excessive accumulation results in fibrosis. Fibrosis stiffens the myocardium and hampers the diastolic filling [12]. Prolonged ischemia, hypertrophy and fibrosis, where the heart is unable to pump sufficiently and maintain proper blood flow, will eventually lead to heart failure.

The pathophysiological processes of heart failure are highly complex and unfortunately current therapy is based on a regimen of drugs that only target symptoms [2]. The most common drugs used for the treatment of heart failure are angiotensin-converting enzyme (ACE) inhibitors and β-blockers, which aim to delay or even reverse the maladaptive remodeling process [8]. ACE inhibitors work by reducing the production of angiotensin II and increasing bradykinin production, which results in a drop of blood pressure, while β-blockers reduce heart rate. Both can be used together to improve symptoms associated with heart failure [14]. While these drugs can be effective they may cause adverse side effects and are not suitable for all patients. Diagnosis of heart failure can be quite difficult as most symptoms are non-specific and can be interpreted as other problems [14]. Heart failure can be defined as acute heart failure and chronic heart failure. Acute heart failure is due to a fall in left ventricular stroke volume which can lead to hypotension or cardiogenic shock [2; 15]. Chronic heart failure is due to prolonged ventricular remodeling or dilatation [2]. Dilation and subsequent thinning of the ventricular wall results in increased diastolic and systolic wall stress in the right and left ventricular chambers. Cardiac contractility and relaxation will decrease as chamber dilation continues, leading to heart failure [16]. While heart failure is complex, all of the processes that lead to heart failure (ischemia, hypertrophy, remodeling etc.) appear to involve oxidative stress. Therefore, a better understanding of the oxidative stress mechanism may enable the development of novel and effective therapeutic strategies against heart disease.

Oxidative Stress

Oxidative stress occurs when there is an increase in free radicals, resulting in an imbalance between antioxidants and reactive oxygen species (ROS). Excess free radicals can damage DNA, cell membranes, proteins and other macromolecules [17]. Free radicals are formed when a molecule contains one or more unpaired electron(s) in the outermost orbital, making the molecule highly reactive [18; 19]. Due to its unique diradical configuration, oxygen is a major source of free radicals [18]. Types of ROS include free radicals such as superoxide anion ($O_2^{\circ-}$) and hydroxyl radical ($^{\bullet}OH$), and compounds that are not free radicals per se, such as hydrogen peroxide (H_2O_2) [20]. ROS are generated by the mitochondrial electron-transport chain, the major source of ROS in the heart, and oxygen-metabolizing enzymatic reactions such as xanthine oxidase, uncoupled nitric oxide synthases and NADPH oxidases [17; 21]. Mitochondria provide energy in the form of adenosine triphosphate (ATP) to the cell. Electrons flow along the respiratory transport chain through a series of electron transport carriers located on the inner mitochondrial membrane called complexes I, II, III and IV. Normally, only 1% to 2% of electrons leak out and form $O_2^{\bullet-}$ which is scavenged by manganese superoxide dismutase (Mn-SOD). Typically, ROS act as signaling molecules that regulate numerous cellular processes [21]. ROS are also important for immune defense, in particular for oxidative burst reaction which is essential for phagocytosis [17; 22]. However, under pathophysiologic conditions, the electron transport chain may become uncoupled and lead to increased $O_2^{\bullet-}$ production [20]. Leaked $O_2^{\bullet-}$ converts ferric iron to ferrous iron in the Haber-Weiss reaction. Ferrous iron reacts with H_2O_2 in the Fenton reaction generating highly reactive $^{\bullet}OH$, which can cause significant damage [21]. High amount of ROS are implicated in many pathological diseases. In fact, numerous studies strongly suggest a role for ROS in cardiovascular pathophysiology. ROS have been implicated in the progression of atherosclerosis [4]. Increased levels of ROS observed following myocardial

infarction is shown to be directly involved in the development of contractile dysfunction through modification of proteins important for excitation-contraction coupling [20; 23]. ROS has also been shown to be involved in the development of cardiac hypertrophy by activating hypertrophy signaling kinases and transcription factors as well as remodeling proteins [20; 22; 23].

Oxidative Stress Mediated Damage

The adverse effects of oxidative stress is mainly due to DNA damage. $^{\bullet}OH$ can react with DNA by addition to double bonds of DNA bases and also by removing a hydrogen atom from the methyl group of thymine and the carbon-hydrogen bonds of 2'-deoxyribose [24; 25]. Hydrogen abstraction in the 2'-deoxyribose of DNA due to $^{\bullet}OH$ causes double stranded breaks [24]. All of the bases can be modified by ROS but guanine is highly susceptible, where ROS causes the oxidation of deoxyguanosine to 8-hydroxyguanine (8-oxodG). If unrepaired this results in 8-oxodG mispairing with deoxyadenosine rather than deoxycytosine resulting in a cytosine–adenine point mutation [26]. 8-oxodG has been implicated in many pathological conditions such as various types of cancer, diabetes and cardiovascular disease [24]. $^{\bullet}OH$ can also cause the modification of cytosine to 5-methylcytosine which results in the generation of thymine. Since thymine is a normal component of DNA the new thymine-guanine base pair may avoid detection by repair mechanisms, creating a point mutation [26]. Cells respond to DNA damage by activating cell cycle checkpoints to provide time for DNA repair machinery to mend the damage, but these processes are imperfect. In fact, exposure of cells to H_2O_2 may suppress DNA repair as well as inducing damage [24; 26; 27]. Excess ROS will also lead to oxidative degradation of lipids in a process known as lipid peroxidation. Free radicals initiate lipid

peroxidation by attacking double bonds associated with polyunsaturated fatty acid (PUFA), resulting in the removal of a hydrogen atom from a methylene group. PUFA peroxyl radicals can abstract hydrogen atoms from adjacent PUFA, forming an hydroperoxide and another lipid radical, creating a chain reaction [28]. When prolonged oxidative stress damages cells beyond repair the cell may activate mechanisms to initiate cell death.

Cardiomyocyte cell death is known to contribute to the development of heart failure. There are three forms of cell death that occur in the heart; necrosis, apoptosis, and autophagy. Necrosis is a disruption of cell membrane resulting in the release of intracellular contents [29]. Apoptosis is tightly regulated/programmed cell death that is essential to organ development, control of cell number and deletion of harmful/abnormal cells. Prolonged increase in apoptosis has been shown to play a major role in the development of various cardiovascular disorders and heart failure [29; 30]. Apoptosis exists as two pathways; the intrinsic pathway and the extrinsic pathway. The intrinsic pathway is activated by biological, chemical, and physical stimuli that send signals to the mitochondria and endoplasmic reticulum [31]. The first step is the activation of pro-apoptotic proteins in the cytoplasm, including B-cell lymphoma (Bcl)-2-associated X protein (Bax). Pro-apoptotic Bax can open mitochondrial channels releasing cytochrome c. Anti-apoptotic Bcl-2 can prevent the release of cytochrome c by binding to Bax, thus preventing the opening of mitochondrial channels. Once released cytochrome c will bind to apoptotic protease activating factor (Apaf)-1, causing a conformational change of the protein. The Cytochrome c/Apaf-1 complex then activates caspase-9, creating an apoptosome. The apoptosome cleaves and activates caspase-3 and -7. These activated caspases then translocate to the nucleus and cleave DNA repairing enzymes and activate endonucleases which cleave DNA, resulting in

apoptosis [29-31]. The extrinsic pathway involves cell surface death receptors and is activated when a death ligand binds to its receptor. This results in the formation of the death-inducing signaling complex which activates caspase-8. Caspase-8 has two roles: it can cleave and activate caspase-3, resulting in apoptosis, or can lead to the release of cytochrome c by the mitochondria, causing intrinsic apoptosis [31]. Apoptotis is characterized by cell shrinkage, plasma membrane blebbing, chromatin condensation, DNA fragmentation and finally, fragmentation of the cytoplasm and nucleus into membrane-enclosed apoptotic bodies that undergo phagocytosis [31; 32]. Increased apoptosis has been shown to be involved in many cardiovascular diseases including atherosclerosis, myocardial ischemia/reperfusion injury, diabetic cardiomyopathy, and chronic heart failure [29; 33-35]. Oxidative stress induced cardiomyocyte death is associated with the structural and biochemical changes indicative of apoptosis [30]. Previous studies have shown that cardiomyocyte apoptosis in atherosclerosis, myocardial infarction, ischemia/reperfusion injury, cardiomyopathy, and heart failure is triggered by oxidative stress [30; 36; 37]. It is clear that oxidative stress induced apoptosis is involved in cardiovascular disease.

Autophagy

While the role of apoptosis in cardiovascular disease is well established the role of autophagy is not completely clear. Autophagy is a catabolic pathway for bulk turnover, or recycling, of long-lived proteins and organelles via lysosomal degradation and is induced by signals due to various stressors, such as starvation, metabolic stress, high glucose and hypoxia. There are three types of autophagy: chaperone-mediated autophagy, microautophagy and

macroautophagy. Chaperone-mediated autophagy requires the complete unfolding of the autophagic materials prior to entry into lysosomes. It is initiated by recognition by a hsc70-containing complex. Once bound, protein substrates then translocate into the lysosomal lumen, resulting in unfolding and degradation. This process allows for individual proteins to be singled out [38; 39]. Microautophagy is when lysosomes directly engulf small pieces of the cytoplasm through inward invagination of the lysosomal membrane [38; 40]. Macroautophagy is the most studied of the three and is characterized by the formation of a double-membrane vesicle called the autophagosome. Autophagosome formation involves autophagy-related proteins (ATG), which are downstream of mammalian target of rapamycin (mTOR). In stress response mTOR is inhibited allowing the activation of the unc-51-like kinase (ULK1) complex (ULK1/Atg7/Atg13). This stimulates phagophore formation, and activates the beclin-1 complex which promotes phagophore nucleation and elongation. Membrane elongation involves the ATG12-ATG5 complex and microtubule-associated protein 1 light chain 3 (LC3). LC3-I is normally located in the cytosol until it is conjugated by ubiquitin-conjugating enzyme-like molecules ATG7 and ATG3 to LC3-II. LC3-II is then localized to the autophagosome membrane with the assistance of ATG5. LC3-II remains on the autophagosomes until lysosomes are fused to the autophagosomes to generate autolysosomes. The contents inside the autolysosomes are lysed and degraded and the products are released into the cytosol and used in metabolic pathways [38; 39]. Oxidative stress has been reported to serve as important stimuli of autophagy during periods of stress. Increased ROS degrades inhibitors of beclin-1, allowing for beclin-1 activation and increased autophagy in the cell [39]. Autophagy in the heart is used to maintain homeostasis and is an important survival mechanism when cells need to recycle amino and fatty acids during starvation [29]. A defect in the autophagic pathway can lead to ventricular

dysfunction and heat failure [41]. Autophagy may also be detrimental and lead to excessive self-digestion and degradation of essential cellular components. Autophagy is upregulated in response to ischemia and is thought to promote survival by maintaining energy homeostasis. During ischemia, oxygen and nutrient supplies are decreased causing inactivation of mTOR, leading to autophagy for cell survival [42]. During reperfusion though, beclin 1 is markedly upregulated due to an increase of ROS from reoxygenation after ischemia. This leads to excessive activation of autophagy that could cause cell death [38; 42]. Autophagy is also involved in heart failure, but whether autophagy serves a protective or a deleterious role is not clear. Autophagy may be an adaptive response to heart failure by increasing protein degradation and decreasing cardiac hypertrophy. Though, excessive autophagy in load-induced heart failure leads to cell death, loss of cardiomyocytes, and may contribute to the worsening of heart failure [31; 38; 42]. Therefore, further research is needed to fully understand the role of autophagy in cardiovascular health.

Antioxidant Potential

To maintain homeostasis the cell contains antioxidants that scavenge ROS. An antioxidant is a molecule capable of inhibiting the oxidation of other molecules by being oxidized themselves, so antioxidants are often reducing agents. Antioxidants remove free radical intermediates and inhibit other oxidation reactions, providing protection against oxidative stress induced damage. Both enzymatic and non-enzymatic antioxidants offer protection against ROS [18]. Three of the most important enzymatic antioxidants are SOD, glutathione peroxidase (GPx) and catalase [43]. SOD catalyzes the dismutation of $O_2^{\bullet-}$ to H_2O_2 and O_2. Mn-SOD is the primary

defense against mitochondrially generated ROS as it is located inside the mitochondria [21; 43]. Catalase is found in the cytoplasm and catalyzes the reduction of H_2O_2 to H_2O [43]. Glutathione is also located in the cytoplasm of the cell. Reduced glutathione (GSH) can convert H_2O_2 to H_2O but requires GPx as a catalyst. This reaction will convert glutathione to its oxidized state (GSSG). Glutathione reductase (GSR) can convert GSSG back to GSH by using NADPH as an electron donor. This allows GSH to act as an antioxidant again [18; 43; 44]. Many studies have investigated these antioxidants in cardiovascular disease. SOD, GPx and catalase levels have been shown to decrease in animal models of heart failure [45]. In heart muscle GSH depletion and accumulation of GSSG can occur within minutes of initiating oxidative stress [44; 46]. Many studies have also shown that increasing these antioxidants can improve cardiovascular health in models of disease [43]. Several studies have shown increased SOD offers protection against ischemia-reperfusion injury [18; 47-49]. SOD and catalase have been shown to cause reduction in infarct size in dogs that underwent 90 min of coronary occlusion and 24 h of reperfusion [43; 48]. The therapeutic role of various non enzymatic antioxidants, such as vitamin E, has been greatly studied. Treatment with vitamin E in guinea pigs increased GSH/GSSG ratio, decreased lipid peroxides, decreased oxidative stress and attenuated heart failure [45; 50]. Also, studies with vitamin A, C and E in a rat model of ischemia/reperfusion reported that redox ratio was increased and lipid peroxidation was decreased [18; 51; 52]. Vitamin A, C and E also decreased lipid peroxides and improved cardiac function in myocardial infarction patients [18]. It is clear the antioxidants may have a therapeutic role in oxidative stress induced cardiovascular disease.

The main objective of this study was to use different models of oxidative stress in order to study the molecular effects and mechanistic response of the heart. Also, if/how different

models of oxidative stress lead to different or similar cellular responses. Furthermore, the role of various antioxidants was also studied. Since many cardiovascular diseases are due to oxidative stress where high levels of free radicals overwhelm the enzymatic antioxidant line of defense, supplementation with non-enzymatic antioxidants may provide a promising treatment option. Both a mouse and rat model was used to measure different parameters of oxidative stress response and cardiac remodeling, such as, cell death, antioxidant levels/activity, inflammation, fibrosis and cardiac function and any possible protective effects of antioxidant supplementation. The three different studies investigated oxidative stress over a broad timeline; 21 days-120 days after oxidative stress inducing treatment. This allowed the visualization of the response of the heart to oxidative stress at different time points and how it differs. Also, all three studies investigated pre-treatment with antioxidants versus co-treatment/post-treatment and how pre-treatment may be a better antioxidant treatment option. These studies aim to further our understanding of cardiac oxidative stress and potential benefits of antioxidant supplementation.

Chapter 2 - Impact of a Complex Dietary Supplement on Radiation-Induced Cardiac Damage

Abstract

A high dose of whole body radiation has been shown to lead to oxidative stress and cardiovascular disease. Studies have recently shown that a complex dietary supplement consisting of anti-oxidants and anti-inflammatory compounds can increase longevity, decrease markers of ageing and impart protection against radiation induced oxidative stress and inflammation in irradiated mice. Although autophagy is induced in response to oxidative stress its role in radiation induced cardiac damage has not been investigated. We tested the hypothesis that a complex dietary supplement can attenuate cardiac oxidative stress and apoptosis in mice exposed to a high dose of ionizing radiation. C57BL/6J male mice were fed a complex dietary supplement before (30 days) and after (48 hours, 30 days or 120 days) a whole body 5 Gy dose of radiation or just after (48 hours, 30 days or 120 days) the radiation exposure. Hearts were collected and the protein levels of antioxidants Mn-SOD and catalase, apoptosis markers caspase 3, Bax and Bcl_2 and autophagy marker LC3b I and II were examined. Protein levels of both Mn-SOD and catalase increased 48 hours after irradiation in both supplement fed groups but did not change after 30 or 120 days when compared to time matched 5 Gy radiation treatment alone. Pro-caspase 3 and Bax:Bcl_2 ratio decreased in both supplement fed groups 48 hours after treatment when compared to time matched 5 Gy radiation treatment alone. 30 and 120 days after treatment pro-caspase 3 decreased only when supplement was fed after irradiation. LC3bII:I ratio increased only at 48 hours after treatment in both supplement fed groups when compared to 5 Gy radiation treatment alone. Our results suggest that a dietary supplement design to offset the effects of oxidative stress may provide some protection to the heart against a high whole body dose of radiation.

Introduction

Ionizing radiation (IR) is an electromagnetic wave or particle that can remove an electron from an atom or molecule, leading to the formation of chemically reactive ions. Types of IR include α particles, β particles and γ rays. α and β particles have a high ionizing power but a low penetrating power. Photons of relatively low energy are able to interact with electrons of organic molecules to generate 'excited' states where the energy levels of the molecular orbitals are raised. In the case of γ rays, when the photon energies are high, the electronic excitation is sufficient for electrons to be ejected from their orbital, resulting in molecular ionization [53]. The absorption of IR in living cells can directly disrupt atomic structures, producing chemical and biological changes. The absorbed dose measures the energy absorbed in a specified region and depends on the particular material or tissue placed in an X-ray beam [54]. The basic unit of measurement of absorbed dose is gray (Gy), which is 1 joule of initial energy per kilogram of tissue. An effective dose, called sievert (Sv), is obtained by adding the dose equivalent to each organ modified by each organ's radiosensitivity [54]. The damaging effects caused by IR are due to the geometry of the physical energy deposition per unit track length (per μm) of the impacting radiation, referred to as linear energy transfer (LET) effects [26; 55]. The density of ionization events is higher for radiation with heavy ions than for photons and protons. Heavy ions deposit a large amount of energy in a small distance, while low LET radiation, such as γ rays, will deposit energy infrequently along its track [56; 57]. LET determines the relative potency of different types of radiation in causing biological effects. Following exposure to high LET radiations the yield of damaged sites in DNA is greatly increased [26; 58-62].

IR can damage cells by various mechanisms including DNA damage [63]. IR induced DNA damage includes double strand breaks, single strand breaks and base damage. The generation of double-strand breaks triggers DNA damage response and repair pathways. Single strand breaks and base damage are rapidly repaired but can give rise to stalled replication forks [64]. The main two repair pathways for double strand breaks are homologous recombination and non-homologous end-joining. Homologous recombination uses the correct DNA sequence from a homologous strand of undamaged DNA, achieving high fidelity even if sequence information is lost at the site of the break [63; 64]. Non-homologous end-joining repairs double strand breaks via strand re-extension and functions predominantly during G1 when HR repair is not available [63; 65]. Successful repair of DNA lesions will allow the cell to continue in the cell cycle but unsuccessful repair can trigger the death of the damaged cells, and uncorrected repair will generate mutations [63; 66]. Biochemical modifications that occur after radiation exposure are not only caused by the IR itself. Cellular damage is also caused by oxidative changes, which may continue to arise for days and months after the initial exposure, likely due to continuous generation of reactive oxygen species (ROS) [26; 67]. IR can generate reactive chemical species through radiolysis of water in the cells and by stimulation of oxidases and nitric oxide synthase (Figure 1) [26]. ROS that are directly or indirectly created by IR that exist in an aerobic cellular environment at physiological pH are $O_2^{\bullet-}$, $^{\bullet}OH$ and H_2O_2 [26; 68]. ROS derived from water in the cell damage DNA via a variety of mechanisms, including base damage, base release, depolymerization, cross-linking, and strand breakage [63; 69]. As well as directly causing DNA damage $^{\bullet}OH$ generated by IR may also induce oxidative damage of the mitochondria through peroxidation of mitochondrial inner membrane phospholipids, resulting in enhanced generation of $O_2^{\bullet-}$ from the mitochondria and persistent oxidative stress caused by IR [70].

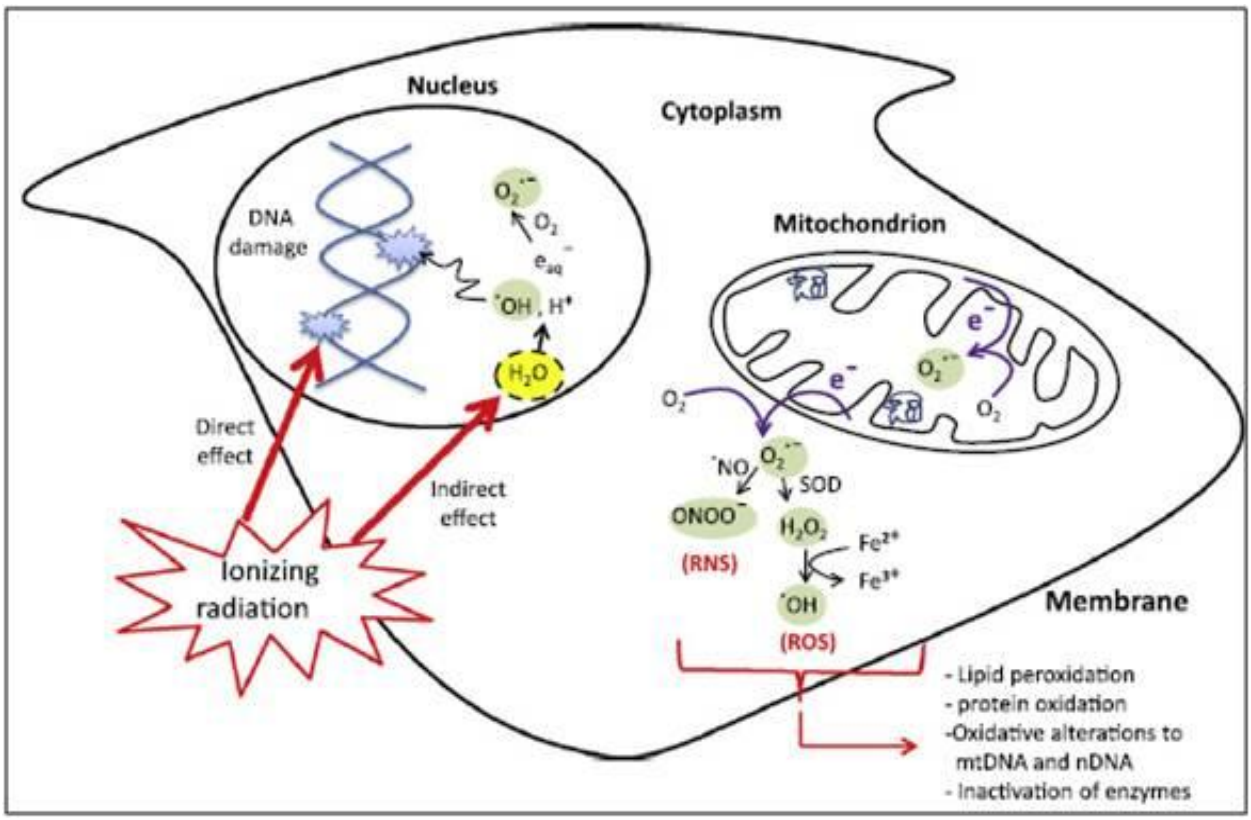

Figure 1. Direct and indirect effects of ionizing radiation on the cell. Ionizing radiation can directly disrupt atomic structures and produce chemical and biological changes. Ionizing radiation can also act indirectly through radiolysis of cellular water and generation of ROS [26].

The detrimental or beneficial effects of IR depends on LET and dose. Increasing LET causes an increase in the yield of H_2O_2. Also, $O_2^{\bullet-}$ is the most abundant radical species produced by radiations with high LET [26; 71; 72]. A high whole body dose (WBD) of IR, which can be defined as >500 mGy, delivered at a high dose rate may cause acute radiation syndrome. The severity of clinical signs and symptoms of acute radiation syndrome are the body volume irradiated, the inhomogeneity of dose exposure, the absorbed dose, the dose rate and the particle type [73]. A whole body dose of 1-4 Gy will cause mild to moderate symptoms, 4-8 Gy will cause severe to very severe symptoms, and >8 Gy is lethal [73; 74]. Acute radiation syndrome is

usually only caused by nuclear accidents, atomic bombs or irradiation as part of cancer therapy [73]. The use of ionizing radiation has become common practice in medical diagnostics and cancer treatment. It is estimated that more than 50% of patients with cancer are treated with radiotherapy [75]. From the early 1980's to 2006 the average radiation dose per individual in the United States increased by a factor of 1.7-6.2 mSv, which is believed to be caused by the growth of medical imaging procedures [76]. As the use of IR in medical procedures increases it is important to understand the biological effects it may lead to in the future.

The heart is an organ that is particularly susceptible to radiation induced damage. High doses of whole body radiation used in cancer treatment has been shown to lead to cardiac stress and cardiovascular disease (CVD) [75]. Radiation induced CVD can include pericarditis, myocardial fibrosis and coronary artery disease (CAD) [77-79]. Chronic or delayed pericarditis may occur anywhere from a few months to years after completion of radiation treatment; with up to 20% of patients developing symptoms of chronic pericarditis within 10 years following irradiation [80]. However, most of the time symptoms are present within 12 months of therapy [81]. Myocardial fibrosis is usually seen at radiation doses above 30 Gy and is often asymptomatic and can occur without an inflammatory reaction. In this case radiation leads to reduced myocardial compliance through microvascular insufficiency and ischemia, resulting in diffuse and patchy interstitial fibrosis [80]. Radiation induced CAD resembles CAD caused by atherosclerosis but has been shown to lead to plaque that is more fibrous with a decrease in lipid component [77; 80]. Also, valvular lesions and calcification have been described in irradiated patients [77; 82]. It is believed that coronary lesions caused by radiation therapy may be the most significant cause of mortality from radiation induced heart disease [81]. The majority of radiation

induced cardiovascular disease is caused by radiation treatment of cancer. Cancer patients treated with radiation as children and adolescents appear to have a high relative risk of fatal cardiovascular complications when compared to non treated in the same age group [83; 84]. Adult patients who receive radiation therapy for cancer treatment, particularly breast cancer, are also at risk of developing heart disease. Early Breast Cancer Trialists' Collaborative Group data has shown that relative risk of cardiac death is related to the estimated mean cardiac dose, and that risk is increased by 3% per Gy [77]. Survivors of acute radiation syndrome also have been shown to develop cardiovascular disease several years after exposure. Studies with survivors of the atomic bombs in Hiroshima and Nagasaki have shown there is a risk of developing cardiovascular disease [76; 85]. Mortality from myocardial infarction 40 years after the radiation exposure is significantly increased in these survivors [76; 85].

Since IR causes an increase in oxidative stress, antioxidants may provide protection and prevent cellular damage. A complex dietary supplement consisting of a wide range of antioxidant and anti-inflammatory compounds has prominently been shown to increase longevity, decrease markers of ageing and impart protection against oxidative stress and inflammation [86-88]. Development of radio-protective diets is a high priority for patients or individuals exposed to IR [88]. The dietary supplement was designed to ameliorate several processes including oxidative stress, inflammatory processes, insulin resistance and mitochondrial dysfunction. Criteria for selecting specific ingredients for the supplement were based on scientifically documented evidence of beneficial effects for one or more of the targets, oral administration and approved for human use [89]. In an age accelerated mouse model that received a WBD of 2 Gy the dietary supplement prevented the formation of chromosomal aberrations. γH2AX and 8-OHdG levels

were significantly reduced in groups that received the supplement when compared to irradiated groups, suggesting that the diet scavenged free radicals before they could cause damage [88]. A similar study investigated the effect of the diet on radiation induced apoptosis in an age accelerated mouse model. Lymphocytes exposed to 2 Gy γ radiation isolated from male mice that received the supplementary diet showed a decrease in amount of apoptotic cells when compared to cells from mice that did not receive the supplement. Interestingly, lymphocytes from female mice were highly radiation resistant compared to males and the supplement provided no additional benefits, suggesting that the effects of IR can depend on several factors including genotype and gender [89]. It is clear the supplementary diet reduces damage caused by IR induced oxidative stress, whether this supplement can provide protection specifically to the heart against IR remains to be seen.

The objectives of this study were to examine the effects of high dose whole body radiation on cardiac oxidative stress and correlate it to cell death. Also, to determine if a dietary supplement designed to offset oxidative stress and inflammation can alter radiation-induced cardiac tissue damage. A mouse model was used and were fed the supplement before and after a WBD of 5 Gy. Previous studies have shown the supplement provides protection against IR if fed before exposure [88; 89] and we were interested if it can also provide protection after radiation exposure. We were also interested in how long the supplement can protect after radiation. Specifically, our focus was on antioxidants and markers of apoptosis and autophagy to provided insight in the mechanism(s) of radiation induced cardiac damage and protection provided from the dietary supplement.

Materials and Methods

Animals

Eight week old male C57BL/6 were purchased from Jackson Laboratories and left for 7 days to recover from transport. Mice were individually housed in 27 x 12 x 15.5 cm cages containing woodchip bedding (Harlan Sani-Chips, 7090). A stainless steel hopper provided food *ad libitum* (Harlan Teklad 8640 22/5 rodent chow) and supported a water bottle. Mice were weighed weekly midway through the photoperiod. The housing room maintained a 12:12-h light:dark photoperiod at 22 ± 2°C. All protocols were approved by the Animal Research Ethics Board at McMaster University and carried out according to the Canadian Council on Animal Care regulations. Mice were placed in 5 groups, 5 mice per group, identified as:

1) Control
2) Supplement only
3) 5 Gy whole body dose (WBD)
4) Supplement + 5 Gy WBD + Supplement
5) 5 Gy WBD + Supplement

All supplement fed mice, except for the 5 Gy WBD + Supplement group, were fed the supplement for 30 days prior to irradiation to allow the compounds within the supplement to reach equilibrium at maximal physiological levels. The 5 Gy WBD + Supplement mice were only fed the supplement after irradiation until their respective time points. Mice were harvested at each of the following time points: 48 hours, 30 days and 120 days post irradiation. Mice were anesthetized with isoflurane and exsanguinated via cardiac puncture. Tissue harvesting followed cervical dislocation, which was performed post blood collection. Tissue collected included heart, liver, kidneys, adrenals, brain, thymus and lungs, which were flash frozen in liquid nitrogen.

Bone marrow and liver, kidneys, adrenals, brain, thymus and lungs remained at McMaster University for future analysis, and hearts were shipped to Lakehead University. Both 30 day and 120 day mice were tested in a novel object/place recognition and modified 8-arm radial maze for cognitive assessment, grip strength and balance tests. Identical tissue harvest as 48h mice followed immediately following completion of testing.

Dietary supplement

Dosages of each component were calculated based on amounts commonly prescribed to humans (Table 1). Values were adjusted for the difference in body size and then increased by a factor of 10 in consideration of the higher gram-specific metabolic rate (and faster nutrient utilization) of mice. Supplement was made for 45 mice for 30 days at a time. Bagels were cut into 1 cm x 1 cm and the crust was removed. All dry components were mixed together before addition of oils. Oils were added and mixed into dry components and dH_2O was added slowly to avoid clumping; 2 mL of this mixture was enough for 6 bagel pieces. Bagel pieces were pre-soaked with 100 mL of dH_2O before addition of supplement. 350 µL of supplement was added to each bagel piece allowed to dry overnight in a fumehood. Dry bagels were sealed in a air free bag and stored in a cool, dark area. Each mouse received one piece of dried bagel daily either with or without the supplement, depending on the treatment group. The mice were given the bagel pieces midway through the photoperiod. Amount of bagel eaten was measured the following day.

Table 1. Components of a Complex Dietary Supplement and Associated Cellular Targets

Component	Target
Vitamin B1	Insulin sensitivity, anti-inflammatory
Vitamin B3	Insulin sensitivity, anti-inflammatory
Vitamin B6	Insulin sensitivity, anti-inflammatory, scavenge O_2^-
Vitamin B12	Insulin sensitivity, anti-inflammatory
Vitamin C	Antioxidant in cytosol, scavenges O_2^-, H_2O_2
Vitamin D	Antioxidant in lipid membrane
Vitamin E	Antioxidant in lipid membrane, scavenges O_2^-, H_2O_2
Acetyl L-carnitine	Mitochondrial support, antioxidant in mitochondria, insulin sensitivity
Alpha lipoic acid	Mitochondrial support, antioxidant in mitochondria, insulin sensitivity
Acetylsalicylic acid	Anti-inflammatory, scavenges NO^-
Beta carotene	Antioxidant in lipid membrane, scavenges O_2^-, H_2O_2
Bioflavonoids	Antioxidant in cytosol and nucleus, scavenge OH^-, O_2^-, metal chelator
Chromium	Insulin sensitivity, scavenges H_2O_2
CoEnzyme Q10	Mitochondrial support, antioxidant in mitochondria
Curcumin	Anti-inflammatory
Folic acid	Antioxidant, maintains glutathione levels, endothelial support
Garlic	Antioxidant in lipid membrane, scavenges O_2^-, H_2O_2
Ginger	Antioxidant in cytosol, scavenges OH^-, O_2^-, $ONOO^-$
Ginkgo biloba	Antioxidant in cytosol, scavenges NO^-
Ginseng	Antioxidant in cytosol and nucleus, scavenges OH^-, O_2^-, $ONOO^-$
Green tea extract	Antioxidant in cytosol, scavenges H_2O_2, OH^-
L-glutathione	Enzymatic antioxidant support, antioxidant in cytosol
Magnesium	Insulin sensitivity, cellular support
Melatonin	Antioxidant in cytosol and nucleus, scavenges OH^-, H_2O_2, O^-, NO, $ONOO^-$
N-acetyl cysteine	Mitochondrial support, antioxidant in mitochondria
Potassium	Insulin sensitivity, cellular support
Quercitin	Anti-inflammatory
Rutin	Antioxidant in lipid membrane, scavenge OH^-, O_2^-, metal chelator
Selenium	Scavenges H_2O_2, enzymatic antioxidant support, insulin sensitivity
Omega 3/6/9	Anti-inflammatory

Irradiation

During irradiation, mice were placed in a polyvinyl chloride (PVC) tube (5 x 12.5 cm) with PVC mesh end caps. To reduce stress, mice were habituated to the restraint devices 30 days

prior to irradiation. Each mouse was given a 5Gy whole-body dose of gamma radiation from a cesium-137 source (Taylor Cesium Source). After irradiation, each mouse was returned to its housing cage. Non-irradiated sham control mice were otherwise exposed to exactly the same conditions as irradiated mice.

Total protein assay

Frozen hearts were washed in cold PBS on ice. Atria was removed and hearts were weighed. ~50 mg of tissue was used to collect protein samples. Hearts were lysed using Pathscan buffer (25mM Tris, 150mM NaCl, 1mM EDTA and 2mL Triton-X) containing sodium fluoride, sodium orthovanadate and protease inhibitor cocktail (Sigma-Aldrich, St. Louis, MO) and kept on ice. Upon addition of ice-cold lysis buffer tissue samples were placed in a Tissue Lyser (Qiagen, Hilden, Germany) for 3 minutes at 30.0 frequency. Lysates were then centrifuged for 10 minutes at 8000 x g. Supernatant was collected and stored at - 80 °C. The amount of protein was measured via a Lowry-based protein assay. Using the *DC* Protein Assay (Bio-Rad, Hercules, CA) 'microplate' method, which requires 5 µL of protein lysate, full-strength and 1/50-strength samples were measured alongside a range of bovine serum albumin (BSA; Fisher Scientific, Hampton, NH) standard concentrations from 0.5-4 mg/mL. Following a 15-minute colour-development period, standard and sample absorbance was measured spectrophotometrically at a wavelength of 750 nm using a PowerWave XS Microplate Spectrophotometer (BioTek, Winooski, VT). Microsoft Excel was used to create a standard curve from the BSA standards, and the equation of the line of best fit was used to calculate the sample protein concentrations. The amount of lysate needed to equal 50 µg/well was calculated.

Sodium dodecyl sulfate-polyacrylamide gel electrophoresis

10 µL of 2x SDS sample loading buffer containing ß-mercaptoethanol (Sigma-Aldrich) was added to the 50 µg sample lysates and dH_2O was used to give a total of 20 µL per sample. Samples were then placed in a 95 °C heat block for 5 minutes and then on ice for an additional 5 minutes. Boiled lysates were quick-spun and loaded into 15 % sodium dodecyl sulfate-polyacrylamide gels, 20 µL per well (Bio-Rad Mini PROTEAN 3 Cell System apparatus was used). Precision Plus Kaleidoscope (Bio-Rad) protein standard was loaded alongside the sample wells. Empty wells were partially filled with 2x SDS loading buffer to ensure even migration across the gel. The electrophoresis apparatus was filled with 1x Running buffer (standard 1x Running buffer was prepared from a 10x stock). Gels were run at 200 V for 1 hour or until the appropriate kDa range had migrated to near the centre of the gel, as indicated by reference to the protein standard indicator.

Electrophoretic transfer

Immediately upon completion of sodium dodecyl sulfate-polyacrylamide gel electrophoresis (to prevent protein band dissociation), gels were removed from the electrophoresis assembly, their edges trimmed and orientation marks added (i.e. diagonal edge cut at top-left), and then were soaked in 1x Transfer buffer for ~10 minutes for equilibration (standard 1x transfer buffer was prepared from a 10x stock). Nitrocellulose transfer membrane (GE Healthcare Life Sciences, Piscataway, NJ) was soaked in 1x transfer buffer for at least 15 minutes. The transfer cassette was assembled as per the manufacturer's instructions, filled with 1x Transfer buffer, and the transfer was performed at 30 V overnight at 4° with a dH_2O ice block.

Protein immunoblot and antibodies

Following electrophoretic transfer membranes were stained with Ponceau S solution (Bio-Rad) for 10 minutes to verify transfer efficiency. Excess Ponceau S stain was removed by dH_2O. The membranes were then soaked in Tris-buffered saline containing 0.1 % Tween-20 detergent (Sigma-Aldrich) (TBST) for 15 minutes to remove Ponceau S, followed by 3x 5 minutes to wash and equilibrate them before being blocked with 5 % milk solution (Oxoid, Nepean ON) for 1 hour 30 minutes at room temperature. Blocked membranes were incubated with primary antibody in 5 % milk on a rocker (Boekel Scientific, Feasterville, PA) overnight at 4 °C. β-actin (1:500), Bax (1:100) and Bcl 2 (1:100) antibodies were purchased from Santa Cruz Biothechnology, Santa Cruz, CA. Caspase 3 (1:500) and LC3B (1:500) antibodies from Cell Signaling Technology, Danvers, MA. MN-SOD (1:1000) antibody was purchased from Millipore (Merck KGaA, Darmstadt, Germany) and Catalase (1:5000) antibody from Sigma-Aldrich. Membranes were then washed in TBST 3x 10 minutes. Following this step, 1:1000 HRP-conjugated goat anti-rabbit (R&D Systems, Minneapolis, MN) or anti-mouse (Pierce Antibody Products, Rockford, IL) IgG secondary antibodies in 5 % milk solution were used to probe the membrane on a rocker for 2 hours at room temperature. Following this step, membranes were again washed with TBST 3x 10 minutes.

Chemiluminescent imaging and densitometry

Standard Enhanced chemiluminescence (ECL) was performed to detect protein-banding patterns on the immunoblots by virtue of the HRP-conjugated secondary antibodies using luminol and coumeric acid (Sigma-Aldrich). Chemiluminescent immunoblots were detected via 5-minute High-Sensitivity Chemiluminescent exposures using a Chemidoc XRS imager (Bio-

Rad) supported by Quantity One software for Windows (Bio-Rad). Brief Epi-White exposures were also collected in order to interpret chemiluminescent banding patterns with the membranes' visible protein ladders. Blots were analyzed via densitometry using the Quanity One software, with reference to β-actin control.

Statistics

Data were presented as mean ± standard error of the mean (SEM), and all data presented here represents n = 5 independent experiments. Statistical analyses were performed using GraphPad Prism software. One-way ANOVA with post hoc Tukey's test were utilized when possible with $p < 0.05$ considered significant. Asterisks are used herein to denote significance according to the following scheme: * = $p < 0.05$; ** = $p < 0.01$; *** = $p < 0.001$.

Results

Protein levels of Catalase After Radiation and Supplement Treatment

48 hours after a 5Gy WBD of radiation protein concentration of catalase did not change (Figure 2). Supplement treatment alone also did not change catalase levels when compared to control (Figure 2). When mice were pretreated for 30 days before irradiation and sacrificed 48 hours after catalase increased when compared to control and 5Gy (Figure 2). When mice were pretreated for 30 days before and treated once 24 hours after irradiation with supplement catalase increased when compared to control and 5Gy (Figure 2). 30 days after radiation treatment protein concentration of catalase did not change (Figure 3). Supplement treatment alone did not change catalase levels when compared to control (Figure 3). When mice were pretreated for 30 days before irradiation and sacrificed 30 days after or pretreated for 30 days before and 30 days

after irradiation catalase did not change when compared to radiation treatment (Figure 3). 120 days after radiation treatment protein concentration of catalase (Figure 4) increased. Supplement treatment alone did not change catalase levels when compared to control (Figure 4). When mice were pretreated for 30 days before irradiation and sacrificed 120 days after or pretreated for 30 days before and 120 days after irradiation catalase did not change when compared to radiation treatment (Figure 4). Catalase levels were increased in hearts of 30 day pre and 120 day post treated mice when compared to control (Figure 4).

Protein levels of Mn-SOD After Radiation and Supplement Treatment

48 hours after a 5Gy WBD of radiation protein concentration of Mn-SOD decreased when compared to control (Figure 5). Supplement treatment alone did not change Mn-SOD levels when compared to control (Figure 5). When mice were pretreated for 30 days before irradiation and sacrificed 48 hours after Mn-SOD increased when compared to 5Gy and was unchanged when compared to control (Figure 5). When mice were pretreated for 30 days before and treated once 24 hours after irradiation with supplement Mn-SOD increased when compared to 5Gy and was unchanged when compared to control (Figure 5). 30 days after radiation treatment protein concentration of Mn-SOD decreased when compared to control (Figure 6). Supplement treatment alone did not change Mn-SOD levels when compared to control (Figure 6). When mice were pretreated for 30 days before irradiation and sacrificed 30 days after or pretreated for 30 days before and 30 days after irradiation Mn-SOD did not change when compared to radiation treatment (Figure 6). Mn-SOD levels were decreased in hearts of 30 day pre and post treated mice when compared to control (Figure 6). 120 days after radiation treatment protein concentration of Mn-SOD did not change when compared to control (Figure 7).

Supplement treatment alone did not change Mn-SOD levels when compared to control (Figure 7). When mice were pretreated for 30 days before irradiation and sacrificed 120 days after or pretreated for 30 days before and 120 days after irradiation Mn-SOD did not change when compared to radiation treatment (Figure 7).

Protein levels of Markers of Apoptosis After Radiation and Supplement Treatment

Pro-caspase 3 and Bax:Bcl_2 ratio were used as indicators of apoptosis. 48 hours after a 5Gy WBD of radiation protein concentration of pro-caspase 3 and Bax:Bcl_2 ratio increased when compared to control (Figure 8 & 11). Supplement treatment alone increased both pro-caspase 3 and Bax:Bcl_2 ratio when compared to control (Figure 8 & 11). When mice were pretreated for 30 days before irradiation and sacrificed 48 hours after or pretreated for 30 days before and treated once 24 hours after irradiation with supplement pro-caspase 3 and Bax:Bcl_2 ratio decreased when compared to radiation treatment and did not change when compared to control (Figure 8 & 11). 30 days after radiation treatment protein concentration of pro-caspase 3 increased (Figure 9) but Bax:Bcl_2 ratio did not change when compared to control (Figure 12). Supplement treatment alone did not change apoptosis protein levels when compared to control (Figure 9 & 12). When mice were pretreated for 30 days before irradiation and sacrificed 30 days after pro-caspase 3 did not change (Figure 9) while Bax:Bcl_2 ratio increased when compared to 5Gy radiation treated and control mice (Figure 12). Hearts from mice treated with supplement 30 days before and after irradiation showed decreased protein levels of pro-caspase 3 (Figure 9) and increased Bax:Bcl_2 ratio when compared to radiation treatment (Figure 12). Pro-caspase 3 did not change (Figure 9) while Bax:Bcl_2 ratio increased when compared to control mice (Figure 12). 120 days after radiation treatment protein concentration of pro-caspase 3 increased (Figure 10) while Bax:Bcl_2

ratio did not change when compared to control (Figure 13). Supplement treatment alone did not change protein levels of pro-caspase 3 when compared to control (Figure 10) but did decrease Bax:Bcl_2 ratio (Figure 13). When mice were pretreated for 30 days before irradiation and sacrificed 120 days after pro-caspase 3 did not change (Figure 10) while Bax:Bcl_2 ratio decreased when compared to radiation treated mice (Figure 13). When compared to control pro-caspase 3 was increased (Figure 10) and Bax:Bcl_2 ratio was decreased (Figure 13). When mice were pretreated for 30 days before and 120 days after irradiation with supplement pro-caspase 3 decreased (Figure 10) while Bax:Bcl_2 ratio did not change when compared to 5Gy radiation treated mice (Figure 13). There was no change in protein levels of pro-caspase 3 or Bax:Bcl_2 when compared to control (Figure 10 & 13).

Protein levels of Autophagy Marker After Radiation and Supplement Treatment

LC3bII:I ratio was used as an indicator of autophagy. 48 hours after a 5Gy WBD of radiation protein concentration of LC3bII:I ratio did not change when compared to control (Figure 14). Supplement treatment alone did not change LC3bII:I ratio when compared to control (Figure 14). When mice were pretreated for 30 days before irradiation and sacrificed 48 hours after or pretreated for 30 days before and treated once with supplement 24 hours after irradiation LC3bII:I ratio increased when compared to 5Gy treated mice and control (Figure 14). There was no change in LC3bII:I ratio after radiation alone or any of the supplement treated mice in the 30 day treatment groups when compared to control (Figure 15). 120 days after radiation treatment LC3bII:I ratio increased when compared to control (Figure 16). Supplement treatment alone did not change LC3bII:I ratio when compared to control (Figure 16). When mice were pretreated for 30 days before irradiation and sacrificed 120 days after LC3bII:I ratio did not change when

compared to radiation treated mice and was increased when compared to control (Figure 16). When mice were pretreated for 30 days before and 120 days after irradiation LC3bII:I ratio decreased compared to radiation treated mice to near control levels (Figure 16).

Conclusion

The heart is particularly susceptible to radiation induced oxidative stress. A dietary supplement was able to provide, in some cases, protection to the heart with regard to protein expression of antioxidants and markers of apoptosis and autophagy. This protection and extent of radiation induced damage appears to be dependent on time.

Figures

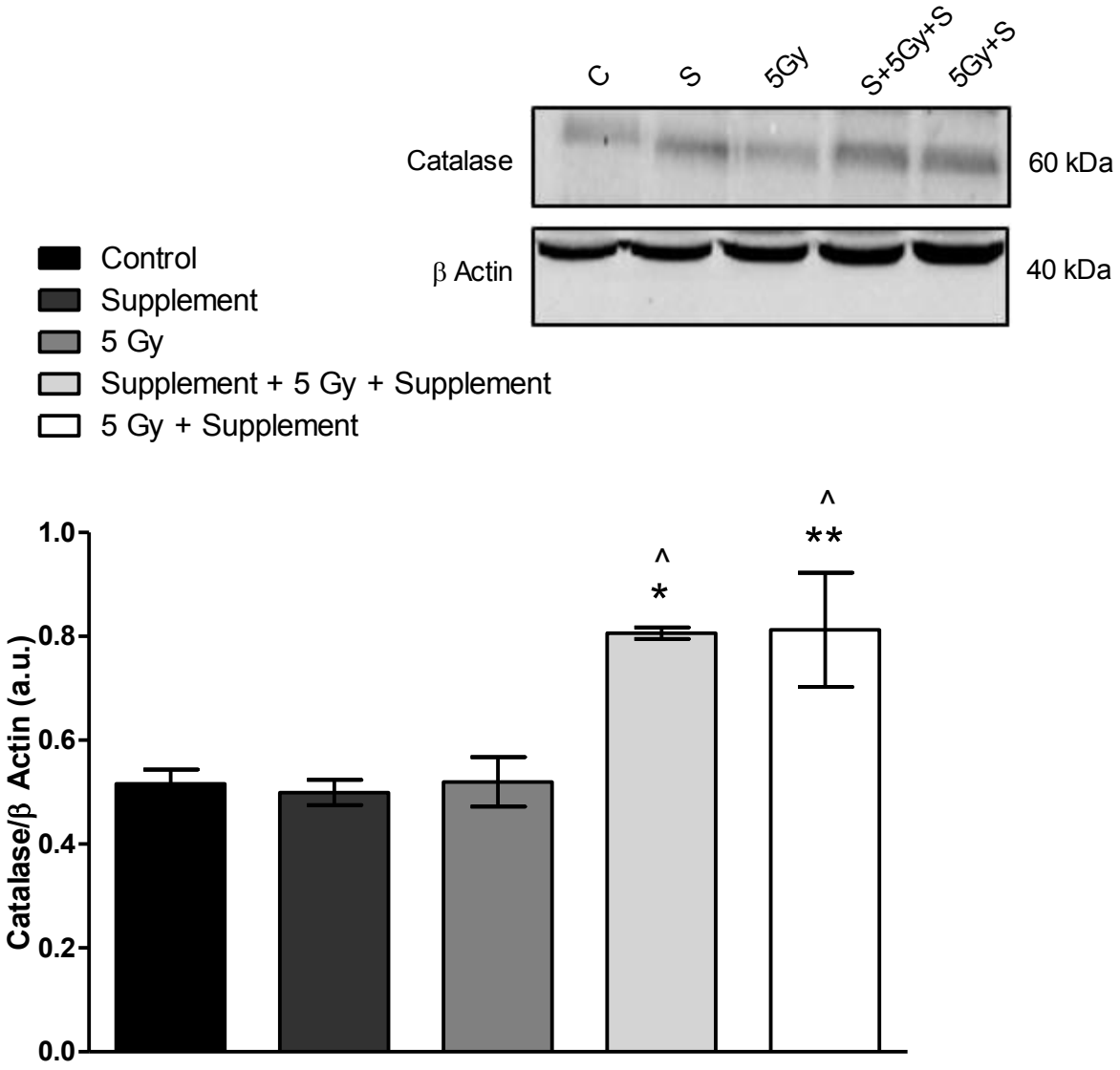

Figure 2. The effect of a dietary supplement on catalase protein expression in the heart at 48 hours after 5 Gy whole body radiation. Protein concentration of catalase was assessed via immunoblotting, where C = control, S = supplement alone, 5Gy = single whole body dose of 5 Gy γ radiation, S+5Gy+S = supplement for 30 days prior radiation and 48 hours after, 5Gy+S = supplement 48 hours after radiation. Bars represent mean ± SEM where n = 5 (** = $p < 0.01$ versus control; * = $p < 0.05$ versus control; ^ = $p < 0.05$ versus 5 Gy).

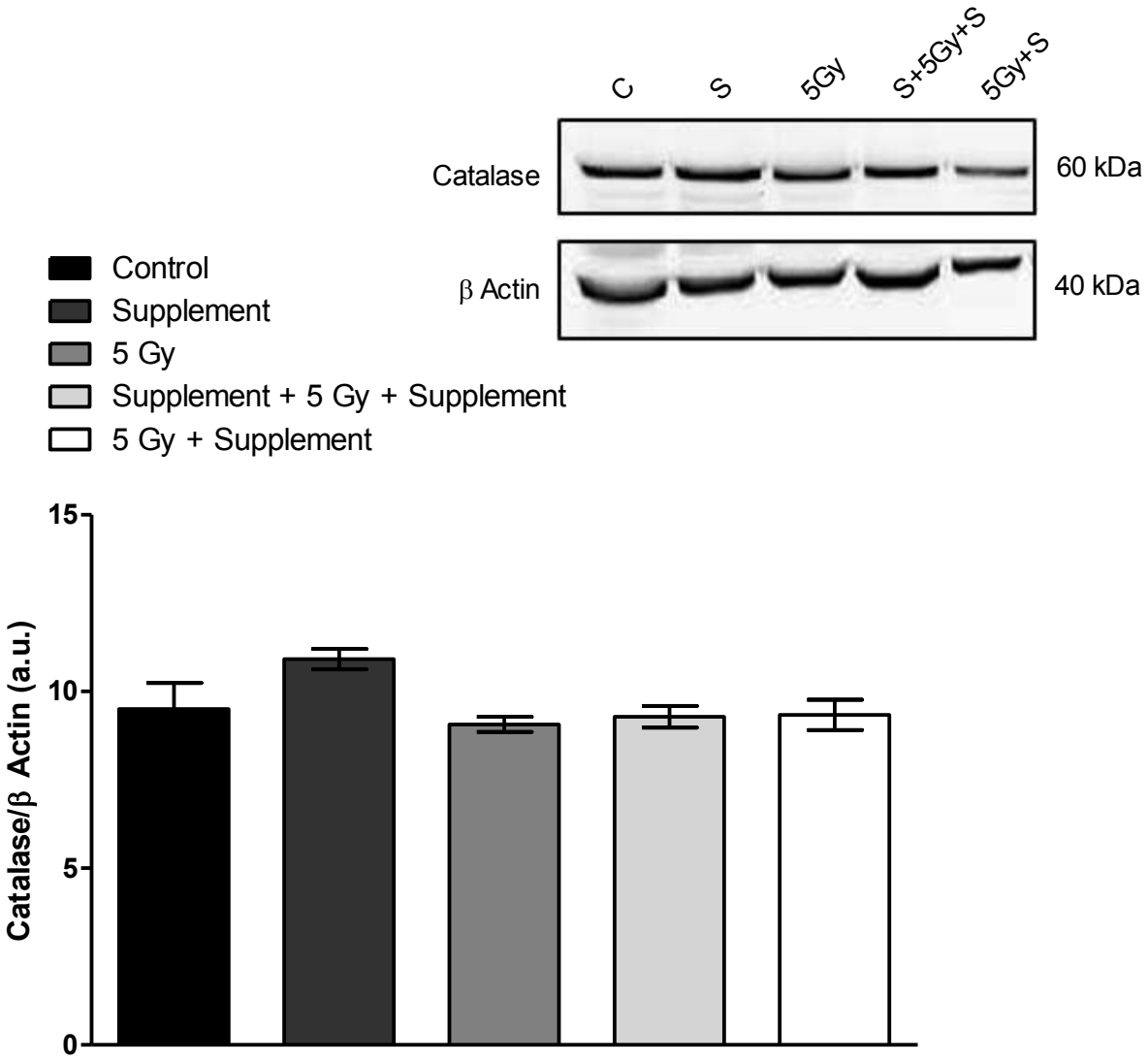

Figure 3. The effect of a dietary supplement on catalase protein expression in the heart at 30 days after 5 Gy whole body radiation. Protein concentration of catalase was assessed via immunoblotting, where C = control, S = supplement alone, 5Gy = single whole body dose of 5 Gy γ radiation, S+5Gy+S = supplement for 30 days prior radiation and 30 days after, 5Gy+S = supplement 30 days after radiation. Bars represent mean ± SEM where $n = 5$.

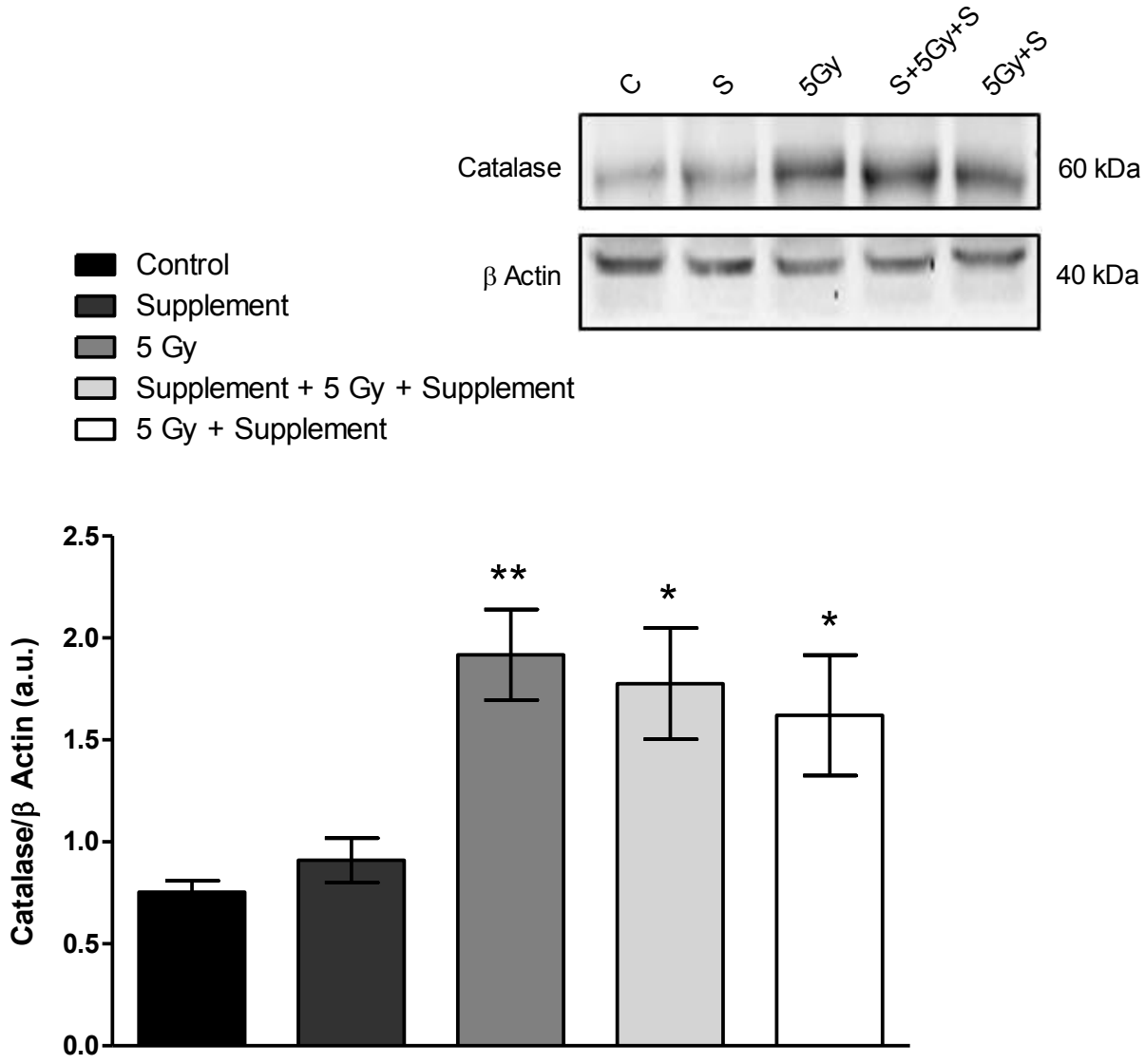

Figure 4. The effect of a dietary supplement on catalase protein expression in the heart at 120 days after 5 Gy whole body radiation. Protein concentration of catalase was assessed via immunoblotting, where C = control, S = supplement alone, 5Gy = single whole body dose of 5 Gy γ radiation, S+5Gy+S = supplement for 30 days prior radiation and 120 days after, 5Gy+S = supplement 120 days after radiation. Bars represent mean ± SEM where $n = 5$ (** = $p < 0.01$ versus control; * = $p < 0.05$ versus control).

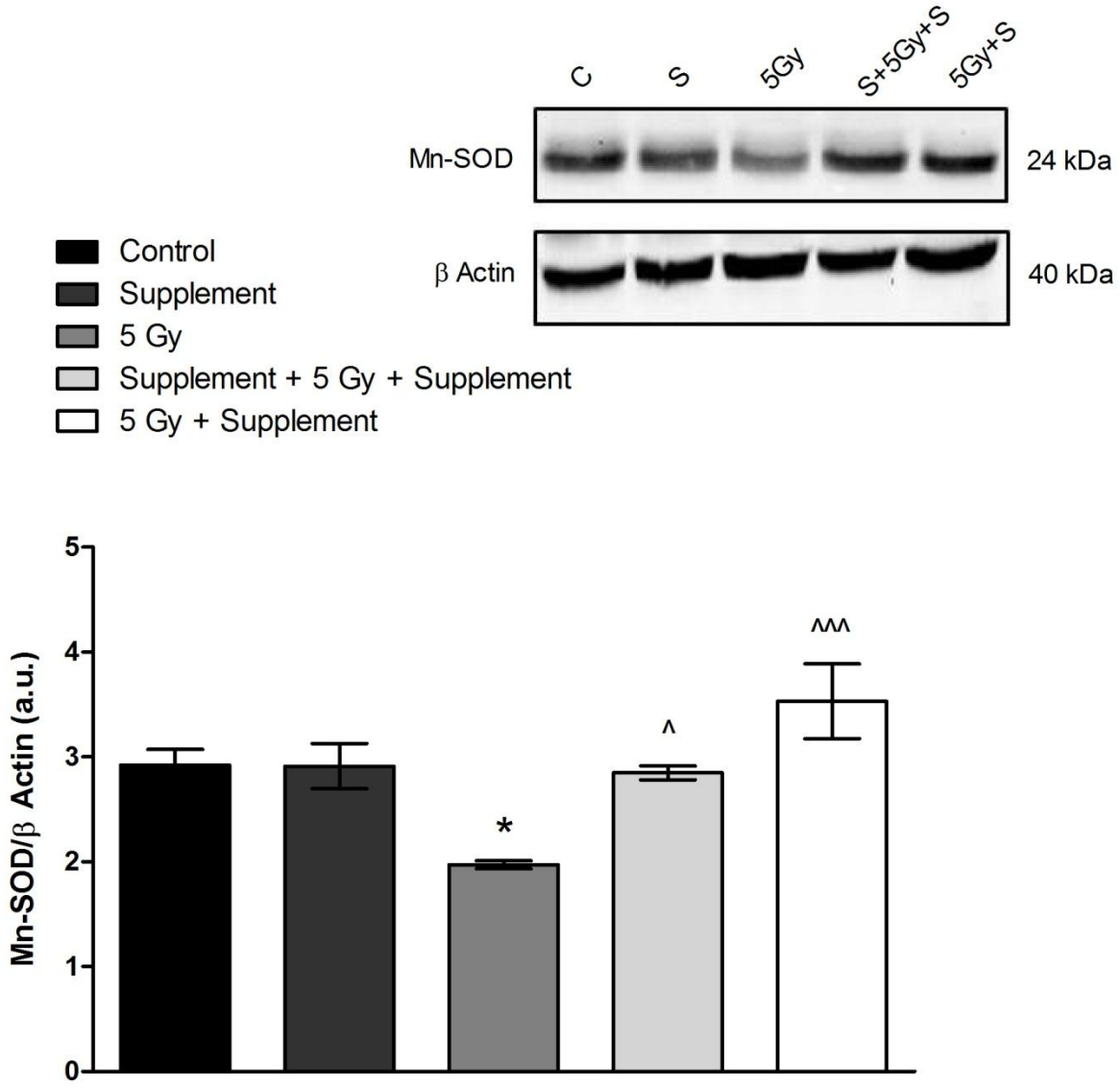

Figure 5. The effect of a dietary supplement on Mn-SOD protein expression in the heart at 48 hours after 5 Gy whole body radiation. Protein concentration of Mn-SOD was assessed via immunoblotting, where C = control, S = supplement alone, 5Gy = single whole body dose of 5 Gy γ radiation, S+5Gy+S = supplement for 30 days prior radiation and 48 hours after, 5Gy+S = supplement 48 hours after radiation. Bars represent mean ± SEM where n = 5 (* = $p < 0.05$ versus control; ^^^ = $p < 0.001$ versus 5 Gy; ^ = $p < 0.05$ versus 5 Gy).

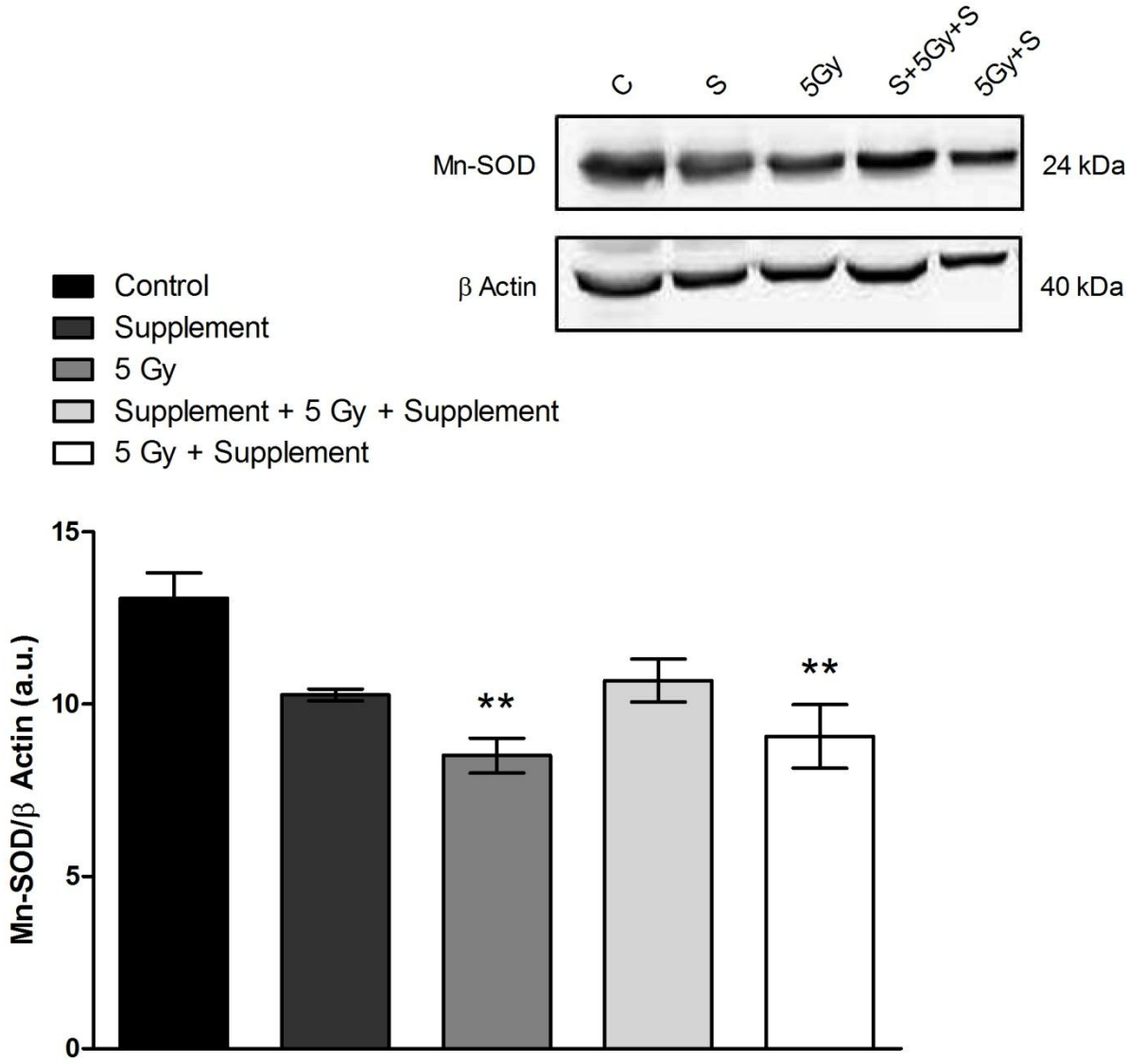

Figure 6. The effect of a dietary supplement on Mn-SOD protein expression in the heart at 30 days after 5 Gy whole body radiation. Protein concentration of Mn-SOD was assessed via immunoblotting, where C = control, S = supplement alone, 5Gy = single whole body dose of 5 Gy γ radiation, S+5Gy+S = supplement for 30 days prior radiation and 30 days after, 5Gy+S = supplement 30 days after radiation. Bars represent mean ± SEM where n = 5 (** = $p < 0.01$ versus control).

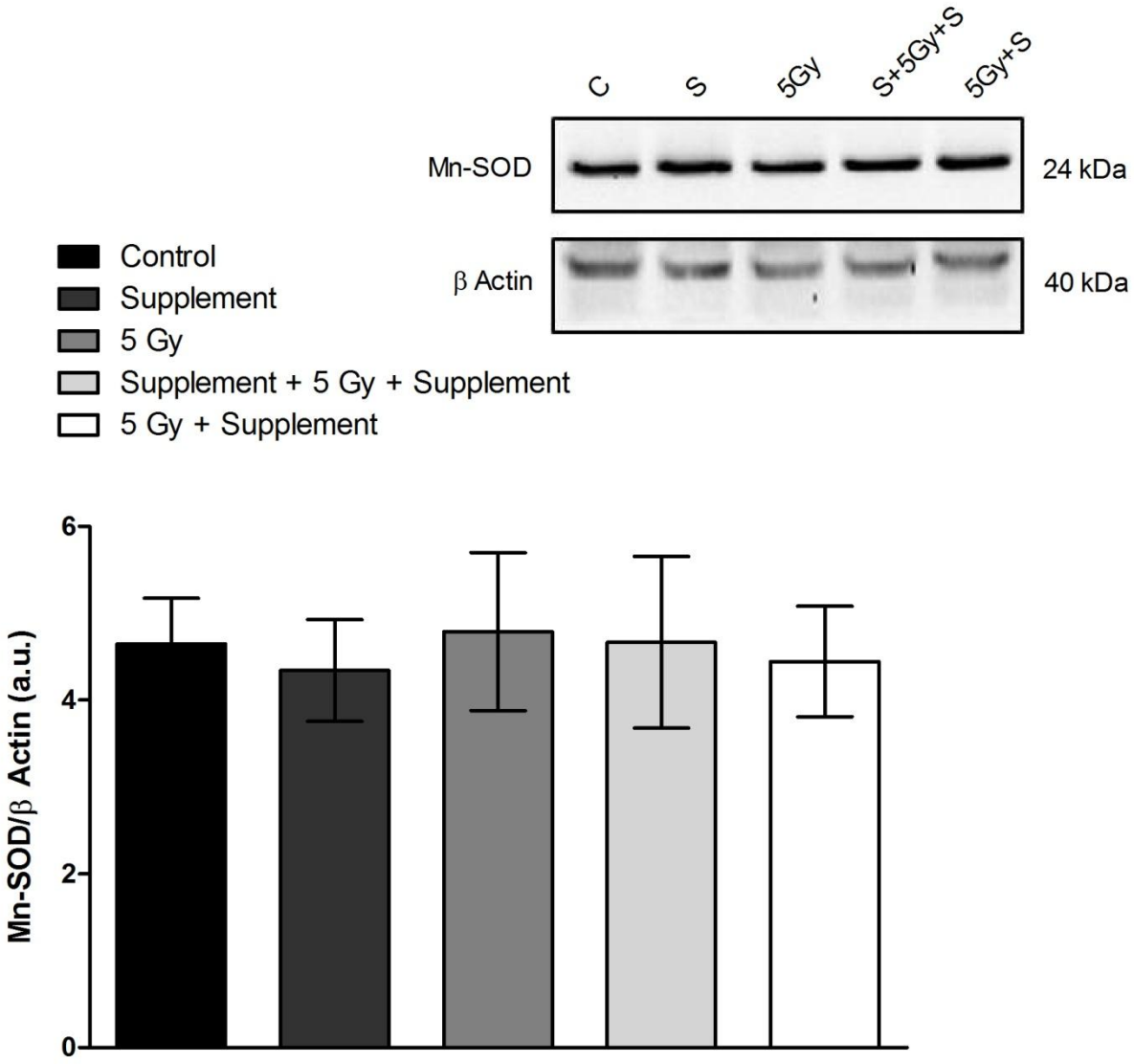

Figure 7. The effect of a dietary supplement on Mn-SOD protein expression in the heart at 120 days after 5 Gy whole body radiation. Protein concentration of Mn-SOD was assessed via immunoblotting, where C = control, S = supplement alone, 5Gy = single whole body dose of 5 Gy γ radiation, S+5Gy+S = supplement for 30 days prior radiation and 120 days after, 5Gy+S = supplement 120 days after radiation. Bars represent mean ± SEM where *n* = 5.

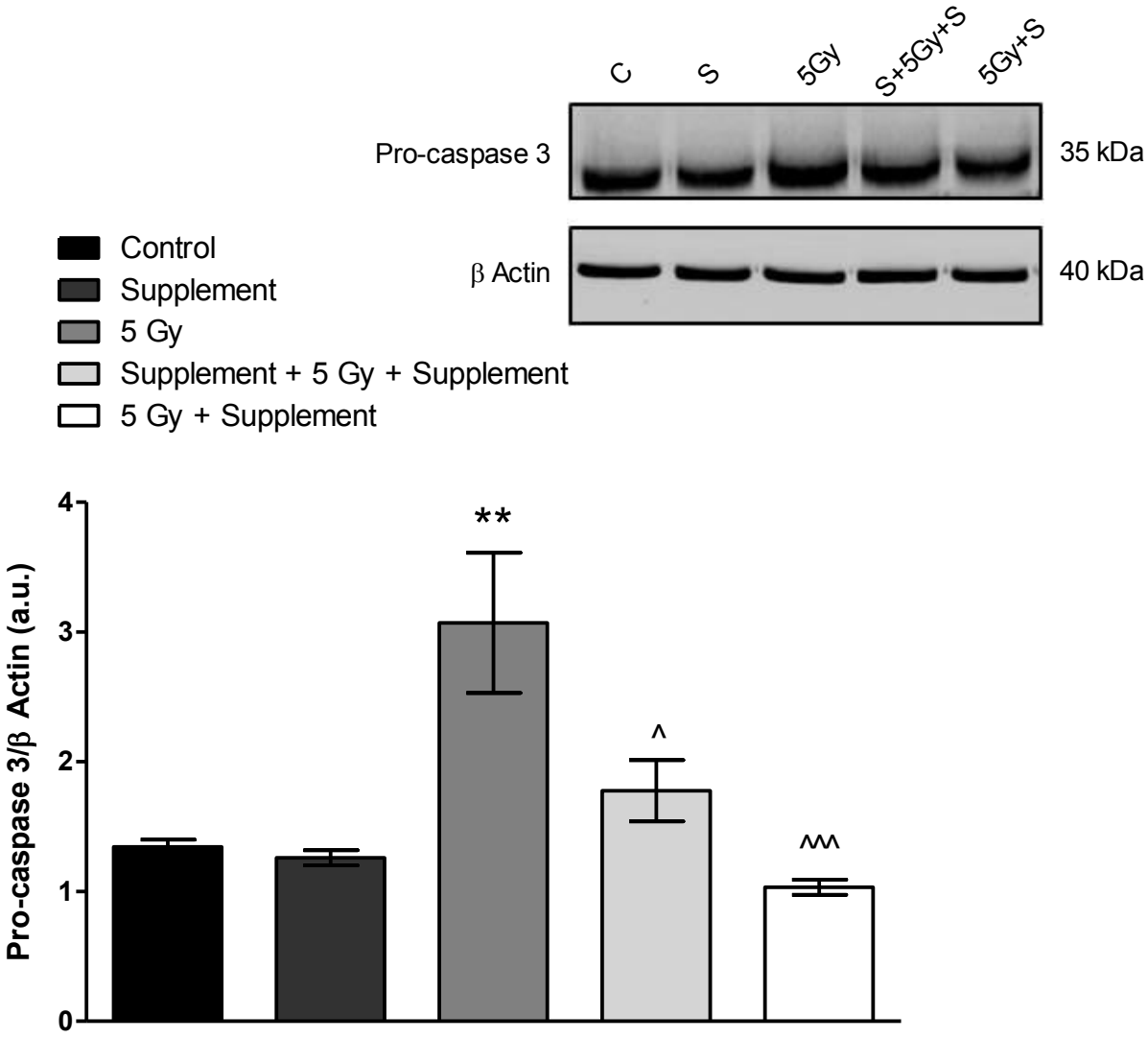

Figure 8. The effect of a dietary supplement on Pro-caspase 3 protein expression in the heart at 48 hours after 5 Gy whole body radiation. Protein concentration of pro-caspase 3 was assessed via immunoblotting, where C = control, S = supplement alone, 5Gy = single whole body dose of 5 Gy γ radiation, S+5Gy+S = supplement for 30 days prior radiation and 48 hours after, 5Gy+S = supplement 48 hours after radiation. Bars represent mean ± SEM where $n = 5$ (** = $p < 0.01$ versus control; ^^^ = $p < 0.001$ versus 5 Gy; ^ = $p < 0.05$ versus 5 Gy).

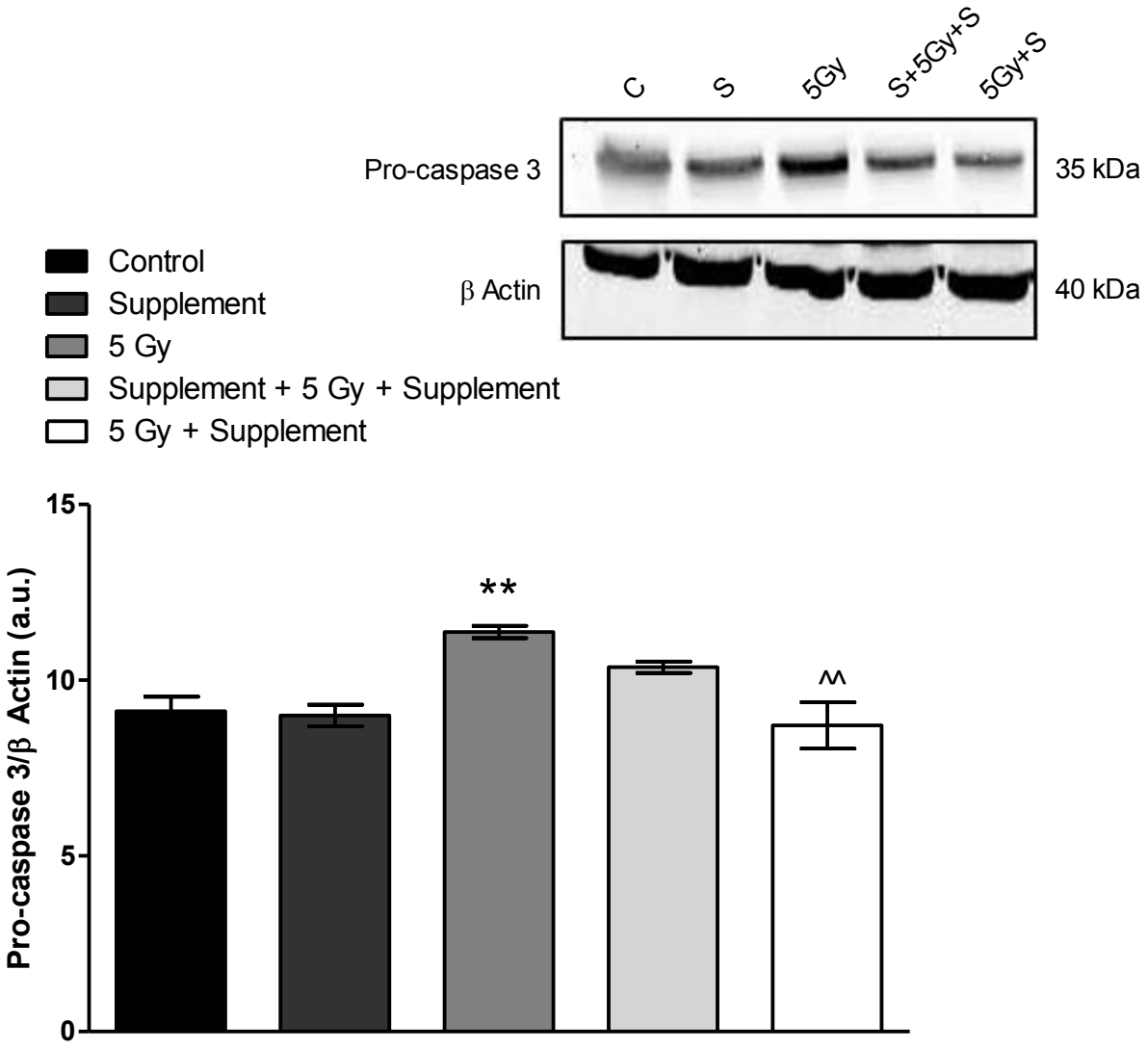

Figure 9. The effect of a dietary supplement on Pro-caspase 3 protein expression in the heart at 30 days after 5 Gy whole body radiation. Protein concentration of pro-caspase 3 was assessed via immunoblotting, where C = control, S = supplement alone, 5Gy = single whole body dose of 5 Gy γ radiation, S+5Gy+S = supplement for 30 days prior radiation and 30 days after, 5Gy+S = supplement 30 days after radiation. Bars represent mean ± SEM where $n = 5$ (** = $p < 0.01$ versus control; ^^ = $p < 0.01$ versus 5 Gy).

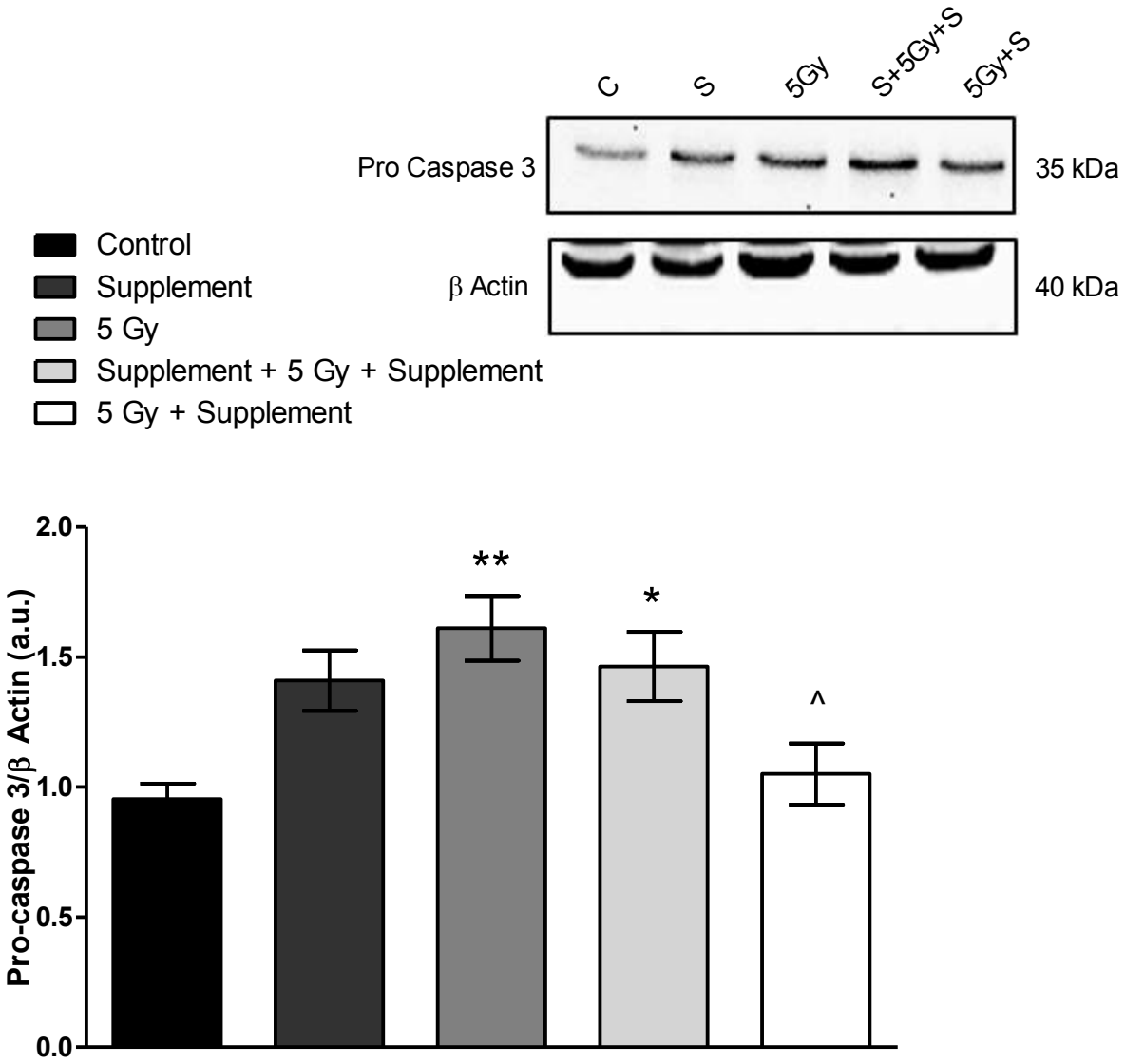

Figure 10. The effect of a dietary supplement on Pro-caspase 3 protein expression in the heart at 120 days after 5 Gy whole body radiation. Protein concentration of pro-caspase 3 was assessed via immunoblotting, where C = control, S = supplement alone, 5Gy = single whole body dose of 5 Gy γ radiation, S+5Gy+S = supplement for 30 days prior radiation and 120 days after, 5Gy+S = supplement 120 days after radiation. Bars represent mean ± SEM where n = 5 (** = $p < 0.01$ versus control; * = $p < 0.05$ versus control; ^ = $p < 0.05$ versus 5 Gy).

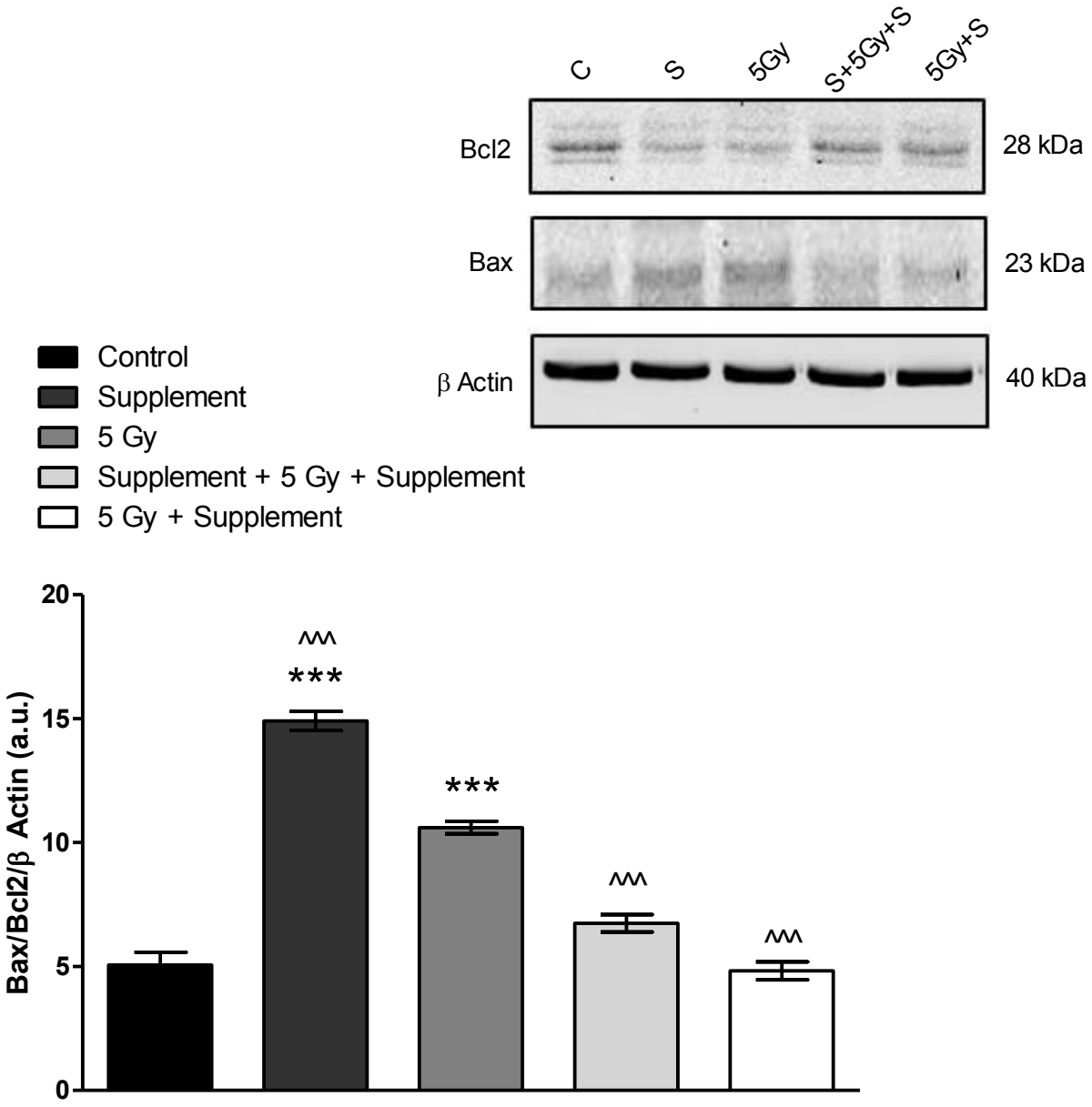

Figure 11. The effect of a dietary supplement on Bax/Bcl_2 ratio protein expression in the heart at 48 hours after 5 Gy whole body radiation. Protein concentration of Bax/Bcl_2 ratio was assessed via immunoblotting, where C = control, S = supplement alone, 5Gy = single whole body dose of 5 Gy γ radiation, S+5Gy+S = supplement for 30 days prior radiation and 48 hours after, 5Gy+S = supplement 48 hours after radiation. Bars represent mean ± SEM where n = 5 (*** = $p < 0.001$ versus control; ^^^ = $p < 0.001$ versus 5 Gy).

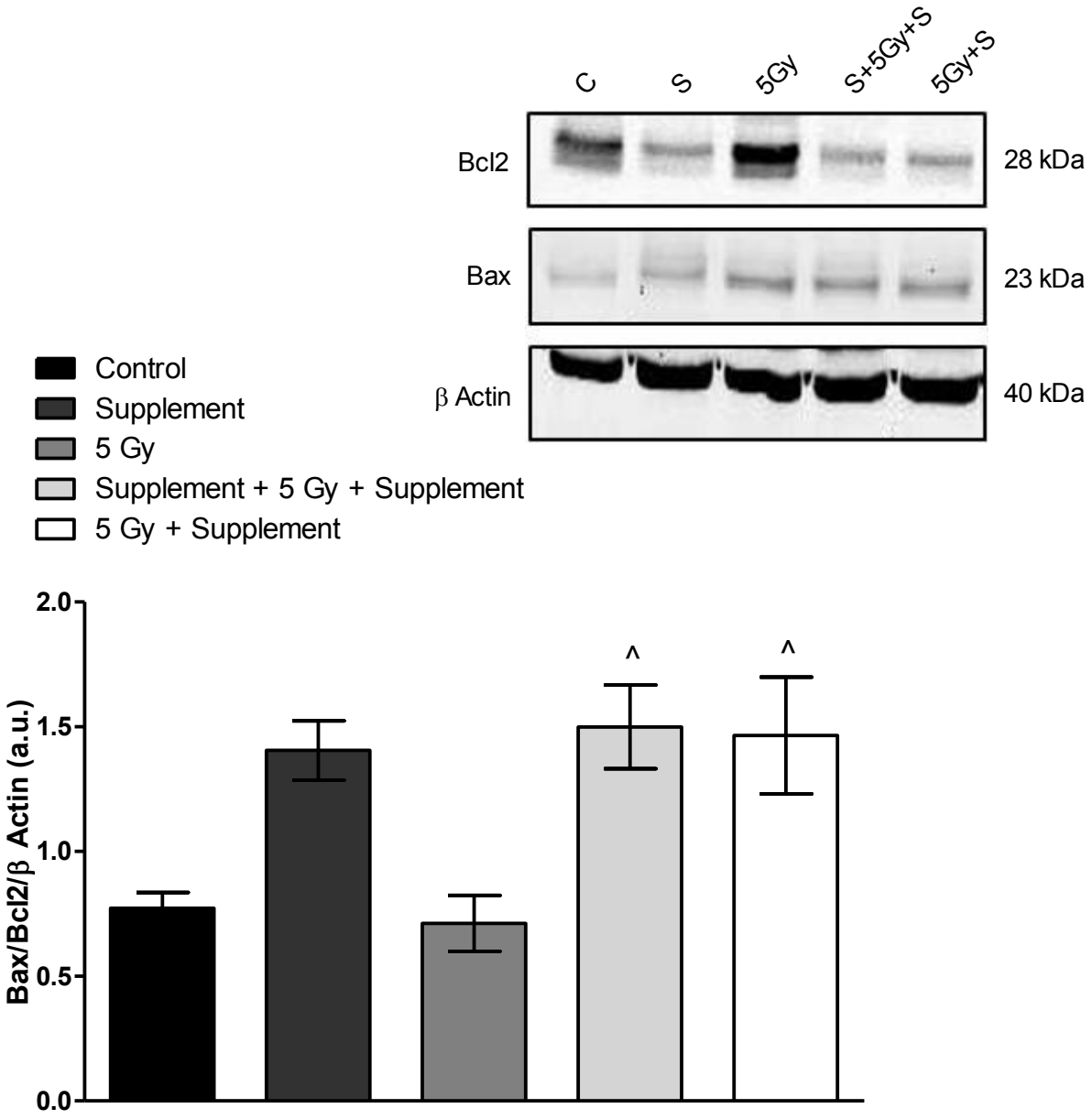

Figure 13. The effect of a dietary supplement on Bax/Bcl_2 ratio protein expression in the heart at 30 days after 5 Gy whole body radiation. Protein concentration of Bax/Bcl_2 ratio was assessed via immunoblotting, where C = control, S = supplement alone, 5Gy = single whole body dose of 5 Gy γ radiation, S+5Gy+S = supplement for 30 days prior radiation and 30 days after, 5Gy+S = supplement 30 days after radiation. Bars represent mean ± SEM where $n = 5$ (^^ = $p < 0.01$ versus 5 Gy).

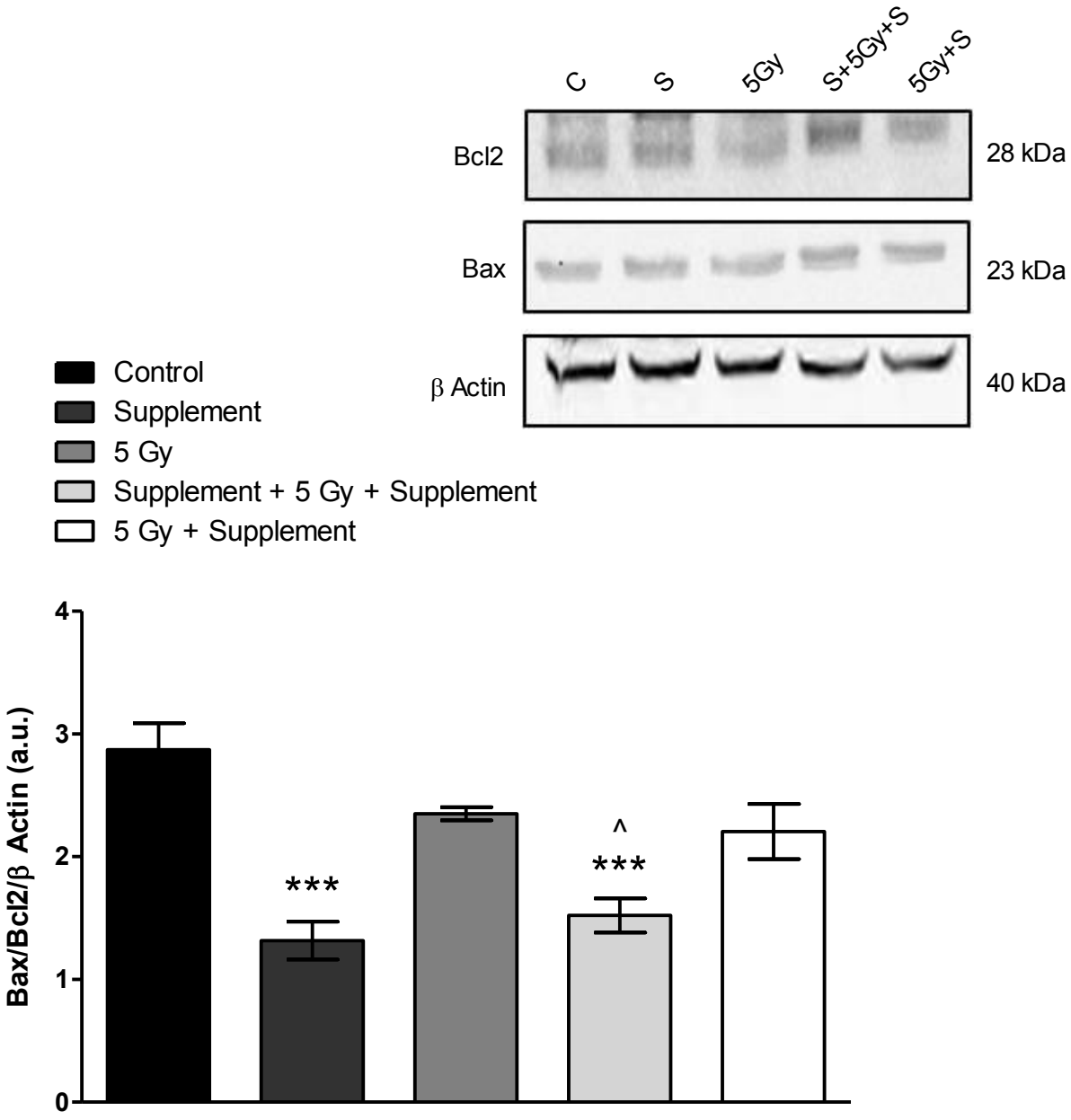

Figure 15. The effect of a dietary supplement on Bax/Bcl_2 ratio protein expression in the heart at 120 days after 5 Gy whole body radiation. Protein concentration of Bax/Bcl_2 ratio was assessed via immunoblotting, where C = control, S = supplement alone, 5Gy = single whole body dose of 5 Gy γ radiation, S+5Gy+S = supplement for 30 days prior radiation and 120 days after, 5Gy+S = supplement 120 days after radiation. Bars represent mean ± SEM where n = 5 (*** = $p < 0.001$ versus control; ^ = $p < 0.05$ versus 5 Gy).

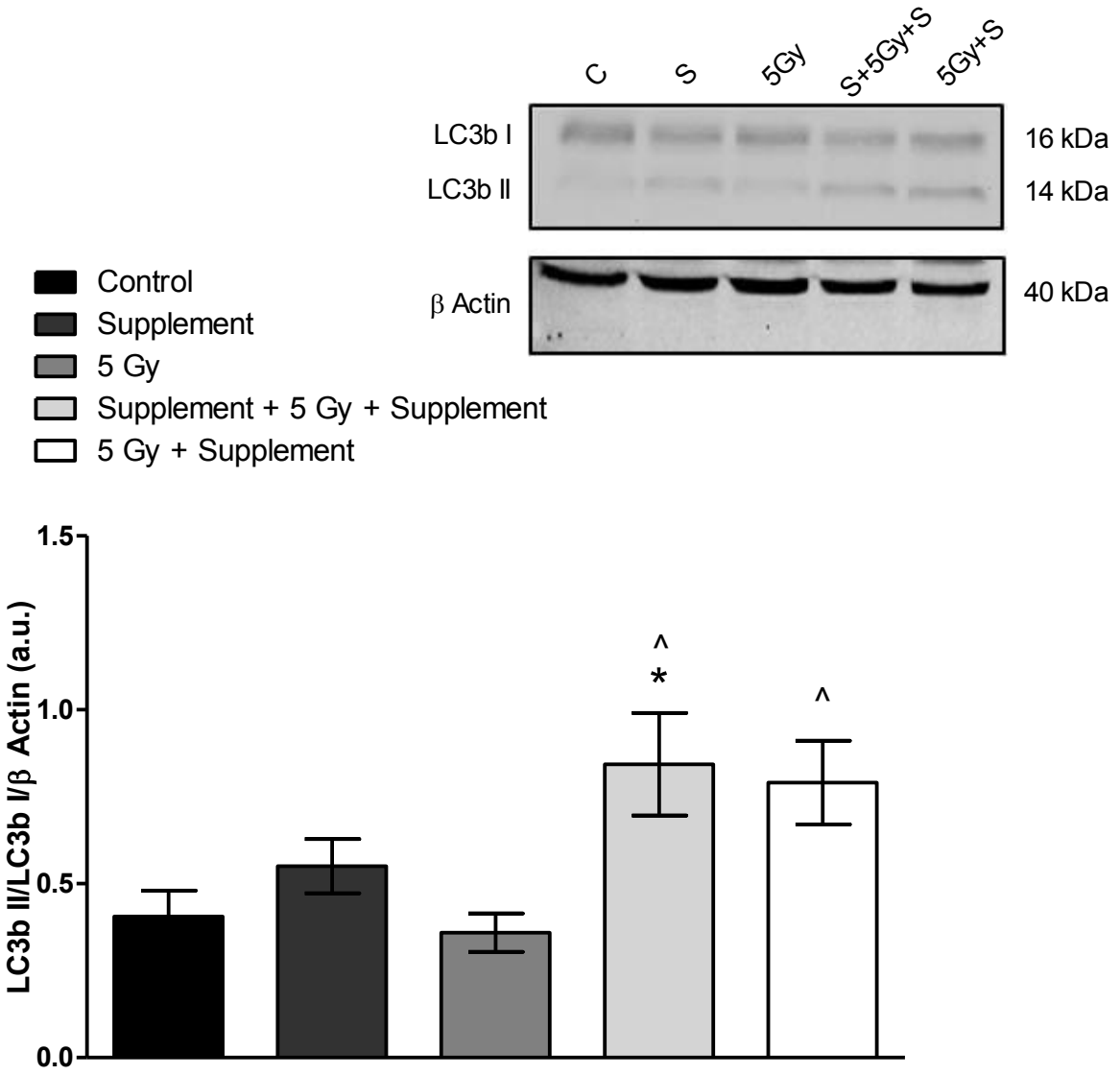

Figure 14. The effect of a dietary supplement on LC3bII/LC3bI ratio protein expression in the heart at 48 hours after 5 Gy whole body radiation. Protein concentration of LC3bII/LC3bI ratio was assessed via immunoblotting, where C = control, S = supplement alone, 5Gy = single whole body dose of 5 Gy γ radiation, S+5Gy+S = supplement for 30 days prior radiation and 48 hours after, 5Gy+S = supplement 48 hours after radiation. Bars represent mean ± SEM where $n = 5$ (*= $p < 0.05$ versus control; ^ = $p < 0.05$ versus 5 Gy).

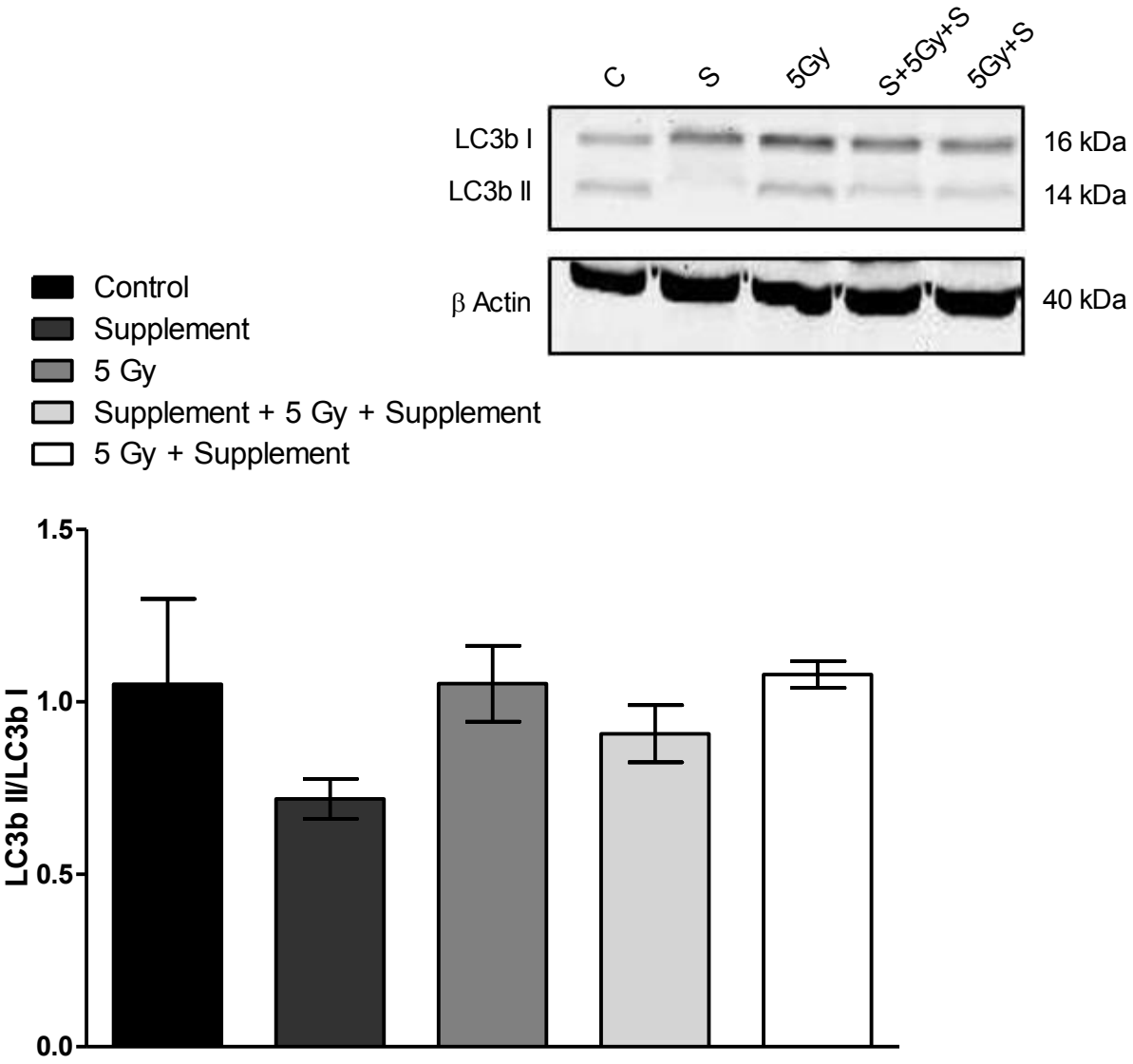

Figure 15. The effect of a dietary supplement on LC3bII/LC3bI ratio protein expression in the heart at 30 days after 5 Gy whole body radiation. Protein concentration of LC3bII/LC3bI ratio was assessed via immunoblotting, where C = control, S = supplement alone, 5Gy = single whole body dose of 5 Gy γ radiation, S+5Gy+S = supplement for 30 days prior radiation and 30 days after, 5Gy+S = supplement 30 days after radiation. Bars represent mean ± SEM where *n* = 5.

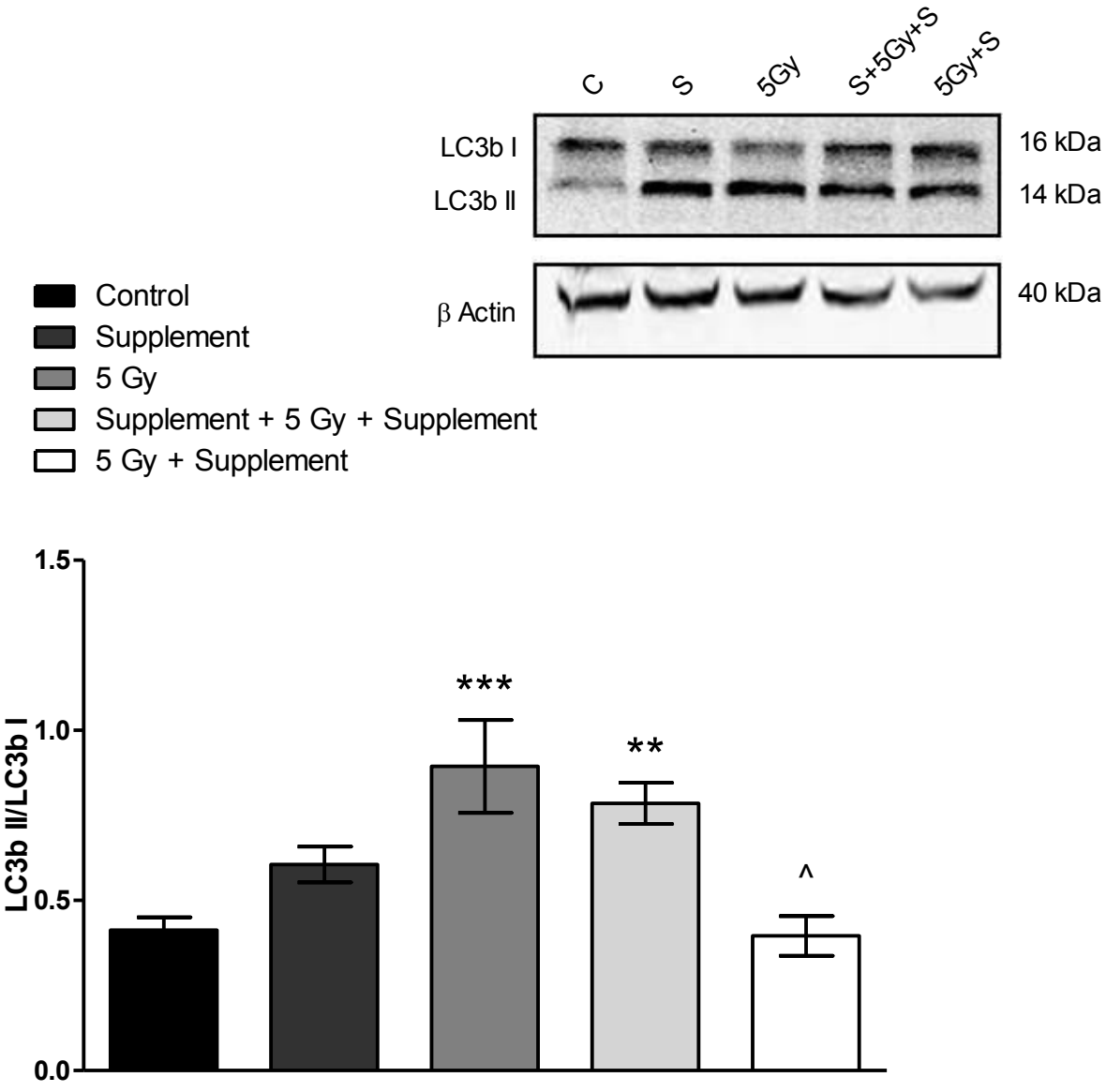

Figure 16. The effect of a dietary supplement on LC3bII/LC3bI ratio protein expression in the heart at 120 days after 5 Gy whole body radiation. Protein concentration of LC3bII/LC3bI ratio was assessed via immunoblotting, where C = control, S = supplement alone, 5Gy = single whole body dose of 5 Gy γ radiation, S+5Gy+S = supplement for 30 days prior radiation and 120 days after, 5Gy+S = supplement 120 days after radiation. Bars represent mean ± SEM where n = 5 (*** = $p < 0.001$ versus control; ** = $p < 0.01$ versus control; ^ = $p < 0.05$ versus 5 Gy).

Chapter 3 - Impact of High Dose Radiation to the Brain on Cardiac Function

Abstract

There is increasing evidence that suggests that radiation may induce DNA damage at sites that are distant from the irradiated target, referred to as the abscopal effect. There are very few studies on the abscopal effect and the heart. We investigated if a high dose of radiation to the head can lead to damage to the heart. Also, we investigated if a complex dietary supplement can attenuate the potential cardiac damage caused by the radiation. Eight week old male Thy1-GFP mice were fed the supplement 30 days before and after radiation or for just 30 days after. Radiation was given as a single 10 Gy dose to the brain. Hearts were collected and fixed in formalin. Hearts were then embedded in paraffin and sectioned at 5 μm at the mid papillary level. Histological staining with Hematoxylin and Eosin, Masson's Trichrome and Picrosirius Red was performed to evaluate inflammation and fibrosis. There was no significant difference in the amount of cardiac inflammation or fibrosis between any of the treatment groups. Therefore, a 10 Gy dose to the brain may not have an effect on cardiac inflammation or fibrosis, at least not within the timeframe of this study. It remains to be seen if a complex dietary supplement can protect against radiation induced damage due to the abscopal effect.

Introduction

In addition to oxidative stress, ionizing radiation has also been shown to induce an increase in inflammation. Inflammation, like oxidative stress, has both beneficial and detrimental effects and is implicated in several cardiac disease conditions. The inflammatory response is an integral component of the host response to tissue injury or invasion but also plays a particularly active role after myocardial infarction. Myocardial stress in the setting of ischemia will rapidly induce cytokines production as a response to oxidative stress [90]. Cytokines are also more implicated in the host's immune response to infections and other forms of stresses. Tumor necrosis factor-alpha (TNF-α) is a pro-inflammatory cytokine that plays an important role in the heart. It can stimulate antigen presentation, inflammatory cell activity, expression of matrix-degrading enzymes and initiate apoptosis [91-93]. ROS are known to initiate the inflammatory response and cause an increase in TNF-α production. H_2O_2 can directly induce myocardial TNF production via the p38 MAPK pathway [90; 94]. TNF-α and other pro-inflammatory mediators contribute to the production of ROS, which further stimulates the production of TNF-α, causing a perpetuating 'vicious cycle' [45]. Studies in irradiated tumors have shown that radiation can up-regulate the expression of inflammatory mediators TNF-α and intercellular adhesion molecule (ICAM)-1 [95-98]. A study by Azimzadeh et al. [99] indicated that total body irradiation can immediately induce cardiac inflammation. Various inflammatory and antioxidative defense proteins were altered when compared to non-irradiated controls. Up-regulation of cytokines such interleukin (IL)-6 and IL-8 has been observed after endothelial cell irradiation in a time and dose dependent manner [78; 100].

TNF-α, have been shown play an important role in regulating collagen deposition post myocardial infarction [90]. A study of a rat model of myocardial infarction found the expression of TNF-α, IL-1β, IL-6, transforming growth factor (TGF)-β1, and TGF-β3 increased after 1 week after myocardial infarction [90; 101]. Elevated cytokines also promote interstitial fibrosis and collagen deposition. There are many types of collagen but the majority of the collagen in the body consists of types I, II, and III. Type I is present in scar tissue, skin, tendons and organs. Type II is found in cartilage. Type III is commonly found with Type I. Type IV is found in basement membranes and used for support [102]. Collagen types I and III are most abundant in the myocardium [103]. Increased cytokines, including IL-1β, TNF-α, IL-6 and TGF-β, have been shown correlate closely to the deposition of type I and type III collagens [90; 104]. This is due to the role of cytokines in the remodeling process. Matrix metalloproteinases (MMP) are synthesized in inflammation and participate in tissue remodeling. MMPs are generally secreted in an inactive form but can be readily activated within minutes of ischemia by cytokines and even ROS, leading to collagen degradation and, subsequently, matrix deposition [90]. TNF-α can also lead to enhanced angiotensin II-mediated effects in favor of fibrosis [90; 105]. Premature differentiation of fibroblasts to myofibroblasts can be induced by ionizing radiation [106]. In hearts from rats that received 15 Gy or 18 Gy γ radiation to the chest, histological staining revealed significant myocardial fibrosis, degeneration and necrosis when compared to the controls [107]. Another study using 10 Gy whole body irradiation examined the impact of high dose radiation on coronary microvasculature and ventricular function in rats. Radiation exposure resulted in cellular peri-arterial fibrosis and irregular collagen deposition [108]. Myocardial cells appear to be sensitive to radiation-induced fibrosis as observed by many reports of arrhythmias occurring after chest radiotherapy [83; 109; 110]

Increasing evidence indicates that inflammatory cells in circulating blood of patients that received irradiation may also induce DNA damage at sites that are distant from the irradiated target, contributing to abscopal effects [26]. It is used to describe the distant tumor regression seen after localized therapeutic irradiation in a different area [111]. The abscopal effect is poorly understood but is believed to be in part immune-mediated. During treatment radiation induces an inflammatory response in tumor tissue that leads to cell death. It has been suggested that this cell death leads to further release of inflammatory cytokines which may be responsible for the abscopal effect after therapy [112-115]. Studies in the Japanese atomic bomb survivors revealed changes in lymphocyte subpopulations patterns and increased levels of parathyroid hormone, both have which might have contributed to the development of cardiovascular disease due to abscopal effects [78; 116; 117]. Oxidative-stress mediators have also been implicated in abscopal effects. These effects may be mediated by redox-sensitive cytokines that are both cytotoxic as well as capable of mediating an antitumor effect by activation of immune activity [26; 118]. It was found that after partial irradiation of rat lung micronucleus formation was observed in other non-irradiated areas of the lung. Pre-treatment with SOD led to a reduced response in the shielded area, indicating the involvement of ROS [111; 119]. While the abscopal effect has been described in various studies, it is rarely recognized as a clinical event [112]. Also, there has been very little study on its effects on the heart.

The objectives of this study were to investigate a possible abscopal effect on the heart after a high dose of radiation to the head in terms of inflammation and fibrosis. Also, to determine if a dietary supplement composed of antioxidants and anti-inflammatories can offset cardiac inflammation and fibrosis caused by the abscopal effect. Levels of inflammation and

fibrosis was measured using histochemistry staining of formalin fixed hearts. There has been no previous studies on cardiac injury induced by a high dose of radiation to the head, therefore this study will provide novel insight on the heart and the abscopal effect.

Materials and Methods

Animals

Eight week old male Thy1-GFP mice were purchased from Jackson Laboratories and left for 7 days to recover from transport. These mice contained green fluorescent protein expression in the Thy1 promoter region. Thy1 is expressed in neurons therefore the brain expresses the green fluorescence. Dendrite size, number and complexity will be examined at the University of California, Irvine. Mice were individually housed in 27 x 12 x 15.5 cm cages containing woodchip bedding (Harlan Sani-Chips, 7090). A stainless steel hopper provided food *ad libitum* (Harlan Teklad 8640 22/5 rodent chow) and supported a water bottle. Mice were weighed weekly midway through the photoperiod. The housing room maintained a 12:12-h light:dark photoperiod at 22 ± 2°C. All protocols were approved by the Animal Research Ethics Board at McMaster University and carried out according to the Canadian Council on Animal Care regulations. Mice were placed in 6 groups, 7 mice per group, identified as:

1) Control
2) Supplement only
3) 10 Gy to the brain only
4) Supplement + 10 Gy Brain
5) 10 Gy Brain + Supplement
6) Scatter dose (WBD equivalent to scatter from 10 Gy inside shield)

All supplement fed mice, except for the 10 Gy + Supplement group, were fed the supplement for 30 days prior to irradiation to allow the compounds within the supplement to reach equilibrium at maximal physiological levels. 10 Gy + Supplement mice were only fed the supplement for 30 days post irradiation. Animals were transferred to a nose cone containing 3% Isoflurane and loss of sensory/reflex response was confirmed by toe pinch. Animals were be immobilized in a drainage pan by extending and taping the forelimbs and securing the torso just above the hindlimbs. The abdominal skin was cut at the level of the diaphragm. The chest cavity was exposed by cutting across the diaphragm and through the ribs, making 2 cuts to free the sternum from ribcage and clamp open to expose the heart and allow drainage of fluids. A blunted 23-gauge winged needle was inserted directly into the left ventricle and saline containing 0.9% heparin was infused using a gravity fed IV set-up, using sharp scissors, cut the right auricle to allow fluid drainage and perfuse until the fluid exiting the heart ran clear. Perfusion fluid was changed to 4% paraformaldehyde solution and approximately 75ml of fixative was perfused into each mouse. Mice were decapitated and the top of the skull was cut along the midline to allow removal of the intact brain. The brain and heart were fixed in 4% paraformaldehyde for 24 hours at 4°C, and then stored in PBS containing 0.05% sodium azide at 4°C until futher analysis.

Dietary Supplement

Dosages of each component were calculated based on amounts commonly prescribed to humans (Table 1). Values were adjusted for the difference in body size and then increased by a factor of 10 in consideration of the higher gram-specific metabolic rate (and faster nutrient utilization) of mice. Supplement was made for 45 mice for 30 days at a time. Bagels were cut into 1 cm x 1 cm and crust removed. All dry components were mixed together before addition of

oils. Oils were added and mixed into dry components and dH_2O was added slowly to avoid clumping; 2 mL/6 bagel piece. Bagel pieces were pre-soaked with 100 mL of dH_2O before addition of supplement. 350 μL of supplement was added to each bagel piece allowed to dry overnight in a fumehood. Dry bagels were sealed in a air free bag and stored in a cool, dark area. Each mouse received one piece of dried bagel daily either with or without the supplement, depending on the treatment group. The mice were given the bagel pieces midway through the photoperiod. Amount of bagel eaten was measure the following day.

Irradiation

During irradiation, mice were restrained in a decapicone mouse restraint (Braintree Scientific) and held in a lead-shielded container which only exposes the head to irradiation. To reduce stress, mice were habituated to the restraint devices 30 prior to irradiation. Each mouse was given a 10 Gy dose of gamma radiation to the head from a cesium-137 source (Taylor Source). After irradiation, each mouse was returned to its housing cage. Non-irradiated sham control mice were otherwise exposed to exactly the same conditions as irradiated mice.

Histochemistry

Formalin fixed hearts were sent to the Laboratory Services Division of the Animal Health Laboratory of University of Guelph for paraffin embedding, sectioning (2 sections per slide) and Hematoxylin and Eosin (H & E) staining. Hearts were sectioned at the mid papillary level at a thickness of 5 μm. Unstained sections were then stained with either Masson's Trichrome or Picrosirius Red. Slides were deparaffinized and rehydrated through xylene (3 x 10 minutes), 100% alcohol (2 x 2 minutes), 95% alcohol (2 x 2 minutes), 80% alcohol (2 x 2 minutes) and

70% (2 x 2 minutes) alcohol washes. For Masson's Trichrome (Sigma) staining slides were re-fixed in Bouin's solution for 1 hour in a 56°C water bath. Slides were then rinsed with running tap water for 10 minutes to remove yellow colour. Slides were stained in Weigert's iron hematoxylin working solution (Sigma) for 8 minutes to stain nuclei then rinsed in running tap water for 10 minutes and washed in distilled water. First, slides were placed in Biebrich scarlet-acid fuchsin solution for 10 minutes then washed with distilled water. Second, slides were differentiated with phosphomolybdic-phosphotungstic acid solution for 10 minutes. Third, slides were placed directly to aniline blue solution and stain for 5 minutes, rinsed briefly in distilled water and differentiated in 1% acetic acid solution for 5 minutes. Slides were washed in distilled water and quickly dehydrated through 100% alcohol and cleared in xylene. A 60% dilution of permount (Sigma) was used to mount slides which were left overnight to dry. For Picrosirius Red (Sigma) staining slides were first stained in Weigert's iron hematoxylin working solution (Sigma) for 8 minutes to stain nuclei then rinsed in running tap water for 10 minutes and washed in distilled water. Slides were then stained in picrosirius red stain composed of piciric acid (Sigma) and sirius red (Sigma) for 1 hour. Slides were washed in 2 changes of acidified water and water was removed by vigorous shaking. Slides were washed in distilled water and quickly dehydrated through 100% alcohol and cleared in xylene. A 60% dilution of permount (Sigma) was used to mount slides which were left overnight to dry. Images at 100x magnification were captured using microscope (OMAX MD827S30L, OMAX, Kent, WA) and camera (ScopeImage 9.0, BioImager Inc., Toronto, ON). Images were analyzed via ImageJ (using the k-means clustering segmentation plugin. Percentage of positive staining was calculated based on number of colour-of-interest pixels by number of total pixels of the whole section.

Statistics

Data were presented as mean ± standard error of the mean (SEM), and all data presented here represents n ≥ 5 independent experiments. Statistical analyses were performed using GraphPad Prism software. One-way ANOVA with post hoc Tukey's test were utilized when possible with $p < 0.05$ considered significant. Asterisks are used herein to denote significance according to the following scheme: * = $p < 0.05$; ** = $p < 0.01$; *** = $p < 0.001$.

Results

Hematoxylin and Eosin Staining of Heart Sections

H & E staining did not show any difference in cell size or morphology between the groups, regardless of radiation or supplement treatment. Also, there was no change in the amount of inflammatory cells between the treatment groups (Figure 17).

Masson's Trichrome Staining of Heart Sections

Type I collagen is seen at the late stage of the fibrotic process and can therefore be an indicator of chronic inflammation. Masson's Trichrome, which stains Type I collagen, was used to measure the percentage of inflammation per section of heart. There was no change in the amount of inflammation between the treatment groups (Figure 18).

Picrosirius Red Staining of Heart Sections

Picrosirius Red, which stains Type I and III collagen, was used to measure the percentage of fibrosis per section of heart. There was no change in the amount of fibrosis between the treatment groups (Figure 19).

Conclusion

Evidence suggests that radiation may induce damage at sites that are distant from the irradiated target due to the abscopal effect. There are very few studies on the abscopal effect and the heart. In this study, neither a high dose of radiation to the head nor a dietary supplement had an effect on inflammation or fibrosis in mouse hearts. It is important to consider that our model may not be appropriate to see cardiac damage caused by the abscopal effect.

Figures

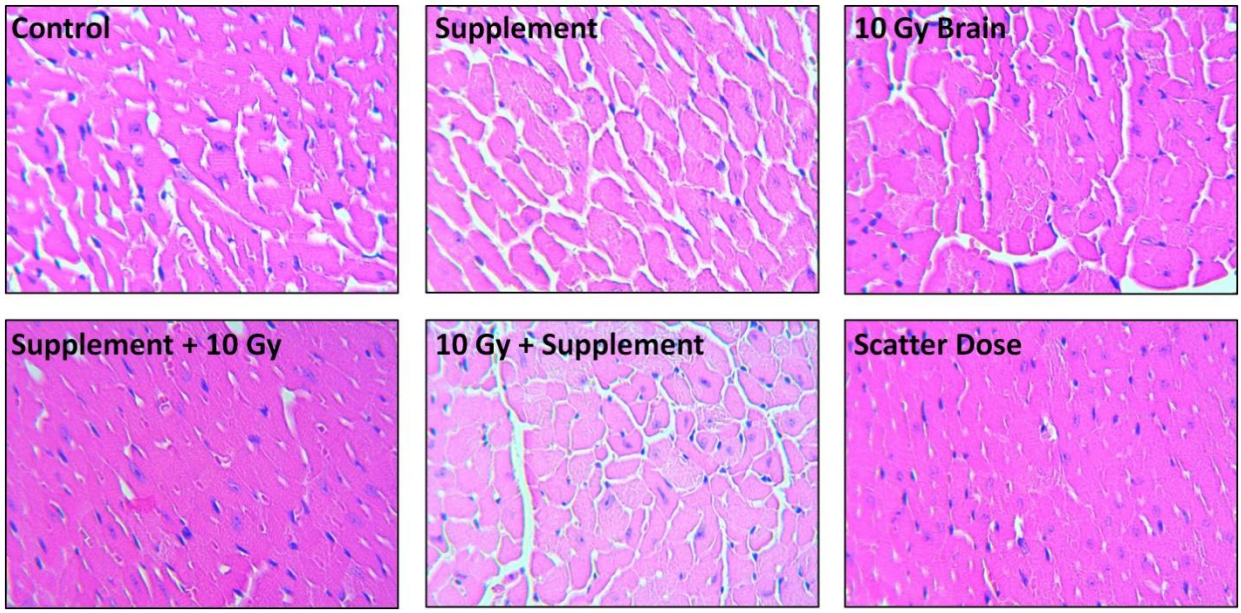

Figure 17. Heart sections stained with Hematoxylin and Eosin stain. Heart sections were stained with Hematoxylin and Eosin stain. Treatments include Control, Supplement (30 days before and after radiation), 10 Gy Brain (single dose to the head), Supplement + 10 Gy (supplement for 30 days before and after 10 Gy), 10 Gy + Supplement (supplement for 30 days after 10 Gy) and Scatter Dose (whole body dose equivalent to scatter from 10 Gy inside shield). Image representations are at 400x magnification, $n = 6$.

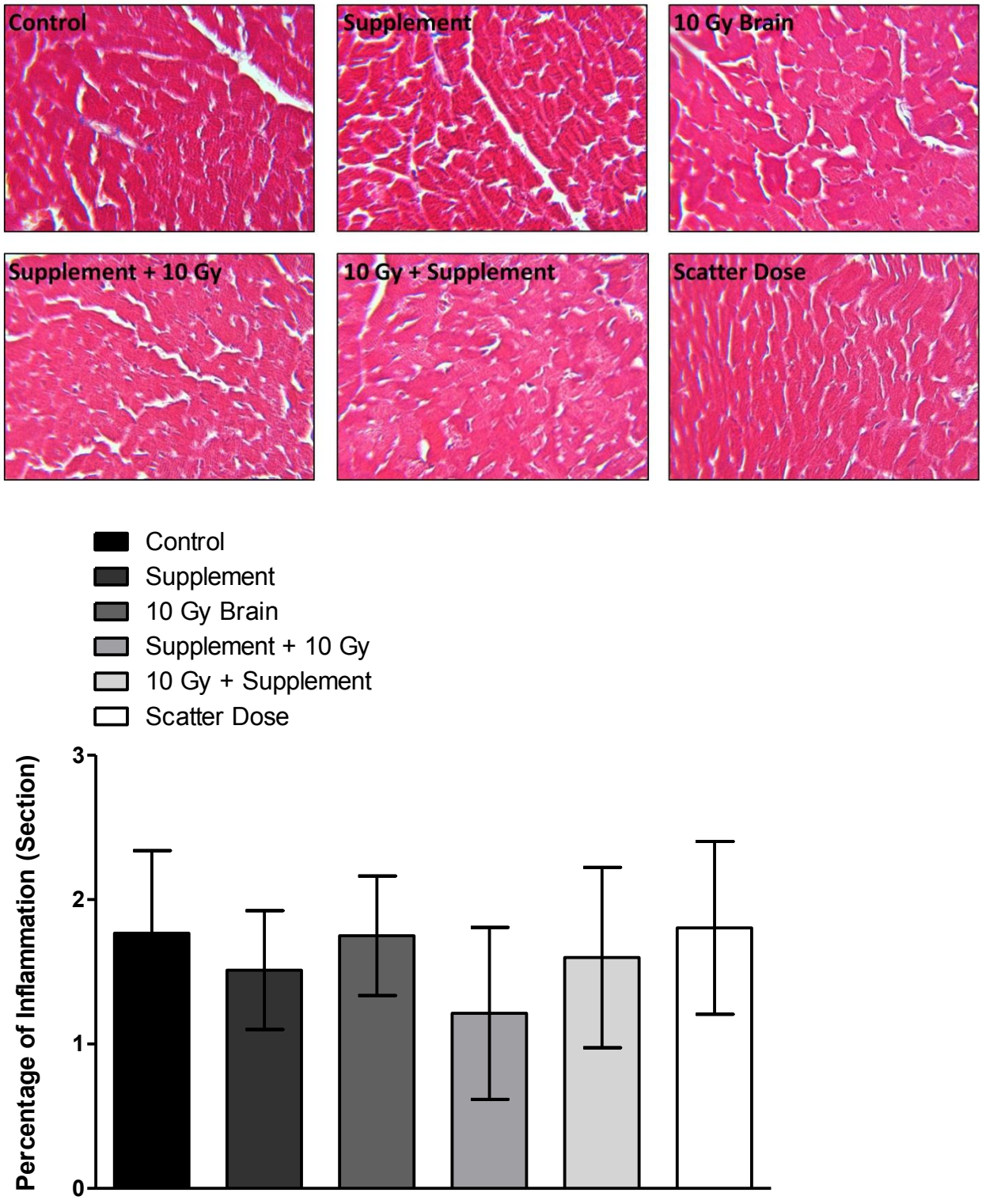

Figure 18. The percentage of cardiac inflammation per section via Masson's Trichrome stain. Level of inflammation per section of heart stained with Masson's Trichrome stain and

evaluated using ImageJ. Treatments include Control, Supplement (30 days before and after radiation), 10 Gy Brain (single dose to the head), Supplement + 10 Gy (supplement for 30 days before and after 10 Gy), 10 Gy + Supplement (supplement for 30 days after 10 Gy) and Scatter Dose (whole body dose equivalent to scatter from 10 Gy inside shield). Image representations are at 400x magnification. Bars represent mean ± SEM where $n = 6$.

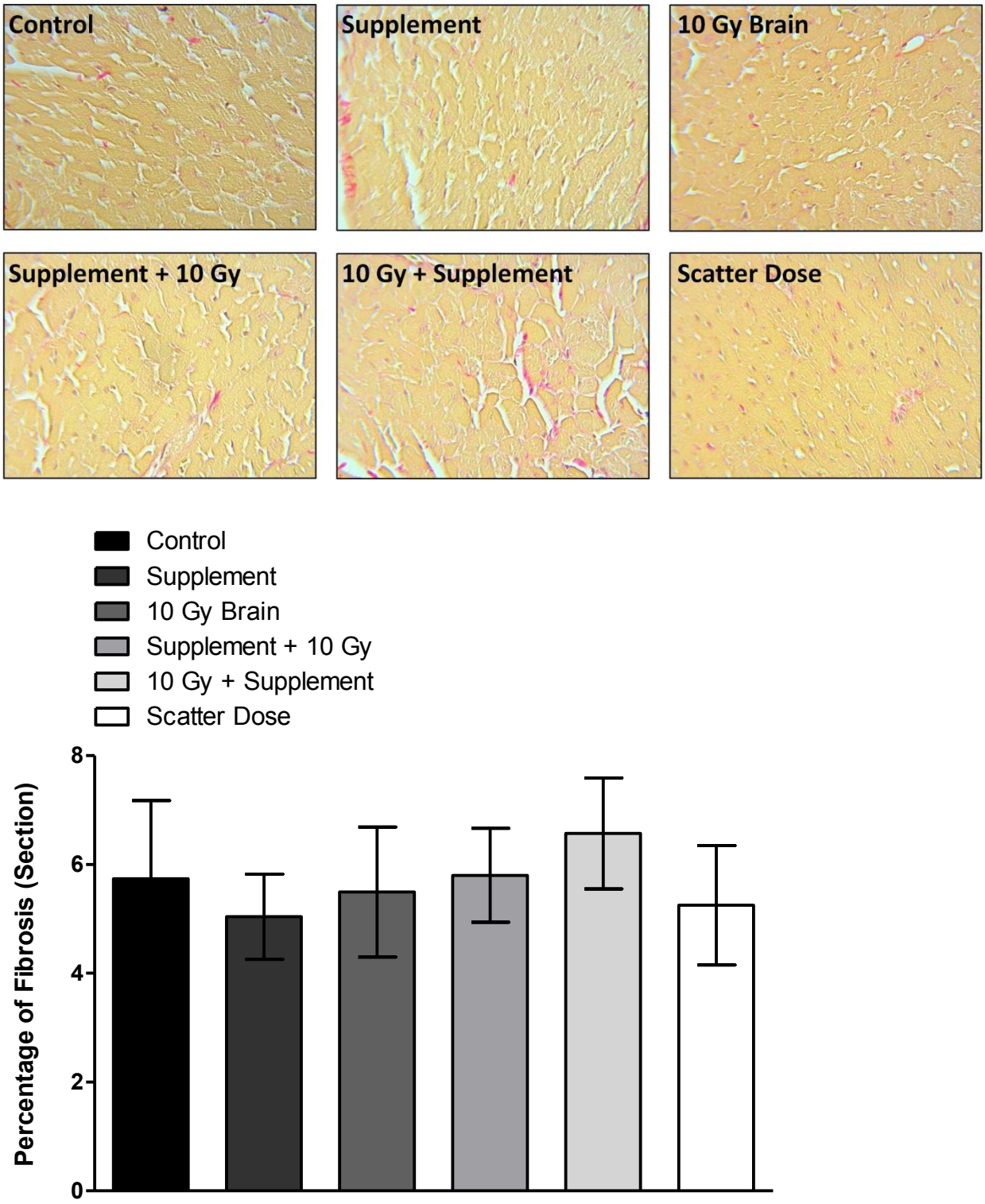

Figure 19. The percentage of cardiac fibrosis per section via Picrosirius Red stain. Level of fibrosis per section of heart stained with Picrosirius Red stain and evaluated using ImageJ.

Treatments include Control, Supplement (30 days before and after radiation), 10 Gy Brain (single dose to the head), Supplement + 10 Gy (supplement for 30 days before and after 10 Gy), 10 Gy + Supplement (supplement for 30 days after 10 Gy) and Scatter Dose (whole body dose equivalent to scatter from 10 Gy inside shield). Image representations are at 400x magnification. Bars represent mean ± SEM where $n = 6$.

Chapter 4 - The Effect of Secoisolariciresinol Diglucoside on Oxidative Stress and Antioxidants in Monocrotaline Induced Cardiac Dysfunction

Abstract

Pulmonary arterial hypertension (PAH) occurs when proliferation and remodeling of pulmonary arterioles leads to pulmonary vascular resistance and pulmonary arterial pressure, resulting in right ventricle hypertrophy leading to dilation and eventually failure. Oxidative stress has been implicated in the pathogenesis of PAH and may play an important role in the regulation of cellular signaling involved in cardiac response to pressure overload. Secoisolariciresinol diglucoside (SDG) is a component from flaxseed that has been shown to reduce cardiac oxidative stress in various pathophysiological conditions. We investigated the potential protective capabilities of SDG in a monocrotaline induced model of PAH. Six week old male Wistar rats were given a single intraperitoneal injection of monocrotaline and sacrificed 21 days later where right ventricles were collected. SDG was given either for 21 days (co-treatment with monocrotaline) or for 35 days with a pre-treatment for 14 days before monocrotaline administration and sacrificed 21 days later. Monocrotaline treatment led to increases in right ventricle hypertrophy, lipid peroxidation and plasma levels of alanine transaminase and aspartate transaminase. Co-treatment with SDG did not change hypertrophy or alanine transaminase and aspartate transaminase levels but decreased reactive oxygen species levels, catalase and superoxide dismutase activity compared to monocrotaline treatment. Also, pre-treatment with SDG decreased right ventricle hypertrophy, reactive oxygen species levels, lipid peroxidation, catalase, superoxide dismutase and glutathion peroxidase activity and plasma levels of alanine transaminase and aspartate transaminase when compared to monocrotaline treatment alone. These findings indicate that pre-treatment with SDG provided protection in this model of heart failure, suggesting an important role for SDG in PAH and right ventricular remodeling.

Introduction

Pulmonary hypertension is a chronic disease characterized by an elevation of mean pulmonary artery pressure above 25 mm Hg [120]. Currently, there are five major categories of pulmonary hypertension recognized; Pulmonary arterial hypertension, Pulmonary hypertension with left heart disease, Pulmonary hypertension associated with lung disease and/or hypoxemia, Pulmonary hypertension due to chronic thrombotic and/or embolic disease and Miscellaneous [121]. Pulmonary arterial hypertension (PAH) occurs when the proliferation and remodeling of pulmonary arterioles causes an increase in pulmonary vascular resistance and pulmonary arterial pressure [122]. This eventually leads to the development of right ventricular hypertrophy and congestive heart failure due to a progressive increase in pulmonary vascular resistance (PVR) and pulmonary arterial pressure [121; 122]. In PAH the primary vascular changes leading to increased PVR are vasoconstriction, remodeling of the pulmonary vascular wall and thrombosis [122]. Vasoconstriction is the result of endothelial dysfunction caused by an imbalance in the availability of dilators and an excess in constrictors [123]. Excess vasoconstrictors stimulates cellular proliferation of vascular smooth muscle cells and induces fibrosis [122]. Vascular remodeling includes medial hypertrophy and arteriole plexiform lesions resulting from intimal hyperplasia eventually leading to luminal occlusion and arteriolar pruning [122; 123]. As PAH progresses there is an increased afterload on the right ventricle promoting right ventricular hypertrophy. The right ventricle can compensate with enhanced contractility, but as afterload increases the right ventricle decompensates, resulting in right ventricle failure [123]. Risk of developing PAH is increased in patients with congestive heart failure, blood clots in the lungs, hereditary mutations, HIV, liver disease, portal hypertension and other conditions linked to high

blood pressure [121]. Symptoms are often nonspecific and may mimic other common disorders. These symptoms can include fatigue or weakness, angina, peripheral edema, and the most common symptom of exertional dyspnea [122]. PAH pathogenesis is complicated and it is likely that one factor alone is not sufficient to activate all of the necessary pathways leading to the development of the disease [122]. This makes it difficult to diagnose and treat the disease, and in fact there is currently no cure available.

PAH induced right ventricle failure is characterized by diminished myocardial perfusion and ischemia, increased end diastolic volume, right ventricle dilation, reduced stroke volume, and reduced cardiac output [123] and is defined as *Cor pulmonale* [124]. Initially, cardiac remodeling and hemodynamic and neurohumoral activation occurs [124; 125]. This results in a period of cardiomyocytes hypertrophy, followed by a reduction in cell number due to apoptosis [124; 126]. This continuous remodeling, hypertrophy and apoptosis eventually leads to heart failure [124; 125]. Currently there are several therapeutic options available that are targeted to specific molecular mechanisms of PAH. Calcium-channel blockers that act as vasodilators have been shown to improve survival, but is only a suitable option for patients with a positive vasodilator challenge, which is present in fewer than 10% of patients with PAH [121; 122; 127]. Protacyclins promote vasodilation and inhibit vascular proliferation and platelet aggregation and have been shown to lead to improvement in exercise capacity, hemodynamics, and quality of life [121]. Unfortunately, due to the short half life of protacyclins, treatment is done intravenously which may cause complications after long term therapy [122]. Endothelin antagonists block vasoconstrictor endothelin-1 and have been shown to improve cardiopulmonary hemodynamic variables but may also cause liver toxicity, anemia, edema, teratogenicity, male infertility, and

testicular atrophy [121; 122; 128]. Nitric oxide and phosphodiesterase inhibitors act as a vasodilator, platelet inhibitor, and antiproliferative agent on vascular smooth muscle cells and have shown to improve symptoms, but long term effects are not yet known [121; 122]. Since available treatments can cause adverse side effects and are not suitable for all patients, further study on possible treatment options for PAH are needed.

Increased production of ROS has been shown to be involved in PAH pathogenesis. Oxidant stress has been demonstrated in the lungs and right ventricle of several animal models of PAH [123]. ROS from the mitochondrial electron-transport chain promote vasculopathy through increased cellular senescence, necrosis, or apoptosis [129; 130]. Studies have shown that increases in mitochondrial-derived ROS contribute to hypoxic pulmonary vasoconstriction [129; 131; 132]. A commonly used model of PAH is the rat monocrotaline (MCT) model. MCT is a pyrrolizidine alkaloid present in the plant *Crotalaria spectabilis*. It causes endothelial injury and an imbalance between vasodilators and vasoconstrictors which leads to vessel wall thickening, increased pulmonary resistance and right ventricle hypertrophy [133-135]. Pichardo et al. [136] demonstrated in right ventricles from rats treated with MCT, Vitamin E levels were decreased and lipid hydroperoxide concentrations were increased, indicating an increase in oxidative stress. Farahmand et al. [134] also reported that ROS are involved in PAH, right ventricular hypertrophy, and failure induced by MCT. PAH induced oxidative stress in rat cardiomyocytes has been shown to be due to ROS generated from NADPH oxidase and the mitochondria [137]. The role of ROS in PAH induced heart failure suggests that treatment with antioxidants may be beneficial. Studies on MCT treated rats pretreated with grape juice, which is rich in flavonoids and poses antioxidant properties, have shown that grape juice can offer some protection to the

right ventricle through decrease of lipid peroxidation, decreased cleaved caspase-3 and improvement of hemodynamic parameters [124; 133]. Treatment with synthetic antioxidant EUK-134 attenuated cardiomyocyte hypertrophy, reduced right ventricle oxidative stress, reduced proapoptotic signaling and prevented interstitial fibrosis in MCT treated rats [138]. Therefore, antioxidants may provide an useful therapeutic treatment option of PAH, but further studies are needed.

Flax (*Linum usitatisimum*) is grown as a food or fiber crop. Flaxseed is the richest source of a lignan called secoisolariciresinol diglucoside (SDG) [139; 140]. When ingested SDG is converted to aglycone secoisolariciresinol, which is structurally similar to known antioxidant nordihydroguaiaretic acid. Therefore, SDG can inhibit the production of ROS and remove ROS already produced through antioxidant and anti-platelet-activating factor-(PAF) activity [141]. There have been numerous studies on the effect of SDG on oxidative stress and cardiovascular health. In streptozotocin induced diabetic rats, treatment with SDG reduced glucose levels and lipid profile, restored antioxidant enzymes and improved insulin levels [142]. Pretreatment with SDG was able to significantly prevent the development of diabetes in streptozotocin treated rats [143], diabetic prone BioBreeding rats [141] and type 2 diabetes prone Zucker rats [144]. In a rabbit model of atherosclerosis, SDG treatment reduced the development of atherosclerotic lesions by causing a decrease in serum cholesterol, LDL-C, and lipid peroxidation product and an increase in HDL-C and antioxidant reserve in rabbits [145]. Penumathsa et al. [146] investigated the effects of SDG treatment on hypercholesterolemic rat hearts after ischemia/reperfusion injury. There was a significant reduction in total cholesterol, LDL-cholesterol, triglycerides and an significant increase in HDL-cholesterol levels in SDG treated

rats as compared to the non-treated. Decreased infarct size, reduced ventricular remodeling and improvement in left ventricular functions was also observed in the SDG treated group. The angiogenic properties of SDG have been investigated in three different models. In an *in vitro* model, human coronary arteriolar endothelial cells treated with SDG showed a significant increase in tubular morphogenesis. In an *ex vivo* ischemia/reperfusion model, SDG-treated showed an increased level of aortic flow and functional recovery. Also, SDG reduced infarct size and decreased cardiomyocyte apoptosis. In an *in vivo* myocardial infarction model, SDG increased capillary density and myocardial function as evidenced by increased fractional shortening and ejection fraction [147]. Prasad [148] investigated the effect of Angiotensin I and treatment with SDG. SDG treatment produced reductions in systolic, diastolic, and mean arterial pressure [148]. In an H9c2 model of cardiac iron overload pretreatment with SDG reduced levels of ROS, expression of inflammatory cytokines and remodeling proteins and protein levels and activity of markers of apoptosis [149]. It is clear that SDG has protective antioxidant capabilities in many models of oxidative stress, but a possible role in PAH has not been investigated.

The objectives of this study were to examine the molecular mechanism(s) of MCT induced right heart failure and also, to determine if treatment with SDG can reduce damage caused by MCT induced oxidative stress. Based on previous work with this model, rats received a single MCT injection to induce PAH after 21 days. For the co-treatment group SDG treatment began on the day of MCT and continued for 21 days until the end of the study. We also pretreated a group of rats for 2 weeks prior to MCT injection and for 21 days after to see if pretreatment of SDG provided any additional benefical effects against PAH. Specifically, our

focus was to examine ROS and antioxidants to provide insight in the mechanism(s) of MCT induced cardiac damage and protection provided from SDG.

Materials and Methods

Animals

Five to six week old male Wistar rats were purchased from the Central Animal House at Universidade Federal do Rio Grande do Sul (UFRGS). Rats were housed in 270 x 260 x 310 mm cages with the floor covered in sawdust and with 4 rats per cage. During the treatment period animals were housed in the animal sector of the Pharmacology Department located in the Instituto de Ciências Básicas da Saúde (ICBS) at UFRGS. The housing room maintained at 22 ± 2°C with a 12:12-h light:dark photoperiod. Rats were placed in 5 groups, 8 rats per group, identified as:

1) Control
2) SDG only
3) MCT only
4) SDG + MCT (co-treatment)
5) SDG pre treatment + MCT

Rats received a daily dose of 25 mg/kg of SDG (kindly provided by Dr Prasad from the University of Saskatchewan) via gavage or water for control groups for the duration of the study. Monocrotaline (Sigma-Aldrich) was given as a single intraperitoneal injection of 60 mg/kg (pH=7.4) at the beginning of SDG treatment. SDG pre treatment + MCT group followed the same protocol but instead SDG treatment began 2 weeks prior to monocrotaline treatment. After 21 days rats were anesthetized with ketamine (90 mg/kg) and xylazine (10 mg/kg) and sacrificed

via decapitation. Blood was collected in heparinized tubes and centrifuged for 10 minutes at 1000 x g. Separated plasma was collected and stored at -80°C.

Tissue Weight Determination

Hearts were collected and total heart, right ventricle (RV) and left ventricle weights were measured. In order to obtain the wet/dry weight ratio of the lungs and livers the organs were freed from adhering tissues. Lungs and livers were weighed and placed in the oven at 40°C until a constant weight was observed. Collected tissues were stored at -80°C until further analysis.

Hemodynamic Evaluation

Hemodynamic parameters were measured at the end of the treatment period just before animals were sacrificed. Rats were anesthetized with ketamine (90 mg/kg) and xylazine (10 mg/kg) and catheterization of the right carotid artery was acheived with a PE 50 catheter connected to a transducer Strain Gauge (Narco Biosystem Pulse Transducer RP-155, Houston, TX) connected to a pressure amplifier (HP 8805C, Hewlett Packard, Palo Alto, CA). Pressure analysis was stored on a computer equipped with an analog-to-digital conversion board (Biopac 1 kHz sampling frequency, Biopac Systems, Inc., Goleta, CA). Heart rate and ventricular systolic and ventricular diastolic pressure were recorded and analyzed using the Windaq software (Dataq Instruments, Inc., Akron, OH).

Homogenization of tissue and total protein for enzymatic activity

A section of about 1/3 of each right ventricle was cut, weighed and placed in a separate eppendorf tube to be homogenated. Buffer composed of 1.15% KCl and 1% PMSF was added to

each section. Tissue was homogenized for 40 seconds then centrifuged for 20 minutes at 3000 rpm. Supernatant was aliquoted and stored at -20°C. Protein concentration was measured via the Lowry method where bovine serum albumin was used to calculate protein concentration of samples read at 625 nm.

Reactive oxygen species indicator assay

DCF-DA (2′, 7′ - dichlorofluorescein diacetate; Sigma-Aldrich) was used as an indicator of ROS. Homogenized samples were diluted in 1.15% KCl buffer. DCF-DA (Sigma-Aldrich) was added to each sample and then incubated for 30 minutes. Samples were added to a 96 well plate and read at 488 nm (Perkin Elmer LS 55 Fluorescence Spectrometer, Waltham, MA). A standard curve was calculated using different concentrations of DCF (0, 0.2, 1, 2 pmol/mg) and used to calculate the amount of ROS per mg of protein.

Lipid peroxidation

To determine lipid peroxidation tert-butyl hydroperoxide–initiated chemiluminescence was measured in a liquid scintillation counter in the out-of-coincidence mode (LKB Rack Beta Liquid Scintillation Spectrometer 1215, LKB-Produkter AB, Sweden). Measurements were started by the addition of tert-butyl hydroperoxide to right ventricle homogenates. The reaction was allowed to initiate for 1 minute 30 seconds before being read. Each sample was read for 30 seconds in triplicate until tert-butyl hydroperoxide reaction began to decrease. Data was expressed as counts per second (cps)/mg of protein.

Antioxidant Enzyme Activity

Catalase activity was calculated based on amount of H_2O_2 measured over 1 minute. In a cuvette 478 µL of 50mM potassium phosphate buffer, pH 7.4, was added followed by 5 µL of homogenated heart sample. The cuvette was then placed in the spectrophotometer. After 'zeroing' the absorbance 17.5 µL of H_2O_2 was added to the cuvette to start the reaction. Changes in absorbance was read at 240 nm (Cary 1E UV-Spectrophotometer, Agilent Technologies, Santa Clara, CA) for 1 minute where absorbance was recorded every 20 seconds. Absorbance was used to calculate nmol of catalase/mg of protein/ minute [150].

To calculate SOD activity homogenized hearts (1:10) were added to 50 mM Tris-HCl, pH 8.2, containing 1 mM diethylenetriamine pentaacetic acid. SOD activity was determined by measuring the inhibition of pyrogallol (Sigma-Aldrich) autoxidation that is catalyzed by the superoxide radical. Pyrogallol (25 mM) was prepared in 10 mM HCl and stored at 4°C. Catalase (30 µM, prepared in an alkaline buffer, pH 9.0) was used to eliminate H_2O_2 from the reaction. 25 µL of pyrogallol and 10 µL of catalase was added to samples in Tris Base (50 mM and 1 mM EDTA) and absorbance was measured at 420 nm (Agilent Technologies) for 2 minutes where absorbance was recorded at 0.5 and 1.5 minutes. Absorbance was used to calculate Units of SOD/mg of protein [151].

GPx activity was determined by measuring the consumption of NADPH in the reduction reaction of GSSG to GSH. Heart homogenates (50 µL) was added to a cuvette containing 165 µL of 75 mM phosphate buffer, pH 7.0. Then the following solutions were added: 250 µL of NADPH, 5 µL of sodium azide (143mM and 4mM EDTA), 25 µL of glutathione and 5 µL of glutathione reductase. The cuvette was then placed in the spectrophotometer. After 'zeroing' the

absorbance 25 µL of TBOOH (2 uL of tert-butyl hydroperoxide in 867 µL of H_2O) to start the reaction and absorbance was measured at 340 nm (Agilent Technologies) for 2 minutes where absorbance was recorded at 0.5 and 1.5 minutes. Absorbance was used to calculate µmol activity of GPx/mg of protein [152].

Liver Toxicity Test - AST and ALT

Toxicity was measured via asparatate aminotransferase (AST) and alanine transaminase (ALT) tests. An increase in AST and ALT is indicative of liver toxicity. AST catalyzes the conversion of aspartate and ketoglutarate to oxaloacetate and glutamate. The AST/GOT Liquiform kit (Labtest, Lagoa Santa, MG, Brazil) was used to analyze AST levels. Plasma was diluted (1:10) in dH_2O, added to Reagent 1 + 3 mixture and incubated for 5 minutes at 37°C. Reagent 2 was added and samples were read at 340 nm (T60 UV-Visible Spectrophotometer, PG Instruments, Leicestershire, UK) where absorbance was recorded at 1 minute and 2 minutes of reading. ALT catalyzes the conversion of alanine and ketoglutarate to pyruvate and glutamate. ALT was measured in a similar way but with the ALT/GPT Liquiform kit (Labtest).

Statistics

Data were presented as mean ± standard error of the mean (SEM), and all data presented here represents n = 8 independent experiments. Statistical analyses were performed using GraphPad Prism software. One-way ANOVA with post hoc Tukey's test were utilized when possible with $p < 0.05$ considered significant. Asterisks are used herein to denote significance according to the following scheme: * = $p < 0.05$; ** = $p < 0.01$; *** = $p < 0.001$; * = vs. control, # = vs. MCT, ^ = vs. MCT + SDG.

Results

Weekly Weight Gain

Rats in control, SDG and SDG pre treatment + MCT had a similar average weekly weight gain between the groups (Figure 20). The weekly weight gain in MCT and SDG + MCT groups were similar to each other but slightly less than the average weekly weight gain of control, SDG and SDG pre treatment + MCT groups (Figure 20).

Cardiac Hypertrophy and Liver and Lung Congestion

Cardiac hypertrophy was calculated by measuring heart or RV weight to total body weight. MCT treatment led to an increase in total heart/body weight and RV/body weight compared to control (Table 2), suggesting an increase in right ventricle hypertrophy. Co-treatment of SDG with MCT also led to increased total heart/body weight and RV/body weight compared to control (Table 2), suggesting an increase in right ventricle hypertrophy. Heart/body weight and RV/body weight were near control levels in SDG pre-treatment group animals (Table 2). Liver and lung congestion was calculated by measuring wet weight/dry weight. There was no change in lung wet weight/dry weight between any of the groups (Table 2). Liver wet weight/dry weight was increased in MCT + SDG animals compared to control (Table 2).

Hemodynamics

Hemodynamic parameters were measured in the right ventricles of animals. RV systolic pressure (RVSP) was increased in MCT ($P<0.001$) and MCT + SDG ($P<0.05$) groups compared to control. RVSP was significantly less ($P<0.001$) in the SDG + MCT group compared to MCT

(Table 2). RV end diastolic pressure (RVEDP) was increased in the MCT ($P<0.001$) and MCT + SDG ($P<0.05$) groups compared to MCT. RVEDP was significantly less ($P<0.05$) in the SDG + MCT group compared to MCT and MCT + SDG groups (Table 2). dP/dt min and max was increased in MCT ($P<0.01$; $P<0.05$, respectively) compared to control (Table 2).

Oxidative Stress

Oxidative stress was measured via DCF-DA (indicator of ROS levels) and chemiluminescence (indicator of lipid peroxidation). ROS levels did not change in MCT treated animals compared to control but did decrease in MCT + SDG and SDG + MCT groups compared to both control and MCT (Figure 21). Lipid peroxidation increased in MCT treated animals compared to control but was not significantly different in the MCT + SDG group compared to control or MCT. Lipid peroxidation did decrease in the SDG + MCT group compared to MCT (Figure 22).

Antioxidants

Enzymatic activity of antioxidants catalase, SOD and GPx was measured spectrophotometrically. Catalase (Figure 23), SOD (Figure 24) and GPx (Figure 25) activity did not change in MCT treated animals compared to control. Both catalase (Figure 23) and SOD (Figure 24) activity decreased in MCT + SDG and SDG + MCT groups compared to MCT. Only in the SDG + MCT group did GPx activity decrease compared to MCT (Figure 25).

Liver Toxicity

Plasma levels of ALT and AST (indicators of liver toxicity) were measured spectrophotometrically. ALT (Figure 26) and AST (Figure 27) levels were increased in MCT and MCT + SDG groups compared to control. SDG + MCT animals had decreased ALT and AST levels compared to MCT (Figure 26 & 27).

Conclusion

PAH is known to lead to the development of right ventricular hypertrophy and heart failure. Our study has shown that treatment with SDG may offer some protection to the heart against oxidative stress in a model of PAH. Interestingly, pretreatment with SDG has shown to be a better treatment option rather than cotreatment.

Tables

Table 2. Morphometric and hemodynamic measurements of right ventricle

Parameters	Control	SDG	MCT	MCT + SDG	SDG + MCT
Morphometric					
Body Weight (g)	272±22	270±24	243±22*	243±15**	303±46$^{\#\#/\wedge\wedge}$
Total Heart Weight (g)	0.92±0.06	0.95±0.18	0.99±0.16	1.03±0.09	1.04±0.16
RV Weight (g)	0.19±0.04	0.19±0.06	0.24±0.05	0.26±0.06*	0.21±0.03
Total Heart/BW (mg/g)	3.39±0.2	3.51±0.6	4.08±0.7*	4.25±0.5***	3.43±0.1$^{\#/\wedge}$
Total Heart/Tibia Length (mg/cm)	299±23.4	313±58.2	326±51.5	339±30.3	340±50.8
RV/BW (mg/g)	0.69±0.1	0.70±0.2	0.97±0.2**	1.07±0.3**	0.71±0.1$^{\#\#/\wedge\wedge}$
RV/Tibia Length (mg/cm)	61.20±14.8	62.31±18.4	77.84±16.3	85.15±20.7*	69.79±9.0
Liver Wet/Dry Weight (g/g)	3.3±0.1	3.4±0.2	3.4±0.1	3.7±0.4*	3.3±0.1
Lung Wet/Dry Weight (g/g)	4.8±0.3	5.1±0.3	4.8±0.2	5.1±0.7	5.2±0.2
Hemodynamic					
RVEDP (mmHg)	1.5±1.1	1.3±0.9	5.7±3.6*	5.7±2.0*	1.9±0.9$^{\#/\wedge}$
RVSP (mmHg)	29.8±2.5	25.0±6.4	82.6±19.9***	50.8±11.1$^{*/\#\#}$	43.4±7.7$^{\#\#\#}$
dP/dt min (mmHg/min)	-1197±323	-1001±303	-2251±107**	-1764±533	-1764±291
dP/dt max (mmHg/min)	1802±530	1434±512	3112±650*	2273±838	2289±179***

Figures

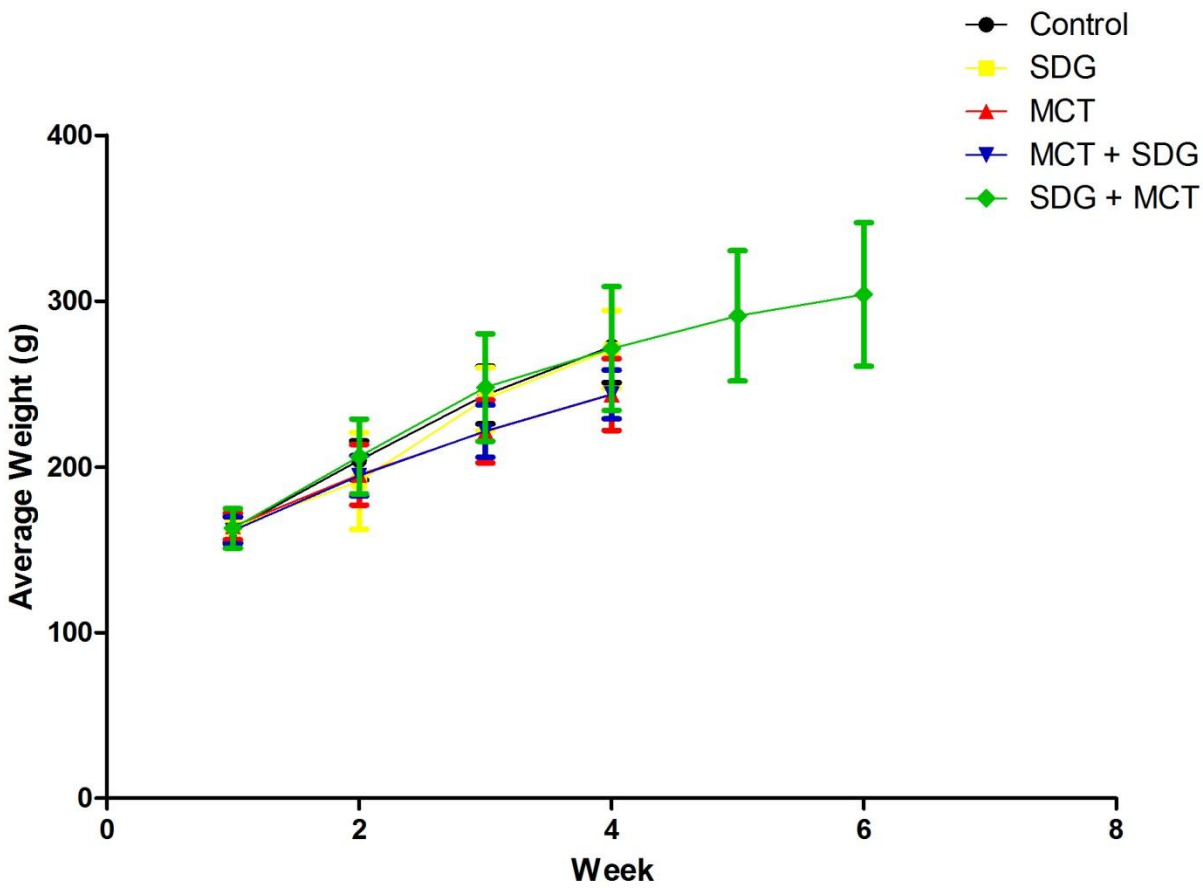

Figure 20. Average weekly body weight gain. All rats were weighed weekly during the study period. Graph represents the average weight of all eight rats per group.

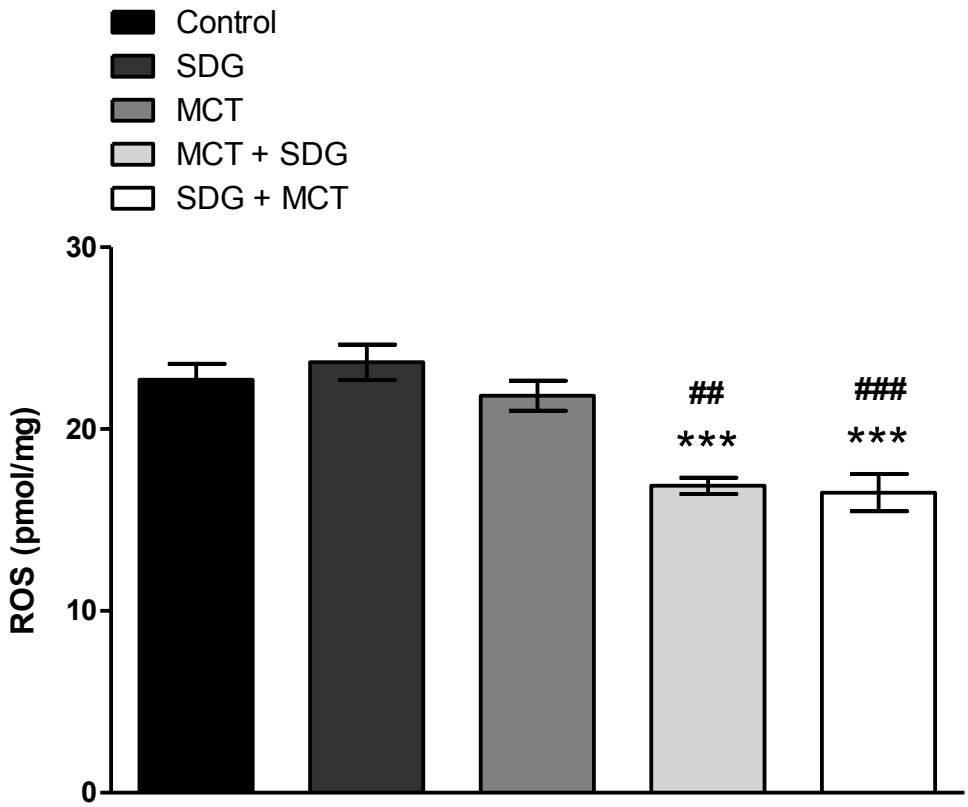

Figure 21. The effect of MCT and SDG on levels of reactive oxygen species in the right ventricle. ROS levels were assessed via DCF-DA. Bars represent mean ± SEM where $n = 8$ (*** = $p < 0.001$ versus control; ### = $p < 0.001$ versus MCT).

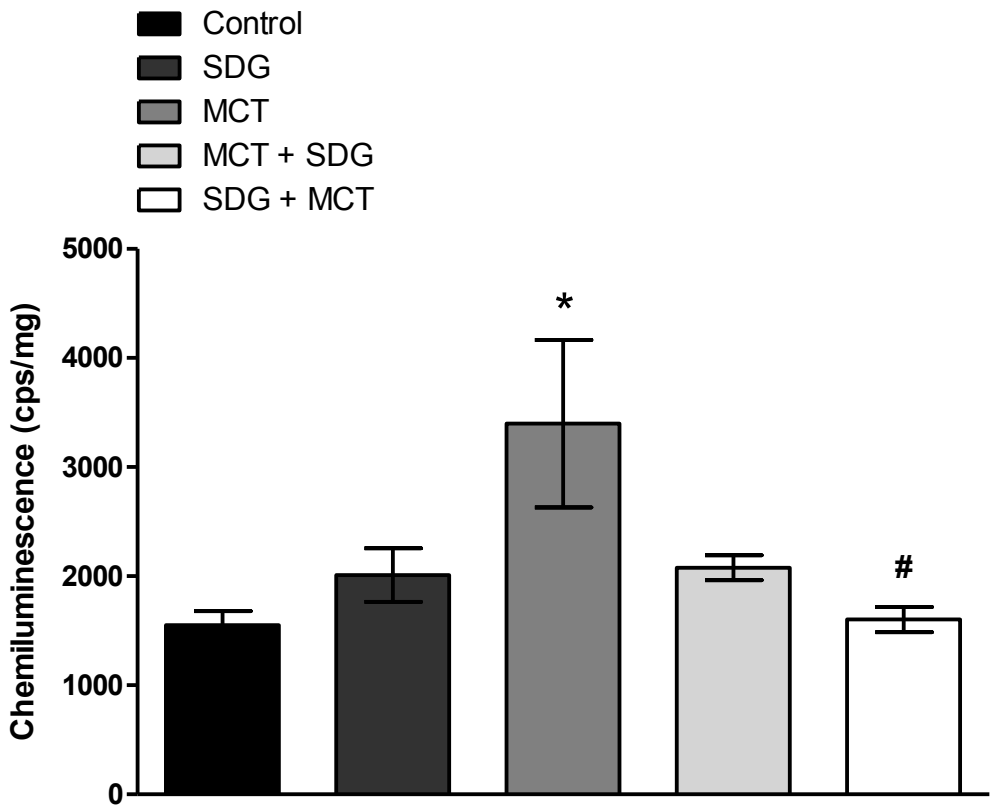

Figure 22. The effect of MCT and SDG on lipid peroxidation in the right ventricle. Lipid peroxidation was assessed via chemiluminescence. Bars represent mean ± SEM where $n = 8$ (*= $p < 0.05$ versus control; # = $p < 0.05$ versus MCT).

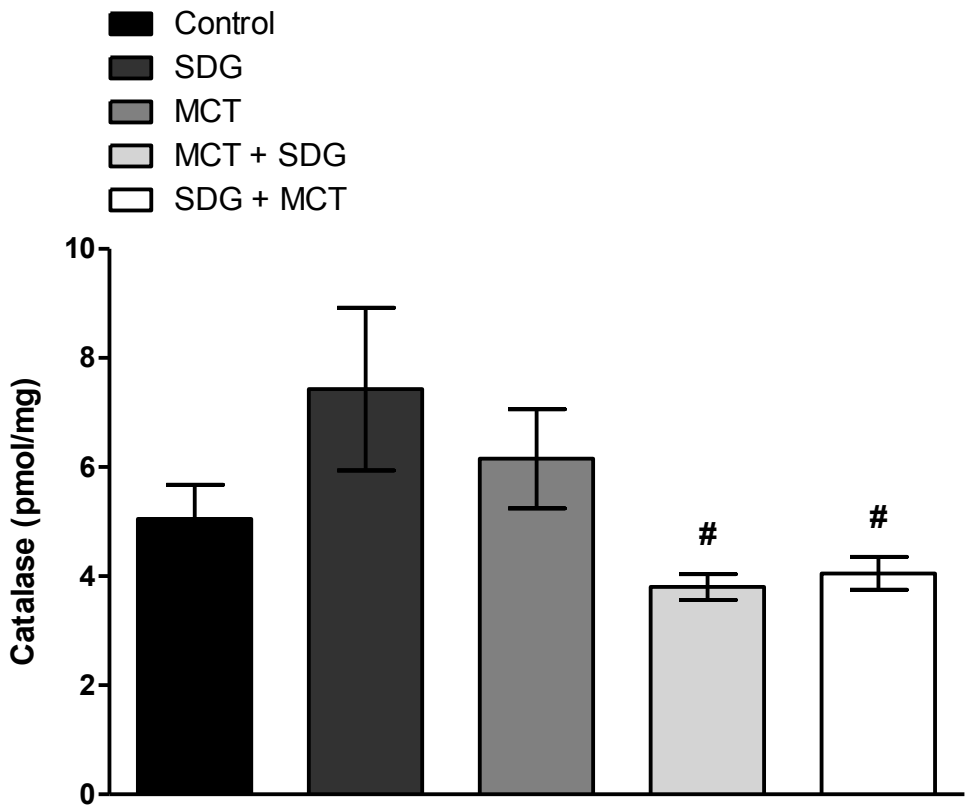

Figure 23. The effect of MCT and SDG on catalase activity in the right ventricle. Enzymatic activity of catalase was assessed via spectrophotometery. Bars represent mean ± SEM where $n = 8$ (# = $p < 0.05$ versus MCT).

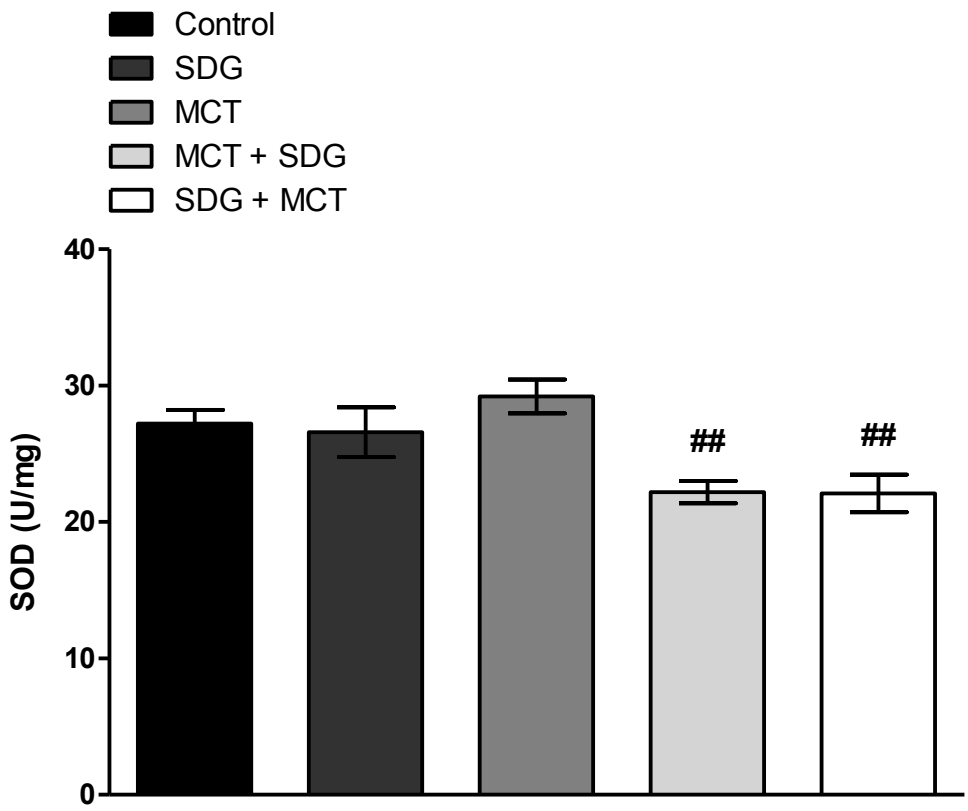

Figure 24. The effect of MCT and SDG on superoxide dismutase activity in the right ventricle. Enzymatic activity of SOD was assessed via spectrophotometery Bars represent mean ± SEM where $n = 8$ (## = $p < 0.01$ versus MCT).

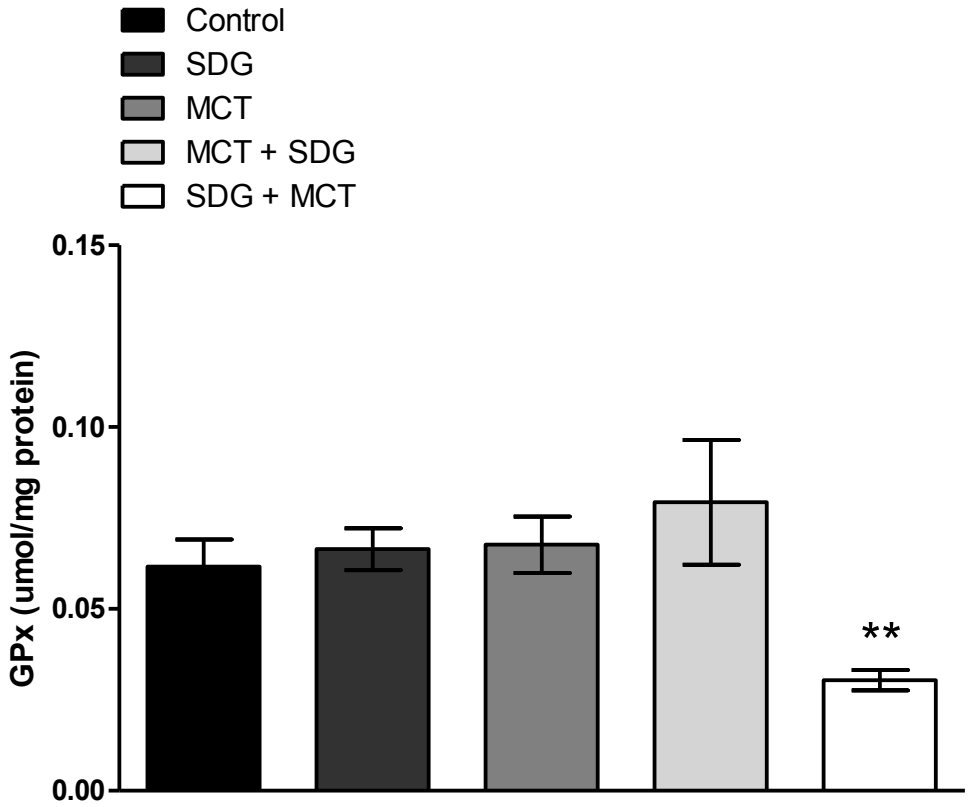

Figure 25. The effect of MCT and SDG on glutathione peroxidase activity in the right ventricle. Enzymatic activity of GPx was assessed via spectrophotometery. Bars represent mean ± SEM where $n = 8$ (** = $p < 0.01$ versus control).

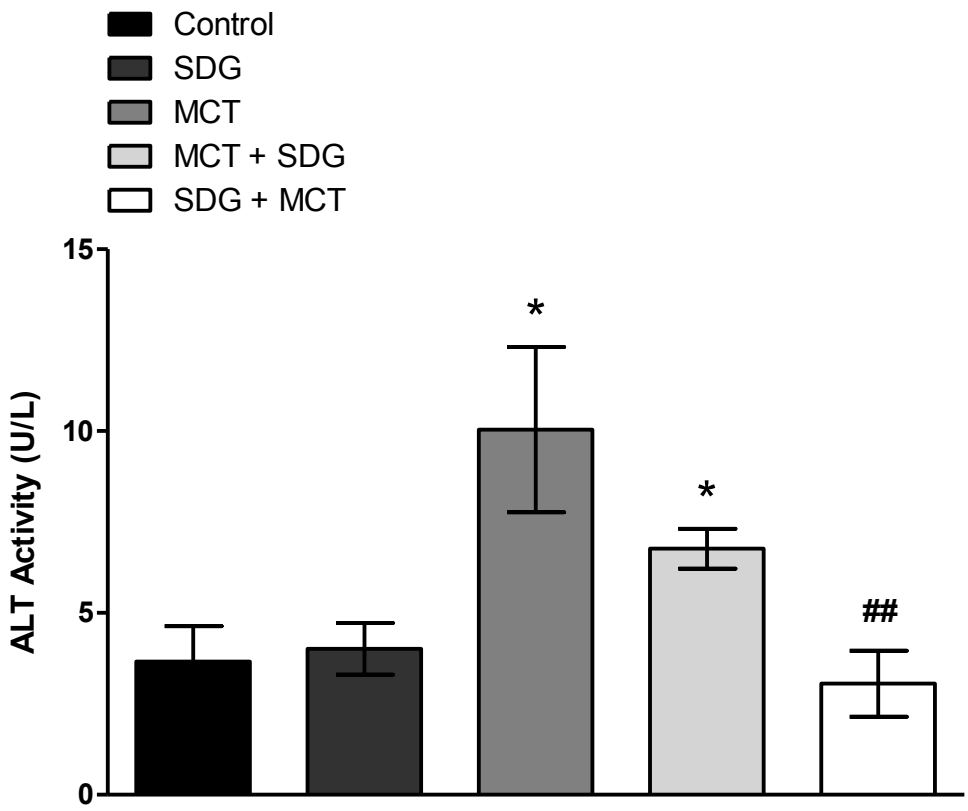

Figure 26. The effect of MCT and SDG on plasma alanine aminotransferase levels. Liver toxicity was assessed by measuring plasma levels of ALT. Bars represent mean ± SEM where $n \geq 4$ (* = $p < 0.05$ versus control; ## = $p < 0.01$ versus MCT).

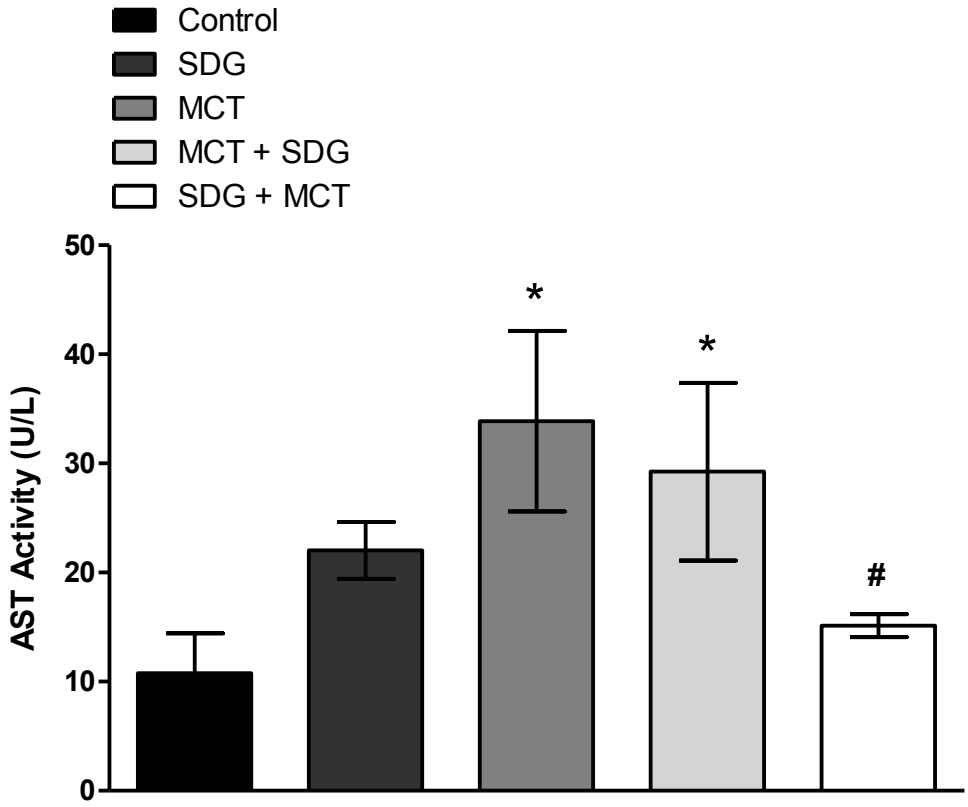

Figure 27. The effect of MCT and SDG on plasma aspartate aminotransferase levels. Liver toxicity was assessed by measuring plasma levels of AST. Bars represent mean ± SEM where $n \geq 4$ (* = $p < 0.05$ versus control; # = $p < 0.05$ versus MCT).

Chapter 5 - Discussion and Conclusion

Discussion

Oxidative stress has been implicated in many cardiovascular diseases including atherosclerosis and ischemia/reperfusion, ultimately leading to heart failure. Oxidative stress is the result of an imbalance of free radicals and enzymatic antioxidants. High levels of ROS can result in DNA, membrane and protein damage [17]. The majority of ROS is due to mitochondrial dysfunction, where $O_2^{\bullet-}$ leaks from the electron transport chain [20]. Leaked $O_2^{\bullet-}$ is readily converted to highly reactive $^{\bullet}OH$ [21]. SOD catalyzes the dismutation of $O_2^{\bullet-}$ to H_2O_2 and O_2 [21; 43]. Catalase catalyzes the reduction of H_2O_2 to H_2O in the cytoplasm [43]. GSH converts H_2O_2 to H_2O in the cytoplasm but requires GPx as a catalyst [43; 44]. During redox imbalance these enzymatic antioxidants are unable to handle the high levels of ROS and damage occurs. Therefore, non-enzymatic antioxidants may be a useful treatment for cardiovascular diseases due to oxidative stress.

Ionizing radiation can cause oxidative stress through the generation of ROS through radiolysis of water and mitochondrial dysfunction [26; 70]. This increase in ROS will damage DNA through base damage, base release, depolymerization, cross-linking, and strand breakage [63; 69]. Also, $^{\bullet}OH$ generated by IR can induce peroxidation of mitochondrial inner membrane phospholipids, resulting in enhanced generation of $O_2^{\bullet-}$ from the mitochondria and persistent oxidative stress [70]. This generation of ROS can continue to arise [26] causing cellular damage long after initial exposure. A complex dietary supplement has previously been shown to prevent damage due to oxidative stress caused by radiation [88; 89]. Though the heart is particularly susceptible to radiation induced damage the use of antioxidants in radiation induced cardiac

damage has not been investigated. Therefore, for this thesis I investigated if the supplement can protect the heart from a whole body dose as well as a high dose to the head of ionizing radiation.

As shown in Chapter 2, when mice were given a 5 Gy whole body dose, radiation did seem to have an effect on protein levels of antioxidants and markers of apoptosis and autophagy at all three time points (48 hours, 30 days and 120 days). Catalase only changed at 120 after radiation, where protein levels increased. Mn-SOD was decreased at 48 hours and 30 days after radiation but was not different than control after 120 days. This likely due to the antioxidants response to the ROS present at each time point. Also, since mitochondria dysfunction is a common result of radiation exposure, this may lead to the decreased levels of Mn-SOD seen after 48 hours and 30 days. Interestingly, both supplement treatment protocols led to an increase in catalase protein levels 48 hours after radiation. Catalase was also increased 120 days after radiation, but this may be due to the radiation rather than supplement as protein levels were similar to when exposed to radiation alone. Pre-treatment with the supplement may have had a positive effect in regards to Mn-SOD where protein levels were similar to control rather than radiation alone both after 48 hours and 30 days. Neither supplement treatment protocols had an effect on Mn-SOD 120 days after radiation, perhaps because at that time point radiation itself did not have an effect on Mn-SOD. In the future it would be interesting to see how other antioxidants are effected, such as glutathione and SOD1 and correlate it to levels of ROS. In regards to apoptosis, both treatment protocols has protective effects against radiation at most time points. Though, only when supplement was given after radiation were pro-caspase 3 levels decreased compared to radiation alone after 120 days. When measuring the Bax:Bcl_2 ratio radiation and supplement had different affects on protein levels at different time points. What's interesting

though is it seems that protein levels of Bcl_2 are affected rather than Bax. Perhaps Bcl_2 is responding to the radiation rather than Bax levels increasing/decreasing. Lc3bII/I ratio was mainly affected after 120 days but since we only measured one marker of apoptosis we don't have enough information to definitively say that autophagy is induced by radiation or the supplement, or if autophagy is beneficial/detrimental. In the future it would be interesting to measure other autophagy markers, such as Atg5 and Beclin 1, to get a better picture of how autophagy is involved in radiation induced cardiac damage. Based on the information we have it does seem that the dietary supplement was beneficial to the heart in some cases.

In Chapter 3 mice were given a 10 Gy dose of radiation to the head and we investigated if the same supplement could protect against cardiac inflammation and fibrosis due to the abscopal effect. Radiation (and supplement) did not have an effect on inflammation or fibrosis in the mouse hearts. Since the abscopal effect to the heart from the brain has not been investigated we cannot say for certain if it does or does not exist. The reason we do not see an increase in inflammation or fibrosis after radiation may be because it is too soon to see a cardiac response. As stated in Chapter 2, patients treated with radiation as children and adolescents are more likely to suffer from cardiovascular complications, but not until later in life [83]. This is the same for patients who underwent radiation therapy for treatment of breast cancer [77]. Mortality from myocardial infarction was seen 40 years after radiation exposure from atomic bombs [76]. In our study, mice were sacrificed 30 days after radiation and, consequently, our model may not be appropriate to see cardiac damage caused by the abscopal effect. This may also explain why we did not see a strong negative effect on the heart after a WBD of 5 Gy in Chapter 2. Even 120 days, our longest time point, may not be long enough to see full detrimental effects of radiation

to the heart in our mouse model. Future studies for both of these projects should use a life span study model to investigate radiation induced cardiac damage and if the dietary supplement can provide protection.

In Chapter 4 we used a different model of oxidative stress; monocrotaline treatment to induce PAH. PAH is known to lead to the development of right ventricular hypertrophy and heart failure [121]. Previously, most of the information on right heart failure was based on work with left heart failure. Farahmand et al [134] investigated antioxidant and oxidative stress changes using an i.p injection of MCT (60 mg/kg) to induce PAH subsequently leading to right heart failure. They found that 1 week after MCT injection right ventricle pressure overload and hypertrophy were increased. They also saw a slight increase in catalase, SOD and GPx activity. 2 weeks after MCT injection there was a significant increase in catalase, SOD and GPx activity, an increase in septal wall thickness and compensated heart failure. 6 weeks after MCT injection they saw right ventrical dilation and failure, lung and liver congestion, decreased catalase, SOD and GPx activity, increased lipid peroxidation and severe bulging of the interventricular septum into the left ventricle. Based on these findings many studies have used a 3 week post MCT injection model to investigate possible treatment options in PAH before reaching the extent of right ventricular damage seen by Farahmand et al [134] at 6 weeks. Pretreatment with grape juice protected the right ventricle through decrease of oxidative stress and improvement of hemodynamic parameters 3 weeks after MCT injection [124; 133]. Studies on the effects of exercise training on MCT induced PAH, where male Wistar rats underwent exercise training for 5 weeks pre MCT then 3 weeks post MCT injection, found that exercise training promoted positive changes in right ventricle and pulmonary artery remodeling and decreased H_2O_2

concentration and apoptotic signaling in the right ventricle [153; 154]. Based on previous positive results we chose to use a 3 week post MCT injection study period.

Treatment with SDG has been shown to protect against other cardiac models of oxidative stress, such as diabetes, atherosclerosis and iron overload. Therefore, we investigated if the same can be observed in our model of PAH. We saw vastly different results between pre-treated animals and co-treated. Pre-treatment with SDG for two weeks provided much better protection against right ventricle damage caused by MCT compared to co-treatment. Right ventricle hypertrophy in the co-treatment group was similar to MCT alone while pre-treatment was similar to control and significantly less than MCT and co-treatment groups. Though, ROS levels and activity of catalase and SOD was significantly less in both pre- and co-treatment groups compared to MCT. These results led us to investigate plasma levels of markers of liver toxicity since both MCT and SDG are metabolized in the liver. ALT and AST were significantly higher in MCT and co-treated groups compared to control and pre-treated groups. Therefore, while we saw the antioxidant properties of SDG in the co-treatment group (reduced ROS and antioxidant activity) it was not enough to prevent the toxicity caused by MCT, which led to increased hypertrophy. In the future, it would be interesting to investigate markers of apoptosis and autophagy in this model. Also, further future directions of this study would be to see if treatment with SDG, particularly pretreatment with SDG, can still protect against MCT induced damage 4, 5 and 6 weeks after injection, when right ventricle damage can be quite severe.

In Chapter 4 we saw that pre-treatment with an antioxidant was significantly better at providing protection against MCT, but there was not much difference between protection

provided by pre- and post-treatment against radiation seen in Chapter 2. This may be because in Chapter 4 only one antioxidant was used, while in Chapter 2 the supplement was composed of many. Or it could be because of the ROS itself. A major factor on the results seen in these studies seems to be the time point where ROS was measured. In Chapter 2 and 3 a high dose of radiation did not have as large of a negative effect as expected. This may be because it takes longer for ROS generation in the heart than the time points we measured at (in human studies oxidative stress is seen in the heart decades after radiation exposure). In Chapter 4 we did not see an increase in ROS as measured via DCF-DA but there was an increase in lipid peroxidation. It is likely that 21 days after MCT treatment is long enough to miss the increase of ROS but instead see the effects ROS (lipid peroxidation). Therefore, when it comes to treatment with antioxidants it is important to consider the extent of oxidative stress and level of ROS present at that time.

It is also important to consider the type of ROS present at a given time. ROS have important physiological functions, such as immune defense [17; 22] and inappropriate removal of ROS may cause paradoxical reductive stress and actually induce or promote disease [155]. Also, as mentioned earlier, different antioxidants, both enzymatic and non-enzymatic, will only react with certain ROS (for example, SOD catalyzes the dismutation of $O_2^{\bullet-}$ to H_2O_2 and O_2 but does not react with $^{\bullet}OH$ or H_2O_2). The complex dietary supplement used in Chapter 2 and 3 was designed to reduce $^{\bullet}OH$, $O_2^{\bullet-}$ and H_2O_2 at multiple cellular sites. Though previous studies have shown positive outcomes of using the supplement [86-88] in many clinical trials antioxidants have almost always failed to show a significant beneficial effects [155; 156]. Schmidt et al [155] state this may due to the fact that many studies showing beneficial effects of antioxidants in animals often do not monitor plasma concentrations of the supplemented antioxidant (which is

done in drug studies to determine safety and effectiveness). Therefore, they believe the possible lack of response to antioxidants in clinical studies is due to pharmacokinetic rather than pharmacodynamic reasons [155].

There are a number of limitations to this study. For Chapter 2 and 3 it would interesting to see if there were any hemodynamic changes due to the dose of radiation, but unfortunately the equipment was not available. In Chapter 2 pro-caspase 3 was used as an indicator of apoptosis via western blot. Though I tried increasing the amount of antibody and protein I could not visualize cleaved caspase 3, which would have given a better indication of apoptosis than pro-caspase 3 alone. In Chapter 3 two stains were used, one for inflammation and one for fibrosis. Though both inflammation and fibrosis have been linked to oxidative stress the study would benefit from a stain specific for oxidative stress, such as 3 nitrotyrosine or 4 hydroxynonenal. Neither we nor the Laboratory Services Division of the Animal Health Laboratory of University of Guelph had the required stains or equipment. In Chapter 4 the enzymatic activity of glutathione peroxidase was measured but not glutathione, which together would give a better indication of antioxidant respone.

Further work needs to be done to determine the long term effects of radiation to the heart. A to-end-of-life study may offer interesting insight on radiation induced ROS in the heart and how antioxidants can be used for treatment. Also, further work is needed on the mechanism(s) of cardiovascular oxidative stress and antioxidant treatment. Though we looked at one marker of autophagy this is not enough do give us a definitive answer on how autophagy was affected in these studies. The role of autophagy may provide some insight into the cardiac response to

oxidative stress. Also, there exists a cross-talk between autophagy and apoptosis that has not been investigated in radiation or MCT induced oxidative stress in the heart. This would give us a better understanding of how the heart responds to oxidative stress and if and when treatment with antioxidants would be appropriate.

Conclusion

Oxidative stress is known to be involved in many types of cardiovascular diseases. The work done in this thesis has shown that treatment with antioxidants may offer some protection to the heart in different models of oxidative stress. Pre-treatment appears to provide better protection against oxidative stress the co-treatment or post-treatment. Though, these studies provide a snapshot of the oxidative stress response at certain time points, and a study over a longer period of time may have different results. Therefore, it is important to consider the extent of oxidative stress and when ROS levels will be increased when developing a antioxidant treatment protocol.

References

1. Mendis, S., Puska, P. & Norrving, B. *Global atlas on cardiovascular disease prevention and control.* (World Health Organization, 2011).
2. MacIver, D. H., Dayer, M. J. & Harrison, A. J. I. A general theory of acute and chronic heart failure. *International Journal of Cardiology* **165,** 25–34 (2013).
3. Organization, W. H. Causes of death 2008: data sources and methods. *Geneva World Heal. Organ.* (2011).
4. Stocker, R. & Keaney, J. F. Role of oxidative modifications in atherosclerosis. *Physiol. Rev.* **84,** 1381–1478 (2004).
5. Rader, D. J. & Daugherty, A. Translating molecular discoveries into new therapies for atherosclerosis. *Nature* **451,** 904–913 (2008).
6. Arslan, F., de Kleijn, D. P. & Pasterkamp, G. Innate immune signaling in cardiac ischemia. *Nat. Rev. Cardiol.* **8,** 292–300 (2011).
7. Rezkalla, S. H. & Kloner, R. A. Coronary no-reflow phenomenon: From the experimental laboratory to the cardiac catheterization laboratory. *Catheterization and Cardiovascular Interventions* **72,** 950–957 (2008).
8. Frey, N., Katus, H. A., Olson, E. N. & Hill, J. A. Hypertrophy of the Heart: A New Therapeutic Target? *Circulation* **109,** 1580–1589 (2004).
9. Dorn, G. W., Robbins, J. & Sugden, P. H. Phenotyping Hypertrophy Eschew Obfuscation. *Circ. Res.* **92,** 1171–1175 (2003).
10. Anversa, P. *et al.* Ischemic cardiomyopathy: myocyte cell loss, myocyte cellular hypertrophy, and myocyte cellular hyperplasia. *Ann. N. Y. Acad. Sci.* **752,** 47–64 (1995).

11. Frey, N., Luedde, M. & Katus, H. a. Mechanisms of disease: hypertrophic cardiomyopathy. *Nat. Rev. Cardiol.* **9,** 91–100 (2012).

12. van Nieuwenhoven, F. A. & Turner, N. A. The role of cardiac fibroblasts in the transition from inflammation to fibrosis following myocardial infarction. *Vascular Pharmacology* **58,** 182–188 (2012).

13. Porter, K. E. & Turner, N. A. Cardiac fibroblasts: At the heart of myocardial remodeling. *Pharmacology and Therapeutics* **123,** 255–278 (2009).

14. McMurray, J. J. V & Pfeffer, M. A. Heart failure. *Lancet* **365,** 1877–1889 (2005).

15. MacIver, D. H. Is remodeling the dominant compensatory mechanism in both chronic heart failure with preserved and reduced left ventricular ejection fraction? *Basic Res. Cardiol.* **105,** 227–234 (2010).

16. Hoshijima, M. & Chien, K. R. Mixed signals in heart failure: cancer rules. *J. Clin. Invest.* **109,** 849–855 (2002).

17. Seddon, M., Looi, Y. H. & Shah, A. M. Oxidative stress and redox signalling in cardiac hypertrophy and heart failure. *Heart* **93,** 903–907 (2007).

18. Khaper, N., Palace, V., Hill, M., Kumar, D. & Singal, P. Heart failure: A failed adaptation to oxidative stress. *Adapt. Biol. Med.* **2,** 13–28 (1999).

19. Singal, P. *et al.* Role of oxidative stress in heart failure subsequent to myocardial infarction. *L'information Cardiol.* **9,** 343–362 (1996).

20. Byrne, J. A., Grieve, D. J., Cave, A. C. & Shah, A. M. Oxidative stress and heart failure. *Arch. Mal. Coeur Vaiss.* **96,** 214–221 (2003).

21. Sarsour, E. H., Kumar, M. G., Chaudhuri, L., Kalen, A. L. & Goswami, P. C. Redox control of the cell cycle in health and disease. *Antioxid. Redox Signal.* **11,** 2985–3011 (2009).

22. Giordano, F. J. Oxygen, oxidative stress, hypoxia, and heart failure. *Journal of Clinical Investigation* **115,** 500–508 (2005).

23. Tsutsui, H., Kinugawa, S. & Matsushima, S. Oxidative stress and heart failure. *Am. J. Physiol. Heart Circ. Physiol.* **301,** H2181–90 (2011).

24. Cooke, M. S., Evans, M. D., Dizdaroglu, M. & Lunec, J. Oxidative DNA damage: mechanisms, mutation, and disease. *FASEB J.* **17,** 1195–1214 (2003).

25. Sonntag, C. *The chemical basis of radiation biology*. (Taylor & Francis London, 1987).

26. Azzam, E. I., Jay-Gerin, J. P. & Pain, D. Ionizing radiation-induced metabolic oxidative stress and prolonged cell injury. *Cancer Letters* **327,** 48–60 (2012).

27. Hu, J. J., Dubin, N., Kurland, D., Ma, B. L. & Roush, G. C. The effects of hydrogen peroxide on DNA repair activities. *Mutat. Res.* **336,** 193–201 (1995).

28. Young, I. S. & McEneny, J. Lipoprotein oxidation and atherosclerosis. *Biochem. Soc. Trans.* **29,** 358–362 (2001).

29. Lee, Y. & Gustafsson, A. B. Role of apoptosis in cardiovascular disease. *Apoptosis* **14,** 536–548 (2009).

30. Kumar, D. & Jugdutt, B. I. Apoptosis and oxidants in the heart. *J. Lab. Clin. Med.* **142,** 288–297 (2003).

31. Whelan, R. S., Kaplinskiy, V. & Kitsis, R. N. Cell death in the pathogenesis of heart disease: mechanisms and significance. *Annu. Rev. Physiol.* **72,** 19–44 (2010).

32. Fellström, B. & Zezina, L. Apoptosis: friend or foe? in *Transplantation proceedings* **33,** 2414–2416 (Elsevier, 2001).

33. Kockx, M. M. *et al.* Apoptosis and related proteins in different stages of human atherosclerotic plaques. *Circulation* **97,** 2307–2315 (1998).

34. Olivetti, G. *et al.* Apoptosis in the failing human heart. *N. Engl. J. Med.* **336,** 1131–1141 (1997).

35. Cai, L. *et al.* Hyperglycemia-induced apoptosis in mouse myocardium: Mitochondrial cytochrome c-mediated caspase-3 activation pathway. *Diabetes* **51,** 1938–1948 (2002).

36. MacLellan, W. R. & Schneider, M. D. Death by design. Programmed cell death in cardiovascular biology and disease. *Circ. Res.* **81,** 137–144 (1997).

37. Haunstetter, A. & Izumo, S. Apoptosis basic mechanisms and implications for cardiovascular disease. *Circ. Res.* **82,** 1111–1129 (1998).

38. Mei, Y., Thompson, M. D., Cohen, R. a & Tong, X. Autophagy and oxidative stress in cardiovascular diseases. *Biochim. Biophys. Acta* **1852,** 243–251 (2014).

39. Essick, E. E. & Sam, F. Oxidative stress and autophagy in cardiac disease, neurological disorders, aging and cancer. *Oxid. Med. Cell. Longev.* **3,** 168–177 (2010).

40 Mizushima, N. & Komatsu, M. Autophagy: Renovation of cells and tissues. *Cell* **147,** 728–741 (2011).

41. Nakai, A. *et al.* The role of autophagy in cardiomyocytes in the basal state and in response to hemodynamic stress. *Nat. Med.* **13,** 619–624 (2007).

42. De Meyer, G. R. Y. & Martinet, W. Autophagy in the cardiovascular system. *Biochim. Biophys. Acta - Mol. Cell Res.* **1793,** 1485–1495 (2009).

43. Singal, P. K., Khaper, N., Palace, V. & Kumar, D. The role of oxidative stress in the genesis of heart disease. *Cardiovascular research* **40,** 426–432 (1998).

44. Li, S. M., Li, X. & Rozanski, G. J. Regulation of glutathione in cardiac myocytes. *J. Mol. Cell. Cardiol.* **35,** 1145–1152 (2003).

45. Khaper, N. *et al.* Targeting the vicious inflammation-oxidative stress cycle for the management of heart failure. *Antioxid. Redox Signal.* **13,** 1033–1049 (2010).

46. Ceconi, C. *et al.* New insights on myocardial pyridine nucleotides and thiol redox state in ischemia and reperfusion damage. *Cardiovasc. Res.* **47,** 586–594 (2000).

47. Myers, M. L., Bolli, R., Lekich, R. F., Hartley, C. J. & Roberts, R. Enhancement of recovery of myocardial function by oxygen free-radical scavengers after reversible regional ischemia. *Circulation* **72,** 915–921 (1985).

48. Jolly, S. R., Kane, W. J., Bailie, M. B., Abrams, G. D. & Lucchesi, B. R. Canine myocardial reperfusion injury. Its reduction by the combined administration of superoxide dismutase and catalase. *Circ. Res.* **54,** 277–285 (1984).

49. Werns, S. W. *et al.* The independent effects of oxygen radical scavengers on canine infarct size. Reduction by superoxide dismutase but not catalase. *Circ. Res.* **56,** 895–898 (1985).

50. Dhalla, A. K. & Singal, P. K. Antioxidant changes in hypertrophied and failing guinea pig hearts. *Am. J. Physiol.* **266,** H1280–H1285 (1994).

51. Bastounis, E. *et al.* Free radical related myocardial mitochondrial damage following limb ischaemia-reperfusion. *Cardiovasc. Res.* **28,** 1868–1871 (1994).

52. Dhalla, A. K., Hill, M. F. & Singal, P. K. Role of oxidative stress in transition of hypertrophy to heart failure. *J. Am. Coll. Cardiol.* **28,** 506–514 (1996).

53. Riley, P. A. Free radicals in biology: oxidative stress and the effects of ionizing radiation. *Int. J. Radiat. Biol.* **65,** 27–33 (1994).

54. Huda, W. Radiation dosimetry in diagnostic radiology. *Am. J. Roentgenol.* **169,** 1487–1488 (1997).

55. Roth, R. A., Sharma, S. C. & Katz, R. Systematic evaluation of cellular radiosensitivity parameters. *Phys. Med. Biol.* **21,** 491–503 (1976).

56. Niemantsverdriet, M. *et al.* High and low LET radiation differentially induce normal tissue damage signals. *Int. J. Radiat. Oncol. Biol. Phys.* **83,** 1291–1297 (2012).

57. Schulz-Ertner, D. & Tsujii, H. Particle radiation therapy using proton and heavier ion beams. *J. Clin. Oncol.* **25,** 953–964 (2007).

58. Kryston, T. B., Georgiev, A. B., Pissis, P. & Georgakilas, A. G. Role of oxidative stress and DNA damage in human carcinogenesis. *Mutat. Res.* **711,** 193–201 (2011).

59. Ottolenghi, A., Merzagora, M. & Paretzke, H. G. DNA complex lesions induced by protons and alpha-particles: Track structure characteristics determining linear energy transfer and particle type dependence. *Radiat. Environ. Biophys.* **36,** 97–103 (1997).

60. Goodhead, D. T. Energy deposition stochastics and track structure: What about the target? *Radiation Protection Dosimetry* **122,** 3–15 (2006).

61. Ward, J. F. Biochemistry of DNA lesions. *Radiat. Res. Suppl.* **8,** S103–S111 (1985).

62. Georgakilas, A. G. From chemistry of DNA damage to repair and biological significance. Comprehending the future. *Mutat. Res.* **711,** 1–2 (2011).

63. Santivasi, W. L. & Xia, F. Ionizing radiation-induced DNA damage, response, and repair. *Antioxid. Redox Signal.* **21,** 251–259 (2014).

64. Jeggo, P. & Löbrich, M. Radiation-induced DNA damage responses. *Radiat. Prot. Dosimetry* **122,** 124–127 (2006).

65. Shibata, A. *et al.* Factors determining DNA double-strand break repair pathway choice in G2 phase. *EMBO J* **30,** 1079–1092 (2011).

66. Haffty, B. G. & Wilson, L. D. *Handbook of radiation oncology: basic principles and clinical protocols*. (Jones & Bartlett Learning, 2009).

67. Petkau, A. Role of superoxide dismutase in modification of radiation injury. *Br. J. Cancer. Suppl.* **8,** 87–95 (1987).

68. Ferradini, C. & Jay-Gerin, J.-P. Radiolysis of water and aqueous solutions - history and present state of the science. *Can. J. Chem.* **77,** 1542–1575 (1999).

69. Bucher, N. & Britten, C. D. G2 checkpoint abrogation and checkpoint kinase-1 targeting in the treatment of cancer. *Br. J. Cancer* **98,** 523–528 (2008).

70. Yoshida, T., Goto, S., Kawakatsu, M., Urata, Y. & Li, T. Mitochondrial dysfunction, a probable cause of persistent oxidative stress after exposure to ionizing radiation. *Free Radical Research* **46,** 147–153 (2012).

71. LaVerne, J. A. Radiation chemical effects of heavy ions. *Charg. Part. Phot. Interact. with Matter. Chem. Physicochem. Biol. Consequences with Appl.* 403–429 (2004).

72. Meesungnoen, J., Jay-Gerin, J. P., Hatano, Y., Katsumura, Y. & Mozumder, A. Radiation chemistry of liquid water with heavy ions: Monte Carlo simulation studies. *Charg. Part. Phot. Interact. with matter Recent Adv. Appl. interfaces. Boca Rat. Taylor Fr.* 355–400 (2011).

73. Macià i Garau, M., Lucas Calduch, A. & López, E. C. Radiobiology of the acute radiation syndrome. *Reports of Practical Oncology and Radiotherapy* **16,** 123–130 (2011).

74. IAEA, W. H. O. Diagnosis and treatment of radiation injuries, Safety Reports Series No. 2. *Vienna IAEA* (1998).

75. Yusuf, S. W., Sami, S. & Daher, I. N. Radiation-induced heart disease: A clinical update. *Cardiol. Res. Pract.* **1,** (2011).

76. Baker, J. E., Moulder, J. E. & Hopewell, J. W. Radiation as a risk factor for cardiovascular disease. *Antioxid. Redox Signal.* **15,** 1945–1956 (2011).

77. Darby, S. *et al.* Radiation-related heart disease: current knowledge and future prospects. *Int. J. Radiat. Oncol. Biol. Phys.* **76,** 656–665 (2010).

78. Schultz-Hector, S. & Trott, K.-R. Radiation-induced cardiovascular diseases: is the epidemiologic evidence compatible with the radiobiologic data? *Int. J. Radiat. Oncol. Biol. Phys.* **67,** 10–18 (2007).

79. Gagliardi, G. *et al.* Radiation dose-volume effects in the heart. *Int. J. Radiat. Oncol. Biol. Phys.* **76,** S77–85 (2010).

80. Heidenreich, P. A. & Kapoor, J. R. Radiation induced heart disease. *Heart* **95,** 252–258 (2009).

81. Filopei, J. & Frishman, W. Radiation-induced heart disease. *Cardiol. Rev.* **20,** 184–188 (2012).

82. Veinot, J. P. & Edwards, W. D. Pathology of radiation-induced heart disease: a surgical and autopsy study of 27 cases. *Hum. Pathol.* **27,** 766–773 (1996).

83. Adams, M. J., Hardenbergh, P., Constine, L. & Lipshultz, S. Radiation-associated cardiovascular disease. *Crit. Rev. Oncol. Hematol.* **45,** 55–75 (2003).

84. Hancock, S. L., Donaldson, S. S. & Hoppe, R. T. Cardiac disease following treatment of Hodgkin's disease in children and adolescents. *J. Clin. Oncol.* **11,** 1208–1215 (1993).

85. Preston, D., Shimizu, Y., Pierce, D., Suyama, A. & Mabuchi, K. Studies of mortality of atomic bomb survivors. Report 13: Solid cancer and noncancer disease mortality: 1950-1997. *Radiat. Res.* **160,** 381–407 (2003).

86. Lemon, J. A., Boreham, D. R. & Rollo, C. D. A complex dietary supplement extends longevity of mice. *J. Gerontol. A. Biol. Sci. Med. Sci.* **60,** 275–279 (2005).

87. Long, J., Aksenov, V., Rollo, C. D. & Liu, J. A complex dietary supplement modulates nitrative stress in normal mice and in a new mouse model of nitrative stress and cognitive aging. *Mech. Ageing Dev.* **133,** 523–529 (2012).

88. Lemon, J. A., Rollo, C. D. & Boreham, D. R. Elevated DNA damage in a mouse model of oxidative stress: Impacts of ionizing radiation and a protective dietary supplement. *Mutagenesis* **23,** 473–482 (2008).

89. Lemon, J. A., Rollo, C. D., McFarlane, N. M. & Boreham, D. R. Radiation-induced apoptosis in mouse lymphocytes is modified by a complex dietary supplement: the effect of genotype and gender. *Mutagenesis* **23,** 465–472 (2008).

90. Nian, M., Lee, P., Khaper, N. & Liu, P. Inflammatory cytokines and postmyocardial infarction remodeling. *Circ. Res.* **94,** 1543–1553 (2004).

91. Kaur, K. *et al.* Biology of TNFalpha and IL-10, and their imbalance in heart failure. *Heart Fail. Rev.* **14,** 113–123 (2009).

92. Han, D., Ybanez, M. D., Ahmadi, S., Yeh, K. & Kaplowitz, N. Redox regulation of tumor necrosis factor signaling. *Antioxid. Redox Signal.* **11,** 2245–2263 (2009).

93. Idriss, H. T. & Naismith, J. H. TNF alpha and the TNF receptor superfamily: structure-function relationship(s). *Microsc. Res. Tech.* **50,** 184–195 (2000).

94. Meldrum, D. R. *et al.* Hydrogen peroxide induces tumor necrosis factor alpha-mediated cardiac injury by a P38 mitogen-activated protein kinase-dependent mechanism. *Surgery* **124,** 291–296; discussion 297 (1998).

95. Multhoff, G. & Radons, J. Radiation, Inflammation, and Immune Responses in Cancer. *Frontiers in Oncology* **2,** (2012).

96. Zhou, D. *et al.* Effects of NF-kappaB1 (p50) targeted gene disruption on ionizing radiation-induced NF-kappaB activation and TNFalpha, IL-1alpha, IL-1beta and IL-6 mRNA expression in vivo. *Int. J. Radiat. Biol.* **77,** 763–772 (2001).

97. Son, E.-W., Rhee, D.-K. & Pyo, S. Gamma-irradiation-induced intercellular adhesion molecule-1 (ICAM-1) expression is associated with catalase: activation of Ap-1 and JNK. *J. Toxicol. Environ. Heal. Part A* **69,** 2137–2155 (2006).

98. Van der Meeren, A. *et al.* Abdominal radiation exposure elicits inflammatory responses and abscopal effects in the lungs of mice. *Radiat. Res.* **163,** 144–152 (2005).

99. Azimzadeh, O. *et al.* Rapid proteomic remodeling of cardiac tissue caused by total body ionizing radiation. *Proteomics* **11,** 3299–3311 (2011).

100. Van Der Meeren, A., Squiban, C., Gourmelon, P., Lafont, H. & Gaugler, M. H. Differential regulation by IL-4 and IL-10 of radiation-induced IL-6 and IL-8 production and ICAM-1 expression by human endothelial cells. *Cytokine* **11,** 831–838 (1999).

101. Yue, P., Massie, B. M., Simpson, P. C. & Long, C. S. Cytokine expression increases in nonmyocytes from rats with postinfarction heart failure. *Am. J. Physiol.* **275,** H250–H258 (1998).

102. Lodish, H. *et al.* in *Molecular Cell Biology* (WH Freeman, 2000). at <http://www.ncbi.nlm.nih.gov/books/NBK21582/>

103. de Jong, S., van Veen, T. A. B., de Bakker, J. M. T. & van Rijen, H. V. M. Monitoring cardiac fibrosis: a technical challenge. *Netherlands Hear. J.* **20,** 44–48 (2012).

104. Deten, A., Hölzl, A., Leicht, M., Barth, W. & Zimmer, H.-G. Changes in extracellular matrix and in transforming growth factor beta isoforms after coronary artery ligation in rats. *J. Mol. Cell. Cardiol.* **33,** 1191–1207 (2001).

105. Peng, J., Gurantz, D., Tran, V., Cowling, R. T. & Greenberg, B. H. Tumor necrosis factor-α-induced AT1 receptor upregulation enhances angiotensin II-mediated cardiac fibroblast responses that favor fibrosis. *Circ. Res.* **91,** 1119–1126 (2002).

106. Herskind, C. & Rodemann, H. P. Spontaneous and radiation-induced differentiation of fibroblasts. *Exp. Gerontol.* **35,** 747–755 (2000).

107. Gao, S., Wu, R. & Zeng, Y. Up-regulation of peroxisome proliferator-activated receptor gamma in radiation-induced heart injury in rats. *Radiat. Environ. Biophys.* **51,** 53–59 (2012).

108. Baker, J. *et al.* 10 Gy total body irradiation increases risk of coronary sclerosis, degeneration of heart structure and function in a rat model. *Int. J. Radiat. Biol.* **85,** 1089–1100 (2009).

109. Orzan, F. *et al.* Associated cardiac lesions in patients with radiation-induced complete heart block. *Int J Cardiol* **39,** 151–156 (1993).

110. Cohen, S. I., Bharati, S., Glass, J. & Lev, M. Radiotherapy as a cause of complete atrioventricular block in Hodgkin's disease: An electrophysiological-pathological correlation. *Arch. Intern. Med.* **141,** 676–679 (1981).

111. Siva, S., MacManus, M. P., Martin, R. F. & Martin, O. A. Abscopal effects of radiation therapy: A clinical review for the radiobiologist. *Cancer Letters* **356,** 82-90 (2013).

112. Kaminski, J. M. *et al.* The controversial abscopal effect. *Cancer Treatment Reviews* **31,** 159–172 (2005).

113. Watters, D. Molecular mechanisms of ionizing radiation-induced apoptosis. *Immunol. Cell Biol.* **77,** 263–271 (1999).

114. Hong, J.-H. *et al.* Induction of acute phase gene expression by brain irradiation. *Int. J. Radiat. Oncol. Biol. Phys.* **33,** 619–626 (1995).

115. Quarmby, S., Kumar, P. & Kumar, S. Radiation induced normal tissue injury: Role of adhesion molecules in leukocyte–endothelial cell interactions. *Int. J. Cancer* **82,** 385–395 (1999).

116. Kusunoki, Y. *et al.* Decreased proportion of CD4 T cells in the blood of atomic bomb survivors with myocardial infarction. *Radiat Res* **152,** 539–543 (1999).

117. Fujiwara, S. *et al.* Levels of parathyroid hormone and calcitonin in serum among atomic bomb survivors. *Radiat. Res.* **137,** 96–103 (1994).

118. Azzam, E. I., de Toledo, S. M. & Little, J. B. Oxidative metabolism, gap junctions and the ionizing radiation-induced bystander effect. *Oncogene* **22,** 7050–7057 (2003).

119. Khan, M. A., Van Dyk, J., Yeung, I. W. T. & Hill, R. P. Partial volume rat lung irradiation; Assessment of early DNA damage in different lung regions and effect of radical scavengers. *Radiother. Oncol.* **66,** 95–102 (2003).

120. Guglin, M. & Khan, H. Pulmonary Hypertension in Heart Failure. *J. Card. Fail.* **16,** 461–474 (2010).

121. Chin, K. M. & Rubin, L. J. Pulmonary Arterial Hypertension. *J. Am. Coll. Cardiol.* **51,** 1527–1538 (2008).

122. Raiesdana, A. & Loscalzo, J. Pulmonary arterial hypertension. *Ann. Med.* **38,** 95–110 (2006).

123. Demarco, V. G., Whaley-Connell, A. T., Sowers, J. R., Habibi, J. & Dellsperger, K. C. Contribution of oxidative stress to pulmonary arterial hypertension. *World J. Cardiol.* **2,** 316–324 (2010).

124. Mosele, F. *et al.* Effects of purple grape juice in the redox-sensitive modulation of right ventricular remodeling in a pulmonary arterial hypertension model. *J. Cardiovasc. Pharmacol.* **60,** 15–22 (2012).

125. Haider, N., Narula, N. & Narula, J. Apoptosis in heart failure represents programmed cell survival, not death, of cardiomyocytes and likelihood of reverse remodeling. *J. Card. Fail.* **8,** S512–S517 (2002).

126. Nadal-Ginard, B., Kajstura, J., Leri, A. & Anversa, P. Myocyte death, growth, and regeneration in cardiac hypertrophy and failure. *Circ. Res.* **92,** 139–150 (2003).

127. Sitbon, O. *et al.* Long-term response to calcium channel blockers in idiopathic pulmonary arterial hypertension. *Circulation* **111,** 3105–3111 (2005).

128. Channick, R. N. *et al.* Effects of the dual endothelin-receptor antagonist bosentan in patients with pulmonary hypertension: A randomised placebo-controlled study. *Lancet* **358,** 1119–1123 (2001).

129. Tabima, D. M., Frizzell, S. & Gladwin, M. T. Reactive oxygen and nitrogen species in pulmonary hypertension. *Free Radic. Biol. Med.* **52,** 1970–86 (2012).

130. Wolin, M. S., Ahmad, M. & Gupte, S. A. The sources of oxidative stress in the vessel wall. in *Kidney International* **67,** 1659–1661 (2005).

131. Leach, R. M., Hill, H. M., Snetkov, V. A., Robertson, T. P. & Ward, J. P. T. Divergent roles of glycolysis and the mitochondrial electron transport chain in hypoxic pulmonary vasoconstriction of the rat: Identity of the hypoxic sensor. *J. Physiol.* **536,** 211–224 (2001).

132. Weissmann, N. *et al.* Effects of Mitochondrial Inhibitors and Uncouplers on Hypoxic Vasoconstriction in Rabbit Lungs. *Am. J. Respir. Cell Mol. Biol.* **29,** 721–732 (2003).

133. Ludke, A. R. L. *et al.* Modulation of monocrotaline-induced cor pulmonale by grape juice. *J. Cardiovasc. Pharmacol.* **55,** 89–95 (2010).

134. Farahmand, F., Hill, M. F. & Singal, P. K. Antioxidant and oxidative stress changes in experimental cor pulmonale. *Mol. Cell. Biochem.* **260,** 21–29 (2004).

135. Jasmin, J.-F., Cernacek, P. & Dupuis, J. Activation of the right ventricular endothelin (ET) system in the monocrotaline model of pulmonary hypertension: response to chronic ETA receptor blockade. *Clin. Sci.* **105,** 647–653 (2003).

136. Pichardo, J., Palace, V., Farahmand, F. & Singal, P. K. Myocardial oxidative stress changes during compensated right heart failure in rats. *Mol. Cell. Biochem.* **196,** 51–57 (1999).

137. Redout, E. M. *et al.* Right-ventricular failure is associated with increased mitochondrial complex II activity and production of reactive oxygen species. *Cardiovasc Res* **75,** 770–781 (2007).

138. Redout, E. M. *et al.* Antioxidant treatment attenuates pulmonary arterial hypertension-induced heart failure. *Am. J. Physiol. Heart Circ. Physiol.* **298,** H1038–H1047 (2010).

139. Prasad, K. Flaxseed and cardiovascular health. *J. Cardiovasc. Pharmacol.* **54,** 369–377 (2009).

140. Westcott, N. D. & Muir, A. D. Process for extracting lignans from flaxseed. (1998).

141. Prasad, K. Oxidative stress as a mechanism of diabetes in diabetic BB prone rats: effect of secoisolariciresinol diglucoside (SDG). *Mol. Cell. Biochem.* **209,** 89–96 (2000).

142. Moree, S. S., Kavishankar, G. B. & Rajesha, J. Antidiabetic effect of secoisolariciresinol diglucoside in streptozotocin-induced diabetic rats. *Phytomedicine* **20,** 237–245 (2013).

143. Prasad, K., Mantha, S. V, Muir, A. D. & Westcott, N. D. Protective effect of secoisolariciresinol diglucoside against streptozotocin-induced diabetes and its mechanism. *Mol. Cell. Biochem.* **206,** 141–149 (2000).

144. Prasad, K. Secoisolariciresinol diglucoside from flaxseed delays the development of type 2 diabetes in Zucker rat. *J. Lab. Clin. Med.* **138,** 32–39 (2001).

145. Prasad, K. Regression of hypercholesterolemic atherosclerosis in rabbits by secoisolariciresinol diglucoside isolated from flaxseed. *Atherosclerosis* **197,** 34–42 (2008).

146. Penumathsa, S. V. *et al.* Secoisolariciresinol diglucoside induces neovascularization-mediated cardioprotection against ischemia-reperfusion injury in hypercholesterolemic myocardium. *J. Mol. Cell. Cardiol.* **44,** 170–179 (2008).

147. Penumathsa, S. V. *et al.* Secoisolariciresinol diglucoside: relevance to angiogenesis and cardioprotection against ischemia-reperfusion injury. *J. Pharmacol. Exp. Ther.* **320,** 951–959 (2007).

148. Prasad, K. Secoisolariciresinol diglucoside (SDG) isolated from flaxseed, an alternative to ACE inhibitors in the treatment of hypertension. *Int. J. Angiol.* **22,** 235–238 (2013).

149. Puukila, S. *et al.* Secoisolariciresinol diglucoside abrogates oxidative stress-induced damage in cardiac iron overload condition. *PLoS One* **10,** e0122852 (2015).

150. Claiborne, A. in *Handbook of methods for oxygen radical research* (ed. Greenwald, R.) 283–284 (CRC Press Boca, 1985).

151. Marklund, S. in *Handbook of Methods for Oxygen Radical Research* (ed. Greenwald, R.) 243–247 (CRC Press Boca, 1985).

152. Paglia, D. E. & Valentine, W. N. Studies on the quantitative and qualitative characterization of erythrocyte glutathione peroxidase. *J. Lab. Clin. Med.* **70,** 158–169 (1967).

153. Colombo, R. *et al.* Effects of exercise on monocrotaline-induced changes in right heart function and pulmonary artery remodeling in rats. *Can. J. Physiol. Pharmacol.* **91,** 38–44 (2013).

154. Colombo, R. *et al.* Aerobic Exercise Promotes a Decrease in Right Ventricle Apoptotic Proteins in Experimental Cor Pulmonale. *J. Cardiovasc. Pharmacol.* **66,** 246–253 (2015).

155. Schmidt, H. H. H. W. *et al.* Antioxidants in Translational Medicine. *Antioxid. Redox Signal.* (2015). doi:10.1089/ars.2015.6393

156. Sesso, H. D. *et al.* Vitamins E and C in the prevention of cardiovascular disease in men: the Physicians' Health Study II randomized controlled trial. *JAMA* **300,** 2123–2133 (2008).